COMPRESSIBILITY FACTORS AND VIRIAL COEFFICIENTS FOR METHANE, ETHYLENE, AND THEIR MIXTURES, USING AN ISOTHERMAL EXPANSION RATIO APPARATUS

By

ROY CARLTON LEE

Bachelor of Science
Oklahoma State University
Stillwater, Oklahoma
August, 1960

Master of Science
Oklahoma State University
Stillwater, Oklahoma
May, 1962

Submitted to the Faculty of the Graduate College
of the Oklahoma State University
in partial fulfillment of the requirements
for the Degree of
DOCTOR OF PHILOSOPHY
May, 1969

COMPRESSIBILITY FACTORS AND VIRIAL COEFFICIENTS

FOR METHANE, ETHYLENE, AND THEIR MIXTURES,

USING AN ISOTHERMAL EXPANSION

RATIO APPARATUS

Thesis Approved:

Wayne C. Edmister
Thesis Adviser

Robert L. Robinson, Jr.

John H. Erbar

David L. Weeks

D. D. Durham
Dean of the Graduate College

PREFACE

An isothermal expansion ratio apparatus was assembled for the precise determination of compressibility factors. Compressibility data were obtained for methane, ethylene, and four of their mixtures, and virial coefficients were derived. The compressibility factors and virial coefficients were compared with values from the literature and with three empirical equations of state.

During the course of this work, many have provided guidance and assistance. I am indebted to Professor W. C. Edmister, my major adviser, for his advice in analyzing the experimental data and in the formulation of this dissertation. Also, appreciation is expressed for the guidance of Dr. R. L. Robinson, Jr., and the interest and help provided by my fellow graduate students.

The financial assistance of the National Science Foundation, the Petroleum Research Fund of the American Chemical Society, and the School of Chemical Engineering is acknowledged.

I wish to express gratitude to my parents and sisters for their encouragement during this work.

TABLE OF CONTENTS

LIST OF TABLES

LIST OF FIGURES

CHAPTER I

INTRODUCTION

This project had three objectives: 1) the design and assembly of an isothermal expansion ratio apparatus for the precise determination of compressibility factors for gases, 2) the use of this apparatus to obtain compressibility factors for the methane-ethylene system, and 3) comparison of experimental compressibility factor and virial coefficient data with existing data and equations of state.

Compressibility data can be of great value in providing needed volumetric data for process design calculations. Also, compressibility data are used to calculate thermodynamic properties, enthalpy and entropy, for example, and to provide a basis for development of methods for estimating thermodynamic properties of gases.

The binary system of methane and ethylene was selected for this study because of its importance in the petrochemical industry and the availability of the pure component data in previous literature, thus providing a convenient comparison. Another important consideration is that no experimental study of compressibility factors for the methane-ethylene system has been reported in the literature. The compressibility factors were determined for methane, ethylene, and four of their binary mixtures at 25, 50, and 75 °C and pressures to 12,000 psia.

CHAPTER II

PVT MEASUREMENTS

In this section, various methods for obtaining compressibility data, including the isothermal expansion ratio method developed by Burnett (6), are discussed. The basic relationships for reducing the data from the isothermal expansion ratio method are shown.

The determination of the PVT properties of gases involves making pressure, temperature, volume, mass, and composition measurements. Accurate pressure and temperature measurements are relatively easy to make compared to the other measurements. Commercially available pressure measuring devices can measure pressure to one part in 10,000. Resistance thermometers are able to measure temperatures to 0.001 °C over a wide range. Special care and techniques are required to make accurate volume, mass, and composition measurements for gases. The volume of the confining vessel is usually determined by weighing the vessel filled with a liquid of known density. The mass of the gas charged into the confining vessel can be determined by weighing the gas sample. Modern chromotography or mass spectrographic methods can be used to measure the composition. Also, gas samples can be prepared of known composition by weighing the amounts of each component put into the confining vessel. Several techniques have been used by previous investigators to determine the PVT properties of gases. These techniques differ usually in the manner in which the volume and mass

of the sample are determined. Some of these techniques will be discussed under the following headings:

1. Constant Volume-Variable Mass
2. Constant Mass-Variable Volume
3. Constant Volume-Constant Mass
4. Variable Volume-Variable Mass

Constant Volume-Variable Mass

In 1930, Bean (2) described a constant volume-variable mass method for PVT determinations. A gas sample of unknown mass was charged into a high pressure bomb of known volume. A portion of the gas sample was expanded to a low pressure, where the PVT properties of the gas were known, into a calibrated burette. The mass of the gas in the low pressure burette was calculated. The expansions from the high pressure bomb were repeated measuring the temperature and pressure and summing the masses for each step.

The compressibility factors were calculated from the temperature and pressure measurements, the bomb volume, and the calculated mass. Several runs were made along an isotherm.

The compressibility factors determined by the Bean apparatus are dependent upon the knowledge of compressibility factors near atmospheric pressure. The errors in the known compressibility data will be reflected in the calculated mass of gas for each expansion and the total mass. Bloomer (5) reported compressibility data for natural gases accurate to 0.1% for temperatures near ambient and pressures to 1000 psi.

A modified Bean apparatus was reported by Solbrig and Ellington (62). The mass of the gas sample that was charged into the high pressure bomb was measured providing an independent check on the sum of the incremental masses. Also before each expansion, several constant volume measurements were made at various temperatures. This procedure reduced the number of runs required for a given amount of data. Data (62) have been reported for hydrogen-methane and hydrogen-ethane mixtures accurate to 0.1% for temperatures from -300 to 300 °F and pressures up to 3000 psi.

Constant Mass-Variable Volume

This technique for determining the PVT properties involves confining a gas sample of known mass in a vessel at constant temperature and determining the change in pressure with change in volume. This method dates from Amagat's work (1).

Michels and Gibson (42) described an apparatus of the constant mass-variable volume type in 1928. The gas sample was confined in a glass piezometer over mercury. The piezometer was contained in a steel pressure vessel filled with mercury and oil. The piezometer consisted of a series of glass vessels connected by capillaries. Platinum wire contacts were placed in the capillaries. The volume of each vessel was calibrated by using mercury.

An experimental run consisted of charging the piezometer with a gas sample of known mass and changing the volume of the sample by pressuring mercury into the piezometer. The platinum contacts indicated the position of the mercury and hence the volume of the gas

sample. The PVT properties were determined from the pressure, temperature, volume, and mass measurements.

The apparatus described by Michels and Gibson (42) was limited to relatively low pressure, to 50 atmospheres. The pressure range of the apparatus could be increased by making the final volume of the piezometer smaller or the initial volume larger. A smaller final volume would decrease the accuracy of the volume measurements and a larger initial volume would require a large apparatus for withstanding high pressures.

An improved apparatus of the constant mass-variable volume type was reported by Michels, Michels, and Wouters (46). The piezometer was designed to be filled to an initial pressure of 20 to 50 atmospheres. The amount of gas charged was determined from previous PVT data. This apparatus could be used to 3000 atmospheres. The authors claimed an accuracy of one part in 2000 at 3000 atmospheres and a higher accuracy at lower pressures.

In both the original and improved apparatus of Michels, the gas sample was confined over mercury. Thus, the temperature range was restricted to avoid freezing the mercury or contaminating the gas sample with mercury vapor at high temperatures.

Another constant mass-variable volume apparatus was reported by Beattie et al. (3) in 1934. A gas sample was sealed in a thin-wall vessel of known volume. The mass of the sample was determined by weighing. The sealed vessel was inverted in a high pressure bomb. Mercury was pumped into the high pressure bomb filling the annular space, and the seal was broken. The change in volume of the original

gas sample was determined by measuring the amount of mercury pumped into the high pressure bomb from a pre-calibrated screw pump.

The effect of pressure and temperature on the volume of the bomb and confining mercury was made using a gas with known PVT properties. The apparatus can be operated along isochors as well as along isotherms.

Douslin et al. (16) have used a Beattie apparatus recently for determining the compressibility factors of fluorocarbons, hydrocarbons, and their binary mixtures over a temperature range of 0 to 350 °C and pressures to 400 atmospheres. The authors reported that the compressibility factors were accurate to 0.03% at the lowest temperature and pressure and to 0.3% at the highest temperature and pressure.

Constant Volume-Constant Mass

A constant volume-constant mass apparatus was developed by Michels et al. (39,45,47) to extend PVT data below 0 °C from their higher temperature measurements using the constant mass-variable volume apparatus. In this method, a gas sample was charged into a high pressure bomb. The gas sample was allowed to equilibrate at 0 °C or 25 °C, where the PVT properties were known, and the pressure measured. Next, the gas sample was cooled to various temperatures below the reference isotherm measuring pressure at each temperature.

In addition to knowing the PVT properties of the gas at a reference isotherm, knowledge of the change in volume of the isochoric apparatus with pressure and temperature was required. Also since the diaphragm cell, which separated the gas sample from the oil of the pressure gage was located outside the thermostat, the isochoric data were corrected for part of the gas sample being at a temperature

other than the gas in the high pressure bomb. This apparatus was operated over a temperature range of 25 to - 180 °C and pressures to 1000 atmospheres. Michels et al. (39,45,47) reported the accuracy to be one part in 10,000. Also, Levelt (33) has presented a detailed discussion of this apparatus.

McMath (38) used an isochoric apparatus to extend the compressibility data from this work for methane, ethylene, and four of their binary mixtures below 25 °C. Also, a detailed discussion of isochoric apparatus was presented by McMath.

The isochoric method of obtaining PVT properties has two major disadvantages. Any errors in the reference isotherm will be reflected in the isochoric data. Changing the temperature of the isochoric apparatus takes considerable time. These disadvantages are offset somewhat by the simplicity of the apparatus. Also, if the same temperatures are used in the course of a series of runs, the method provides isothermal data as well as isochoric data.

Variable Volume-Variable Mass

In 1936, E. S. Burnett (6) reported in a paper a method for determining isothermal compressibility factors of gases. The method consisted of making a series of isothermal expansions from one vessel through a valve into an evacuated vessel, measuring the pressure before each expansion.

The first vessel V_1 is filled to a desired pressure with gas (Figure 1). After allowing the gas to attain thermal equilibrium with

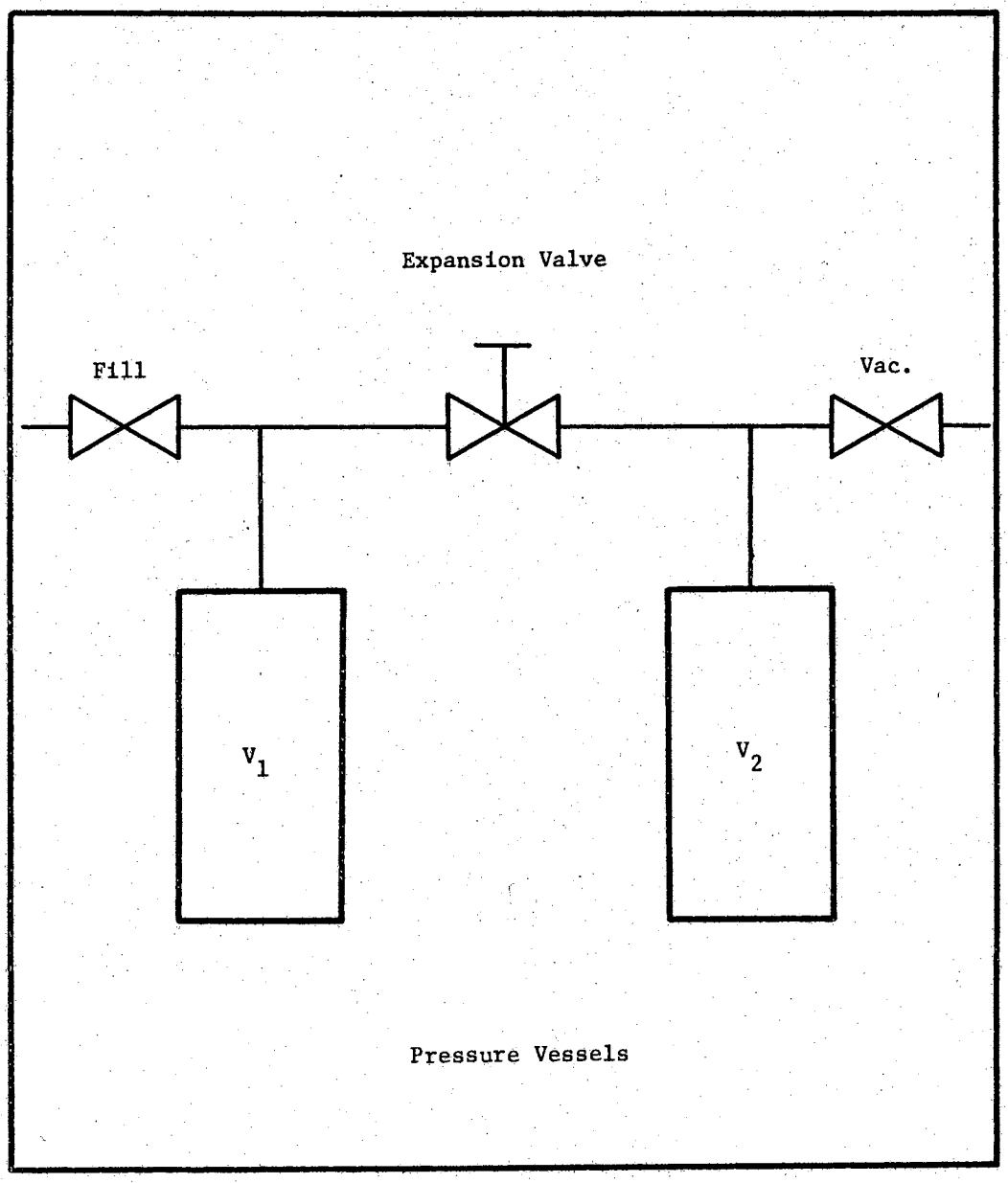

Figure 1. Isothermal Expansion Ratio Apparatus

the thermostat, the initial pressure P_o is measured. The following equation of state can be written for the gas in V_1:

$$P_o V_1 = z_o n_o RT \qquad \text{(II-1)}$$

The valve between the second vessel V_2 and V_1 is closed. Vessel V_2 is evacuated and the gas is expanded from V_1 to V_2. The pressure P_1, after the first expansion of the gas, in V_1 and V_2 is measured after thermal equilibrium is reached. The following equation of state can be written for the gas in V_1 and V_2:

$$P_1(V_1 + V_2) = z_1 n_o RT \qquad \text{(II-2)}$$

Solving Eq. (II-2) for n_o and substituting into Eq. (II-1) gives the following expression:

$$\frac{P_o}{P_1} = \frac{V_1 + V_2}{V_1} \frac{z_o}{z_1} \qquad \text{(II-3)}$$

The expansion valve is closed and V_2 is evacuated. The pressure in V_1 is still P_1, but the number of moles of gas becomes n_1. Then the equation of state for the gas in V_1 is:

$$P_1 V_1 = z_1 n_1 RT \qquad \text{(II-4)}$$

After the second expansion, the following equation of state can be written:

$$P_2 (V_1 + V_2) = z_2 n_1 RT \tag{II-5}$$

Similarly, the pressure ratio can be obtained using Eqs. (II-4) and (II-5).

$$\frac{P_1}{P_2} = \frac{V_1 + V_2}{V_1} \frac{z_1}{z_2} \tag{II-6}$$

Continuing the expansions, the pressure ratio after the j^{th} expansion becomes,

$$\frac{P_{j-1}}{P_j} = \frac{V_1 + V_2}{V_1} \frac{z_{j-1}}{z_j} \tag{II-7}$$

The volume ratio in the above equation is usually defined as the cell constant.

$$N = \frac{V_1 + V_2}{V_1} \tag{II-8}$$

Then Eq. (II-7) is written as follows,

$$\frac{P_{j-1}}{P_j} = N \frac{z_{j-1}}{z_j} \tag{II-9}$$

Another relationship can be developed by solving Eq. (II-3) for P_1 and substituting into Eq. (II-6):

$$z_2 = N^2 \frac{z_o}{P_o} P_2 \qquad \text{(II-10)}$$

Compressibility factors after the first and second expansion are given by Eqs. (II-3) and (II-10), respectively. Similarly, the compressibility factor after the j^{th} expansion can be expressed as,

$$z_j = N^j \frac{z_o}{P_o} P_j \qquad \text{(II-11)}$$

The cell constant is defined using Eq. (II-9) and using the definition of the compressibility factor at zero pressure (z = 1).

$$\underset{P_j \longrightarrow 0}{\text{Limit}} \frac{P_{j-1}}{P_j} = N \qquad \text{(II-12)}$$

The cell constant is usually evaluated by plotting the ratio of the pressure before the j^{th} expansion to the pressure after the j^{th} expansion (P_{j-1}/P_j) versus the pressure after the j^{th} expansion (P_j) and extrapolating to zero pressure as illustrated in Figure 2. Also, the extrapolation can be done using least-mean-square curve-fit procedures.

The compressibility factor before the first expansion is defined using Eq. (II-11) by taking the limit as P_j approaches zero.

$$\underset{P_j \longrightarrow 0}{\text{Limit}} N^j P_j = \frac{P_o}{z_o} \qquad \text{(II-13)}$$

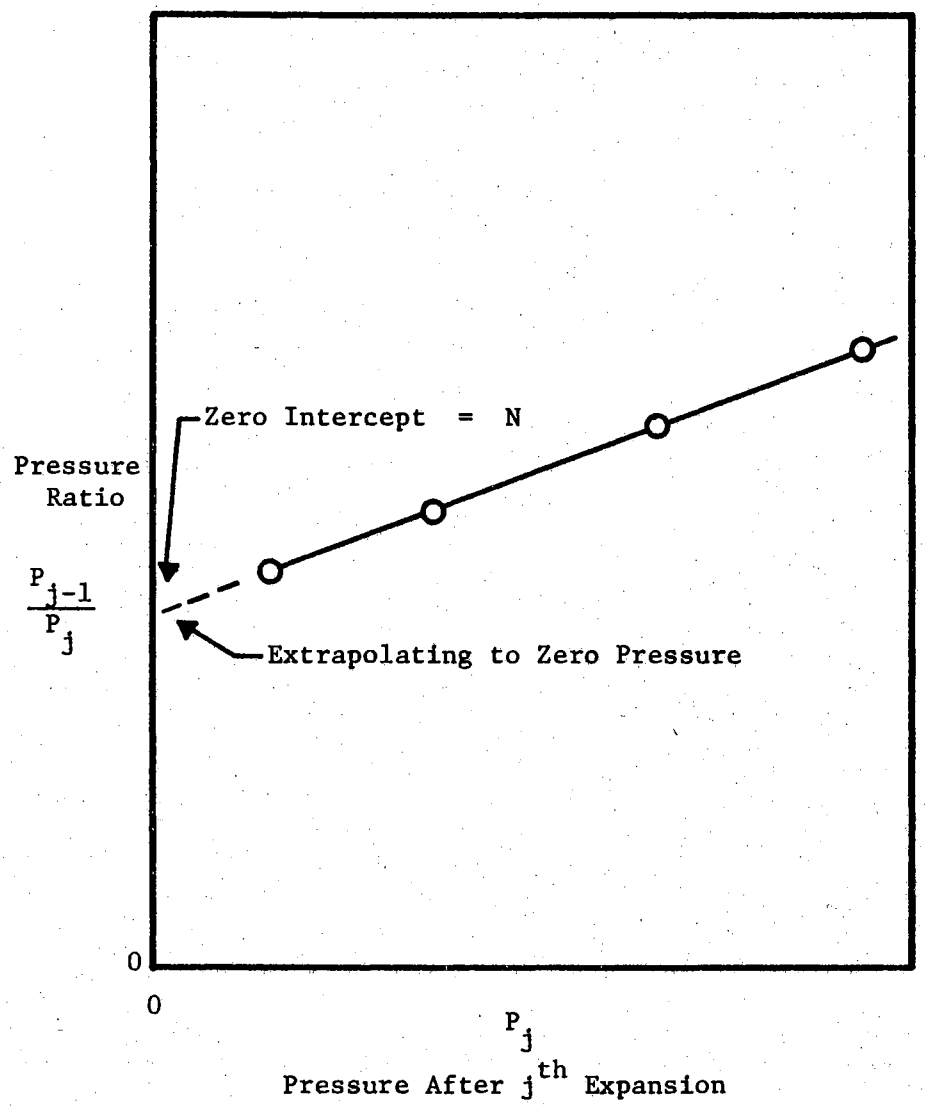

Figure 2. Evaluation of Apparatus Constant, N

The value of P_o/z_o can be calculated graphically by plotting $N^j P_j$ versus P_j and extrapolating to zero pressure as shown in Figure 3 or by curve-fitting.

The equations presented above describing the Burnett method are based on the assumption that the volume of the vessels are not functions of pressure. Vessels which have pressure jackets can fulfill this assumption. Vessels that do have pressure jackets should be treated differently. Canfield (8) has presented relationships for the unjacketed case.

Advantages and Disadvantages

The most commonly used methods for determining compressibility factors involve pressure and temperature measurements of a known mass of a gas in a known volume. Volume measurements can be made accurately at low pressures, but they are more difficult at high pressures. The mass of gas could be determined by weighing in a bomb. Usually the mass of gas is small so that great care must be used to avoid errors.

As shown by the relationships presented for the isothermal expansion method of Burnett, the volume and mass measurements can be eliminated. Only pressure and temperature measurements are required. The expansion method can be used over a wide range of temperatures and pressures. Many of the other methods use mercury or some other liquid which would contaminate the gas sample in the vessel. Canfield et al. (9) reported a maximum error of 0.15% for this method over a wide range of temperatures and pressures.

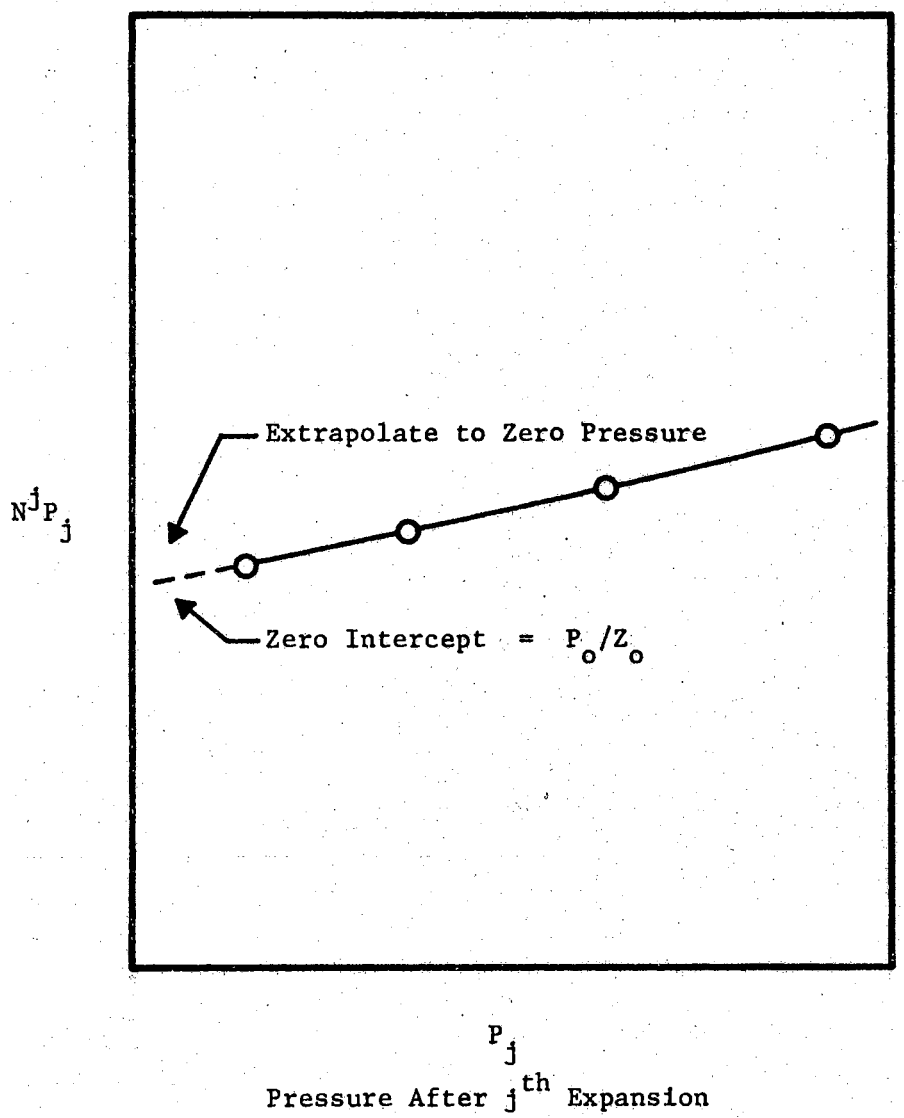

Figure 3. Evaluation of Initial Compressibility Factor

The isothermal expansion method is subject to some disadvantages; namely, it is best suited for measurements above the critical point, and it requires relatively large amounts of gas when compared to other methods.

CHAPTER III

SURVEY OF PREVIOUS WORK

In this chapter, previous work using the isothermal expansion ratio method is reviewed briefly. In addition, a brief review of methods of deriving virial coefficients and of equations of state are presented. For comparison later, compressibility and virial coefficient data for methane and ethylene are reviewed.

Isothermal Expansion Ratio Method

After Burnett (6) introduced the isothermal expansion ratio method in 1936 very little work was reported for several years. The method was briefly mentioned in two Bureau of Mines reports (10,11) in 1940 and 1942. The bulk of the work done using the Burnett method has been done since 1950. Rather, than review each investigator's work, the various investigators who have used the Burnett method are summarized in Table I. The various methods of treating the isothermal expansion ratio data that have been used by various investigators will be presented below.

A large amount of work with the Burnett method has been done by Schneider and his associates (34,35,50,58,59,70,71) at the National Research Council of Canada. Most of their work was done in the temperature range of 0 to 600 °C with pressures to 80 atmospheres on pure component systems. The isothermal pressure ratio data were used to

TABLE I

SUMMARY OF PREVIOUS INVESTIGATIONS USING THE ISOTHERMAL EXPANSION RATIO METHOD OF BURNETT

Temperature Range °C	Pressure Range psia	System	Investigator	Reference
0	to 2,200	Helium	Burnett	(6)
30	to 900	Air		
	to 4,000	Apparatus only	Cattel et al.	(10,11)
26 to 93	to 4,000	Natural gas	Stevens and Vance	(63)
0 to 600	to 1,200	Helium	Schneider	(58)
0 to 600	88-1,200	Helium	Schneider and Duffie	(59)
600 to 1,200	88-900	Helium	Yntema and Schneider	(71)
0 to 600	to 735	Carbon dioxide	MacCormack and Schneider	(34)
0 to 400	to 735	Carbon tetrafluoride	MacCormack and Schneider	(35)
0 to 250	to 735	Sulfur hexafloride		
0 to 600	150-1,200	Argon	Whalley, Lupien, and Schneider	(70)
0 to 700	to 1,200	Neon	Nicholson and Schneider	(50)

TABLE I (Continued)

Temperature Range °C	Pressure Range psia	System	Investigator	Reference
-60 to 30	7-37	Carbon dioxide	Cook	(14)
25	to 1,000	Natural Gas	Bloomer	(5)
30	to 1,800	He, N_2, CO_2, and their binary mixtures	Pfefferle, Goff, and Miller	(54)
30	to 1,800	He and CO_2 mixtures	Harper and Miller	(21)
30	to 1,910	He, N_2, and mixtures	Kramer and Miller	(30)
175 to 475	to 1,500	He - N_2 mixtures	Witonsky and Miller	(69)
50 to 200	to 2,000	Apparatus and data treatment	Silberberg, Kobe, and McKetta	(60)
50 to 200	to 1,000	Isopentane	Silberberg, Kobe, and McKetta	(61)
10 to 250	15-4,600	Sulfur dioxide	Kang et al.	(28)
-30 to 150	15-4,600	Nitrous oxide	Hirth and Kobe	(24)
30 to 200	15-1,000	Neopentane	Heichelheim et al.	(22)
-200 to 50	to 7,000	Methane - H_2 mixtures	Mueller	(48)

TABLE I (Continued)

Temperature Range °C	Pressure Range psia	System	Investigator	Reference
-128 to 10	to 7,000	Methane - H_2 mixtures	Mueller, Leland, and Kobayashi	(49)
-140 to 0	15-7,400	He - N_2 mixtures	Canfield	(8)
-23 to 54	to 4,000	Helium	Stroud, Miller, and Brandt	(64)
21	to 4,000	He - N_2 mixtures		
-10 to 200		CO_2 - ethylene mixtures	Butcher and Dadson	(7)
200 to 350	to 5,000	Methyl chloride	Suh and Storvick	(65)
		Data Treatment	Hoover, Canfield, Kobayashi, and Leland	(25)
-130 to 0	to 7,350	Nitrogen, Argon, and their mixtures	Crain and Sonntag	(13)
-141 to 0	to 600	Methane, ethane, and their mixtures	Hoover, Nagata, Leland, and Kobayashi	(26)

calculate virial coefficients and compressibility factors by expressing the pressure ratios (P_{j-1}/P_j) in terms of the Berlin virial equation of state (see Appendix L).

$$\frac{P_{j-1}}{P_j} = N + (N-1)\frac{B'}{A'} P_{j-1} + (N-P_j/P_{j-1})\frac{C'}{A'} P_{j-1}^2 + \ldots \quad \text{(III-1)}$$

where the coefficients refer to the Berlin virial equation of state shown below:

$$\underline{PV} = A' + B'P + C' P^2 + \ldots \quad \text{(III-2)}$$

The cell constant N was determined usually using a gas, such as helium, that would give a linear relationship of the pressure ratios with pressure. The other coefficients were evaluated by curve-fitting the pressure ratios using a truncated form of Eq. (III-1).

Another method of treating the isothermal expansion ratios has been used by J. G. Miller and his associates (21,30,54) at the University of Pennsylvania. They expressed the compressibility factor as an exponential function of pressure.

$$z = \exp(\alpha P + \beta P^2 + \ldots) \quad \text{(III-3)}$$

By substituting the above relationship into Eq. (II-11), the following equation was obtained:

$$N^i P_i (z_o/P_o) = \exp(\alpha P_i + \beta P_i + \ldots) \quad \text{(III-4)}$$

By taking the natural logarithm of Eq. (III-4), a linear relationship was derived which related the pressure after the i^{th} expansion to a power series in pressure.

$$\ln P_i = -\ln (z_o/P_o) - i \ln N + \alpha P_i + \beta P_i^2 + \ldots \quad \text{(III-5)}$$

The cell constant N and the compressibility factor z_o were determined by fitting the pressure data using a truncated form of Eq. (III-5) as the model. The regression coefficients (α,β, etc.) were related to the virial coefficients by expanding Eq. (III-3) in a power series in pressure and comparing like terms with the Berlin form of the virial equation of state.

$$z = 1 + \alpha P + (\alpha^2/2 + \beta) P^2 + \ldots \quad \text{(III-6)}$$

Then, the following equations were written:

$$B' = \alpha \quad \text{(III-7)}$$

$$C' = \alpha^2/2 + \beta \quad \text{(III-8)}$$

etc.

A treatment of the isothermal expansion data similar to Schneider's method was described by Butcher and Dadson (7). Butcher and Dadson derived an equation by expressing the pressure ratio (P_{j-1}/P_j) in terms of the Leiden virial equation of state.

$$\frac{N(P_{j-1}-NP_j)}{(N-1)\rho_{j-1}^2} = A\left(B + C\rho_{j-1}\frac{(N+1)}{N} + D\rho_{j-1}^2\frac{(N^2+N+1)}{N^2} + \ldots\right) \qquad \text{(III-9)}$$

where ρ = molar density

and the coefficients (B, C, etc.) refer to the Leiden virial equation of state shown below:

$$P\underline{V} = A\,(1 + B/\underline{V} + C/\underline{V}^2 + D/\underline{V}^3 + \ldots) \qquad \text{(III-10)}$$

The cell constant N was determined from the pressure ratios using Eq. (II-12). The values of the densities (ρ_{j-1}) were related to the density at a pressure of a standard atmosphere and at the temperature T.

$$\rho_j = N^{r-j}\rho_{T,1} \qquad \text{(III-11)}$$

where $\rho_{T,1}$ = density at a standard atmosphere and temperature T.

r = number of expansions to reduce pressure to standard atmosphere.

After evaluating r graphically, Eq. (III-9) was used to derive the virial coefficients.

Canfield (8,9) proposed a method of treating the isothermal expansion data that consisted of using the equations presented previously in Chapter II, Eq. (II-11), (II-12), and (II-13), to establish initial values for the cell constant and the compressibility factors. The value of the cell constant was checked using the following equation

based on the Leiden form of the virial equation of state:

$$(z - 1)\,\underline{V} = B + C/\underline{V} + D/\underline{V}^2 + \ldots \qquad \text{(III-12)}$$

According to Eq. (III-12), a plot of $(z - 1)\underline{V}$ versus $1/\underline{V}$ becomes linear at low pressures. Canfield adjusted the value of the cell constant until the plot of $(z - 1)\underline{V}$ versus $1/\underline{V}$ gave a linear relationship at low pressures. The intercept on this plot is the second virial coefficient. The other virial coefficients were derived graphically using the slope-intercept method (slope-intercept method is described in next section).

Most of the investigators have used one of the methods presented here to treat their isothermal pressure ratio data. Other methods not presented here have been described by Silberg, Kobe, and McKetta (60).

Virial Equation of State

The Leiden form of the virial equation of state is an infinite series in density shown below:

$$z = 1 + B(T)/\underline{V} + C(T)/\underline{V}^2 + D(T)/\underline{V}^3 + \ldots \qquad \text{(III-13)}$$

where the coefficients are functions of temperature only for pure components. The equation is derived from considering the interactions between pairs of particles and higher ordered interactions (23). The virial coefficients in Eq. (III-13) are related to these interactions. The derivation is very complicated and lengthly and will not be presented here.

The other form of the virial equation of state known as the Berlin form is an infinite series in pressure.

$$z = 1 + B'(T)P + C'(T)P^2 + D'(T)P^3 + \ldots \quad \text{(III-14)}$$

where the coefficients are functions of temperature only for pure components. The coefficients of the Berlin equation have been related to the coefficients of the Leiden equation (23).

$$B' = B/RT \quad \text{(III-15)}$$

$$C' = (C - B^2)/(RT)^2 \quad \text{(III-16)}$$

etc.

The Leiden form has two advantages over the Berlin form. The Leiden form of the virial equation of state converges more rapidly than the Berlin form. The Leiden coefficients are directly related to the intermolecular potential function which describes the interactions between molecules. The remainder of this section will deal with the Leiden form of the virial equation of state.

The virial coefficients for the Leiden form can be derived from compressibility data. Rearranging Eq. (III-13) gives the following relationship for the second virial coefficient:

$$\lim_{P \to 0} (z - 1)\underline{V} = B(T) \quad \text{(III-17)}$$

The second coefficient can be determined graphically by plotting $(z - 1)\underline{V}$ versus $1/\underline{V}$ and extrapolating to zero density. The intercept is the second virial coefficient.

The third virial coefficient is derived in a similar manner. The third coefficient can be expressed as follows by further rearranging Eq. (III-13).

$$\lim_{P \longrightarrow 0} \; ((z - 1)\underline{V} - B(T))\underline{V} = C(T) \qquad \text{(III-18)}$$

The third coefficient is the intercept at zero density of a plot of $((z - 1)\underline{V} - B(T))\underline{V}$ versus $1/\underline{V}$. The other coefficients can be derived by carring the procedure further.

This procedure known as the slope-intercept method requires accurate low pressure data. Some investigators have based their derivations on curve-fitting higher density data using Eq. (III-13) as their model. The coefficients derived by curve-fitting depend upon the pressure range of the data as well as the degree of the polynomial used. The slope-intercept method has the advantage over curve-fitting of giving coefficients that are functions of temperature only.

The virial equation of state can be used to describe multi-component mixtures. The coefficients in Eq. (III-13) can be applied to the mixture.

$$z = 1 + B_m(T,x_1,x_2,\ldots,x_n)/\underline{V} + C_m(T,x_1,x_2,\ldots,x_n)/\underline{V}^2 + \ldots \qquad \text{(III-19)}$$

where the coefficients are functions of composition in addition to being functions of temperature. The virial coefficients can be derived from the mixture compressibility data using the slope-intercept method.

$$\lim_{P \longrightarrow 0} (z - 1)\underline{V} = B_m(T,x_1,x_2,\ldots,x_n) \qquad \text{(III-20)}$$

$$\lim_{P \longrightarrow 0} ((z - 1)\underline{V} - B_m)\underline{V} = C_m(T,x_1,x_2,\ldots,x_n) \qquad \text{(III-21)}$$

The mixture virial coefficients have been expressed in terms of the composition and the pure component coefficients for a n-component mixture (23).

$$B_m(T,x_1,x_2,\ldots,x_n) = \sum_i^n \sum_j^n x_i x_j B_{ij}(T) \qquad \text{(III-22)}$$

$$C_m(T,x_1,x_2,\ldots,x_n) = \sum_i^n \sum_j^n \sum_k^n x_i x_j x_k C_{ijk}(T) \qquad \text{(III-23)}$$

where x_i , x_j , x_k = mole fraction of i, j, and k^{th} species in mixture.

for $i = j = k$

B_{ii} = pure component second virial coefficient of species i.

C_{iii} = pure component third virial coefficient of species i.

for $i \neq j \neq k$

B_{ij} = second cross coefficient between species i, j.

C_{ijk} = third cross coefficient between species i, j, k.

for $i = j \neq k$

C_{iik} = third cross coefficient between species, i, i, k.

for $i \neq j = k$

C_{ikk} = third cross coefficient between species i, k, k.

Applying Eqs. (III-22) and (III-23) to a binary mixture gives the following expressions:

$$B_m(T,x_1,x_2) = x_1^2 B_{11}(T) + 2x_1x_2B_{12}(T) + x_2^2B_{22}(T) \qquad \text{(III-24)}$$

$$C_m(T,x_1,x_2) = x_1^3C_{111}(T) + x_2^3C_{222}(T) + 3x_1^2x_2C_{112}(T) + 3x_1x_2^2C_{122}(T) \qquad \text{(III-25)}$$

Note that the mixture coefficients are functions of temperature and composition while the coefficients on the right-hand side of Eqs. (III-22), (III-23), (III-24), and (III-25) are functions of temperature only.

Various empirical schemes of combining pure component second virial coefficients have been used to estimate the value of the cross term and subsequently the binary mixture coefficients. These rules allow estimation of low pressure compressibility factors for mixtures by truncating Eq. (III-13) after the second virial coefficient.

A linear combination of the pure component coefficients gives

$$B_{12} = 1/2(B_{11} + B_{22}) \qquad \text{(III-26)}$$

Applying this rule to Eq. (III-24) reduces the mixture value to

$$B_m = x_1 B_{11} + x_2 B_{22} \qquad \text{(III-27)}$$

The linear-square-root combination yields the following expression:

$$B_{12} = 1/4((B_{11})^{1/2} + (B_{22})^{1/2})^2 \qquad \text{(III-28)}$$

Using this value for B_{12} in Eq. (III-24) gives the mixture second virial coefficient. Eq. (III-24) is not simplified as for the linear combination rule.

The following equation gives the square root combination:

$$B_{12} = (B_{11}B_{22})^{1/2} \qquad \text{(III-29)}$$

Substituting Eq. (III-29) into Eq. (III-24) gives the following relationship for the mixture second virial coefficient:

$$B_m = (x_1 (B_{11})^{1/2} + x_2 (B_{22})^{1/2})^2 \qquad \text{(III-30)}$$

The Lorentz combination is given by the following equation:

$$B_{12} = ((B_{11})^{1/3} + (B_{22})^{1/3})^3/8 \qquad \text{(III-31)}$$

This expression does not result in a simplified equation when substituted into Eq. (III-24).

These combination rules will be checked using the experimental values for methane, ethylene, and four of their mixtures in Chapter VI.

Empirical Equations of State

There have been many empirical equations of state used by various investigators. Rather than reviewing these numerous equations, three of the most important equations were selected for comparing with the experimental data presented in Chapter VI. The three equations are: 1) the Benedict-Webb-Rubin (BWR) equation, 2) the Edmister-Vairogs-Klekers generalized BWR equation (GBWR), and 3) the Redlich-Kwong (RK) equation.

BWR Equation

The BWR equation (4) relates either the pressure or the compressibility factor to temperature and specific volume using eight constants. The equation for pressure is

$$P = RT/\underline{V} + (B_oRT - A_o - C_o/T^2)/\underline{V}^2 + (bRT - a)/\underline{V}^3 + a\alpha/\underline{V}^6$$

$$+ (c/\underline{V}^3)((1 + \gamma/\underline{V}^2)/T^2)\exp(- \gamma/\underline{V}^2) \qquad \text{(III-32)}$$

For the compressibility factor the equation is written as

$$z = 1 + (B_o - A_o/(RT) - C_o/(RT^3))/\underline{V} + (b - a/(RT))/\underline{V}^2$$

$$+ a\alpha/(RT\underline{V}^5) + c/(RT^3\underline{V}^2)(1 + \gamma/\underline{V}^2)\exp(- \gamma/\underline{V}^2) \qquad \text{(III-33)}$$

The constants appearing in the BWR equation are evaluated for specific compounds from PVT, critical, and vapor pressure data. The equation has been used primarily to describe data for hydrocarbons and their mixtures. The equation works well up to about twice the critical density ($1/V_c$).

The BWR equation is applied to mixtures by using a set of rules combining the pure component constants. The combination rules are described by the following equations:

$$B_{om} = \sum_i^n x_i B_{oi} \quad \text{(Linear)}$$

$$B_{om} = \sum_i^n \sum_j^n x_i x_j \left((B_{oi})^{1/3} + (B_{oj})^{1/3} \right)^3/8 \quad \text{(Lorentz)}$$

$$A_{om} = \left(\sum_i^n x_i (A_{oi})^{1/2} \right)^2$$

$$C_{om} = \left(\sum_i^n x_i (C_{oi})^{1/2} \right)^2 \qquad \text{(III-34)}$$

$$b_m = \left(\sum_i^n x_i (b_i)^{1/3} \right)^3$$

$$c_m = \left(\sum_i^n x_i (c_i)^{1/3} \right)^3$$

$$a_m = \left(\sum_i^n x_i (a_i)^{1/3} \right)^3$$

$$\gamma_m = \left(\sum_i^n x_i (\gamma_i)^{1/2} \right)^2$$

$$\alpha_m = \left(\sum_i^n x_i (\alpha_i)^{1/3} \right)^3 \qquad \text{(III-34)}$$

The subscript m refers to the constants for the n-component mixture and the i or j refers to the pure component constants. The linear or Lorentz combination has been used frequently for B_{om}. These rules should be regarded as being empirical even though they are based on fundamental considerations.

The BWR equation can be expressed as an infinite series in density $(1/\underline{V})$ to obtain a form similar to the Leiden virial equation of state. This form is derived by expressing the exponential term in an infinite series and rearranging terms.

$$z = 1 + \left(B_o - A_o/(RT) - C_o/(RT^3) \right)/\underline{V} + \left(b - a/(RT) + c/(RT^3) \right)/\underline{V}^2$$

$$+ a\alpha/(RT\underline{V}^5) - c\gamma^2/(2RT^3\,\underline{V}^6) + \ldots \qquad \text{(III-35)}$$

Expressions for the second and third virial coefficients in terms of the BWR constants are obtained by comparing the coefficients of like terms of density in the above equation to the Leiden equation, Eq. (III-13).

$$B(T) = B_o - A_o/(RT) - C_o/(RT^3) \qquad \text{(III-36)}$$

$$C(T) = b - a/(RT) + c/(RT^3) \qquad \text{(III-37)}$$

Notice that the BWR equation does not have any density terms with powers between two and five.

The Edmister-Vairogs-Klekers Generalized BWR Equation

The eight constants in the BWR equation were generalized in terms of the accentric factor, Eq. (III-41), by Edmister, Vairogs, and Klekers (19). The generalized equation is shown below:

$$z = 1 + (B'_o - A'_o/T_r - C'_o/T_r^3)/\underline{V}' + (b' - a'/T_r)/\underline{V}'^2$$

$$+ a'\alpha'/(T_r\underline{V}'^5) + c'/(T_r^3\underline{V}'^2)(1 + \gamma'/\underline{V}'^2)\exp(-\gamma'/\underline{V}/^2) \qquad \text{(III-38)}$$

where $$1/\underline{V}' = RT_c/(P_c\underline{V}) \qquad \text{(III-39)}$$

The generalized constants were determined by plotting the specific constants for the BWR equation versus the accentric factor. The following relationships for the generalized constants were derived from these plots:

$$B'_o = 0.113747 + 0.127349\omega - 0.243280\omega^2$$

$$A'_o = 0.343258 - 0.127521\omega - 0.509131\omega^2 \qquad \text{(III-40)}$$

$$C'_o = 0.098224 + 0.401236\omega - 0,0397267\omega^2$$

$$b' = 0.0275404 + 0.131009\omega - 0.134924\omega^2$$

$$a' = 0.0235866 + 0.290284\omega - 0.295413\omega^2$$

$$c' = 0.035694 + 0.185297\omega - 0.230125\omega^2 \qquad \text{(III-40)}$$

$$\alpha'a' = 0.0000875$$

$$\gamma' = 0.052058 - 0.09064\omega + 0.10506\omega^2$$

where $$\omega = -(\log P_r^o + 1.00) \qquad \text{(III-41)}$$

P_r^o = reduced vapor pressure at $T_r = 0.7$.

The specific constants are related to the generalized constants by the following equations:

$$B_{oi} = B_o' RT_{ci}/P_{ci}$$

$$A_{oi} = A_o' R^2T_{ci}^2/P_{ci}$$

$$C_{oi} = C_o' R^2T_{ci}^4/P_{ci} \qquad \text{(III-42)}$$

$$b_i = b' R^2T_{ci}^2/P_{ci}^2$$

$$a_i = a'R^3T_{ci}^3/P_{ci}^2$$

$$\alpha_i = \alpha'R^3T_{ci}^3/P_{ci}^3$$

$$c_i = c' R^3 T_{ci}^5 / P_{ci}^2$$

$$\gamma_i = \gamma' R^2 T_{ci}^2 / P_{ci}^2$$

Since the generalized constants were evaluated in terms of the specific constants, the combination rules, Eq. (III-34), still apply as well as the equations for the second and third virial coefficients, Eq. (III-36) and (III-37) respectively.

The RK Equation

The RK equation of state (18) is a two constant equation expressing pressure as a function of specific volume and temperature.

$$P = RT/(\underline{V} - b) - a/(T^{1/2}\underline{V}(\underline{V} + b)) \qquad \text{(III-43)}$$

The constants are expressed in terms of the critical pressure and temperature.

$$a = 0.4278\, R^2 T_c^{2.5} / P_c$$

$$b = 0.0876\, R\, T_c / P_c \qquad \text{(III-44)}$$

The RK equation is usually applied above the critical temperature.

The RK equation can be rearranged to give the compressibility factor in terms of the specific volume and temperature.

$$z = \underline{V}/(\underline{V} - b) + a/(RT^{1.5}(\underline{V} + b)) \qquad \text{(III-45)}$$

The RK equation may be applied to mixtures using the following combination rules for a and b:

$$(a_m)^{1/2} = \sum_i^n x_i (a_i)^{1/2}$$

$$b_m = \sum_i^n x_i b_i \qquad \text{(III-46)}$$

The RK equation is written in the form of the Leiden virial equation of state by rearranging Eq. (III-45) as follows:

$$z = 1/(1 - b/\underline{V}) + a/(RT^{1.5}\underline{V}(1 + b/\underline{V})) \qquad \text{(III-47)}$$

Then, the terms $(1 - b/\underline{V})$ and $(1 + b/\underline{V})$ are expanded in infinite series to give the following expression:

$$z = 1 + (b - a/(RT^{1.5}))/\underline{V} + (b^2 - ab/(RT^{1.5}))/\underline{V}^2 + (b^3 - ab^2/(RT^{1.5}))/\underline{V}^3 + \ldots \qquad \text{(III-48)}$$

Comparing the like terms of Eq. (III-13) with Eq. (III-48) gives the virial coefficients in terms of the RK equation constants.

$$B(T) = b - a/(RT^{1.5}) \qquad \text{(III-49)}$$

$$C(T) = b^2 + ab/(RT^{1.5}) \qquad \text{(III-50)}$$

The equations of state presented will not be discussed further at this point. Several publications are available in the literature discussing the application of equations of state.

Methane and Ethylene PVT Data

The volumetric properties of methane have been studied by many investigators. Amagat (1) reported volumetric data in 1881 and Vennix (66) in 1966. Most of the data cover the temperature range from ambient to 350 °C. Some work has been done below ambient. Mueller (48,49), Vennix (66), and Pavlovich and Timrot (53) have reported data below the critical temperature. McMath (38) presented a summary of methane PVT data covering a temperature range of -274 to 650 °F and pressures to 15,000 psia. The sources and the ranges of the data are summarized in Table II.

Some of the same investigators shown in Table II derived second and third virial coefficients from their volumetric data. Douslin (15) and Mueller (48,49) calculated virial coefficients graphically using the slope-intercept method. Michels and Nederbraght (44) and Schamp et al. (57) used a least-squares fit to the data.

The volumetric properties of ethylene have not been studied as extensively as for methane. Michels et al. (40,41) have reported data for pressures to 45,000 psia and from 32 to 302 °F and derived the virial coefficients. Butcher and Dodson (7) determined the virial coefficients from -10 °C to 200 °C. The sources of ethylene volumetric data covering a temperature range of -140 to 500 °F and pressures to 45,000 psia are summarized in Table III.

TABLE II

SUMMARY OF VOLUMETRIC DATA FOR METHANE

From McMath (38)

Temperature Range °F	Pressure Range psia	Investigator	Reference
57 to 212	575-4,400	Amagat	(1)
32 to 650	220-5,900	Douslin	(15)
36 to 392	250-3,150	Fruth and Verschoyle	(20)
32 to 392	470-3,700	Keyes and Burke	(29)
-94 to 392	300-15,000	Kvalnes and Gaddy	(31)
20 to 77	260-2,600	McMath	(38)
-260 to 500	10-1,500	Matthews and Hurd	(36)
32 to 302	295-1,175	Michels et al.	(43)
32 to 302	270-5,600	Michels et al.	(44)
-200 to 50	40-7,000	Mueller et al.	(48,49)
100 to 460	200-10,000	Olds et al.	(51)
-274 to 140	150-2,800	Pavlovich and Timrot	(53)
32 to 302	295-3,400	Schamp et al.	(57)
-226 to 32	10,000	Vennix	(66)
-141 to 0	0-600	Hoover et al.	(26)

TABLE II

SUMMARY OF VOLUMETRIC DATA FOR METHANE

From McMath (38)

Temperature Range °F	Pressure Range psia	Investigator	Reference
57 to 212	575-4,400	Amagat	(1)
32 to 650	220-5,900	Douslin	(15)
36 to 392	250-3,150	Fruth and Verschoyle	(20)
32 to 392	470-3,700	Keyes and Burke	(29)
-94 to 392	300-15,000	Kvalnes and Gaddy	(31)
20 to 77	260-2,600	McMath	(38)
-260 to 500	10-1,500	Matthews and Hurd	(36)
32 to 302	295-1,175	Michels et al.	(43)
32 to 302	270-5,600	Michels et al.	(44)
-200 to 50	40-7,000	Mueller et al.	(48,49)
100 to 460	200-10,000	Olds et al.	(51)
-274 to 140	150-2,800	Pavlovich and Timrot	(53)
32 to 302	295-3,400	Schamp et al.	(57)
-226 to 32	10,000	Vennix	(66)
-141 to 0	0-600	Hoover et al.	(26)

There are no gas phase PVT data available in the literature for the methane-ethylene system.

CHAPTER IV

EXPERIMENTAL APPARATUS

The description of the isothermal expansion ratio apparatus is presented in this chapter. The apparatus consisted essentially of two vessels in an air thermostat, pressure and temperature measuring apparatus, gas compressor, and auxiliary equipment (Figure 4).

Expansion Cell

The expansion cell consisted of two high pressure, jacketed vessels (bombs) and a differential pressure indicating (DPI) cell connected together as shown in the schematic diagram (Figure 4). The expansion valve and most of the other valves were 1/8-inch, 15,000 psi stainless steel needle valves manufactured by High Pressure Equipment, Inc. (Erie, Pennsylvania). The two bombs were connected to the vacuum system, vent, and gas compressor through needle valves. The oil side of the DPI cell was connected to the oil system of the pressure measuring equipment. The pressure jacket of the two bombs was also connected to the oil system.

The bombs were made of 303 stainless steel in the O.S.U. Research Apparatus Development Laboratory. The bombs were fabricated by welding three pieces together, outer shell, inter bomb, and cap. The assembled bombs shown in cross-section in Figure 5 were cylinders approximately 4 inches in diameter by 10 inches long. The internal volume and jacket

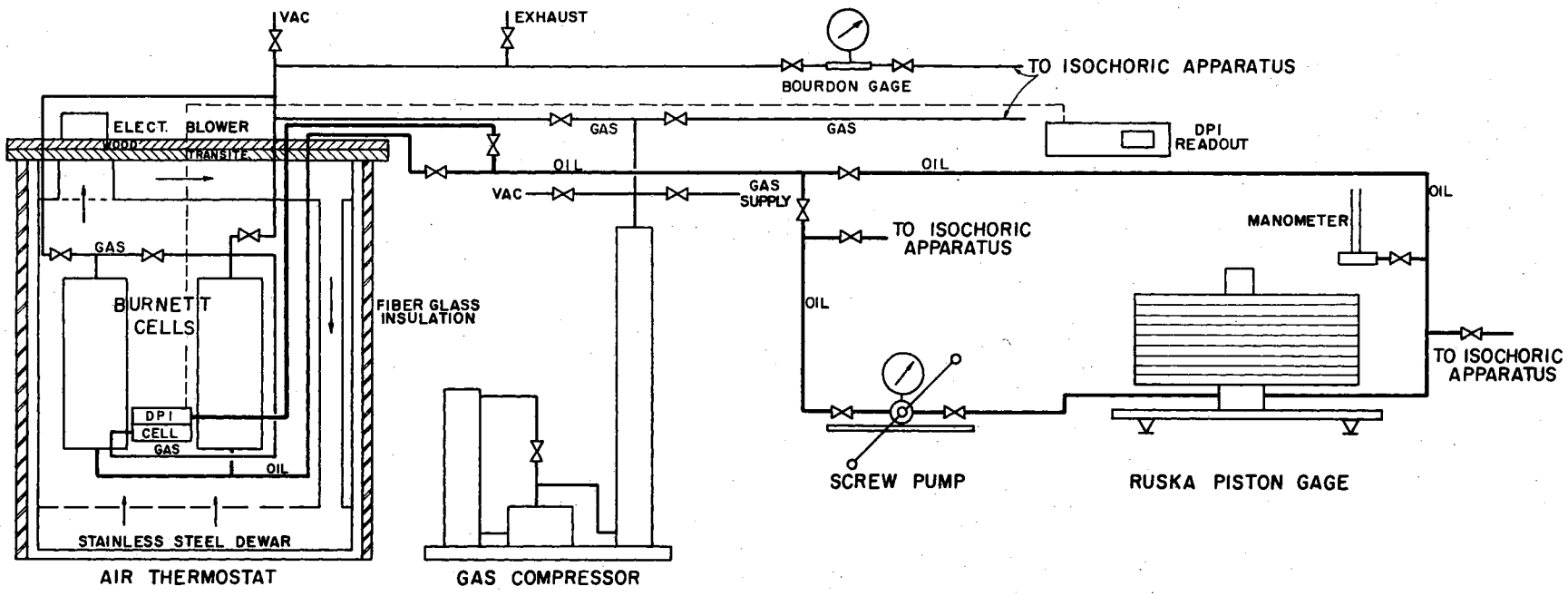

Figure 4. Schematic of Apparatus

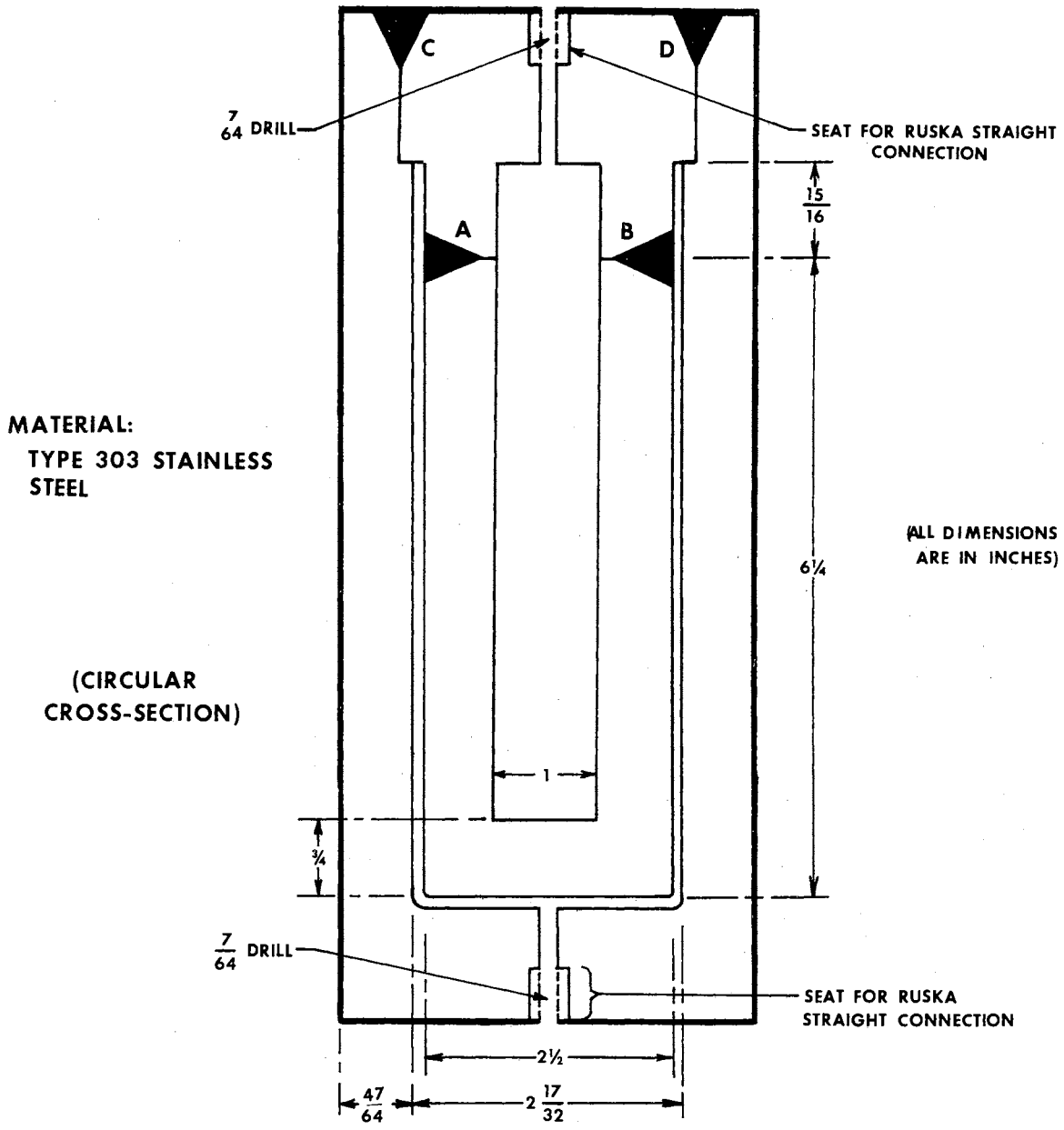

Figure 5. Jacketed Bomb Assembly

were provided with seats for Ruska straight connectors for connecting 1/8-inch tubing. The assembled bombs were pressure tested using oil to 15,000 psi. The geometry of the bombs was such that a jacket pressure 0.8024 of the internal pressure would provide equal total internal and external forces that should minimize volume changes due to pressure distortion (38).

The DPI cell (Cat. No. 2413) was manufactured by Ruska Instrument Corporation of Houston, Texas. The cell is a cylinder with a stainless steel diaphragm separating two internal chambers. The lower chamber was connected to the bombs and the upper chamber to the oil system. A pressure differential between the two chambers deflects the diaphragm. The deflection moves a core relative to a coil in the upper chamber creating an electrical signal. An electric null detector (Ruska Cat. No. 2416) detects the signal and shows the pressure imbalance on a meter.

The DPI cell is capable of operating from 0 to 15,000 psi and can withstand an overpressure in either chamber of 15,000 psi. The DPI cell and null detector can sense a 0.0002 psi pressure differential.

The null detector has a potentiometer for setting the zero point of the indicating meter when the pressure is the same in both chambers. A manometer was placed in the oil system with a reference mark for zeroing the null detector at atmospheric pressure. The zero point changes as pressure is increased in the DPI cell. Ruska provided a calibration curve for zero shift with pressure for ambient temperatures.

Air Thermostat

The air thermostat consisted of a stainless steel dewar containing two baffles, a squirrel cage blower for circulating the air, a cooling coil, electric strip heaters, and a rack for holding the two bombs and DPI cell. The baffles and rack, which were made as a unit, were suspended above the dewar. The dewar was raised to surround the baffles and rack.

The baffles were used to direct the flow of air from the squirrel cage blower, powered by an A.C. synchronous motor located outside the thermostat. The squirrel cage blower was located above the top baffle. The air discharged from the blower passed down a 2-inch tube to the bottom of the dewar. Then, the air passed over a cooling coil (a condenser coil from a refrigeration unit), through a baffle with four 25-watt strip heaters attached, across the two bombs and DPI cell, and through the top baffle to the squirrel cage intake.

A 14-inch square piece of 1/2-inch thick Transite attached to a piece of 3/4-inch plywood served as a lid when the dewar was raised to surround the baffles and rack. A strip of foam rubber provided a seal between the lid and dewar. The tubing and electrical leads were passed through the lid into the air bath. The dewar was covered with a 1-inch layer of Fiberglas. During the 50 and 75 °C runs, the air thermostat was covered with rock wool.

The temperature in the air thermostat was controlled by sub-cooling and supplying heat with controlled heaters. Two of the 250-watt heaters on the bottom baffle served as control heaters; the other two were used as auxiliary heaters. The voltage to the auxiliary heaters was controlled manually using a Powerstat. No sub-cooling was provided in

the air thermostat at 50 and 75 °C. The laboratory served as the heat sink at these two temperatures.

The control heaters were regulated by a temperature control system manufactured by Leeds and Northrup (Philadelphia, Pennsylvania). The temperature control system consisted of a temperature sensing element, a setpoint unit, a D.C. null detector, a current adjusting controller, and a current controlled A.C. power supply (Figure 6). The sensing element was a 100 ohm, platinum resistant thermometer. The platinum element was covered with a ceramic material and epoxy resin. The setpoint unit was a resistance bridge with a range of 20 ohms (25 to 75 °C). The imbalance between the setpoint unit and resistance thermometer was detected and amplified by the D.C. null detector (Cat. No. 9834-2). The null detector had a variable sensitivity range and a meter display of voltage imbalance. The amplified signal was used by the current adjusting controller (Model 60 C.A.T.) to provide an output current between 0 and 5 milliamp. This controller had three modes of control action, proportional, reset, and rate. The output current controlled the A.C. output voltage from the A.C. power supply (Fincor Model No. 1200-2.2-11A). The A.C. output voltage could be varied between zero and 95% of line voltage. The Fincor had two potentiometers for adjusting the upper and lower limits of the output voltage. The output voltage was applied to the control heaters.

For the 25 °C runs, sub-cooling was provided by circulating 18 °C water through the cooling-coil in the bottom of the air thermostat. The temperature of the cooling water was maintained by an auxiliary bath. The auxiliary bath consisted of an insulated container, a temperature controller, two circulating pumps, electric heaters, and a

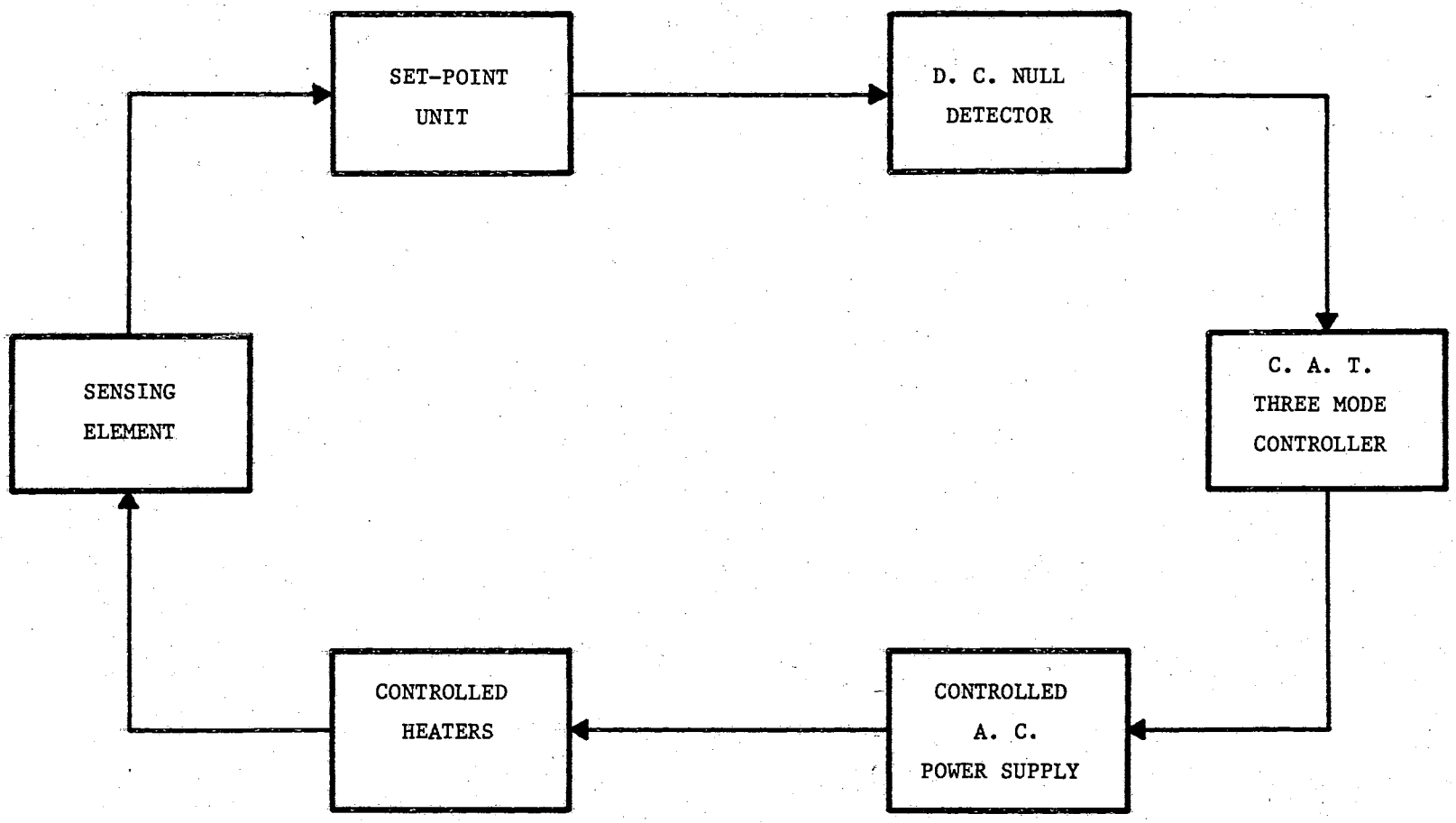

Figure 6. Schematic Diagram of Temperature Control System

Blue M refrigeration unit and insulated tank. One pump circulated water through the air thermostat, and the other through a coil in a tank containing 10 °C water. The temperature in this tank was maintained by the Blue M unit. Make-up heat was supplied to the bath by two knife-blade, 500-watt electric heaters controlled by a thermister, on-off controller. For the 50 and 75 °C runs, the auxiliary bath was not required. The laboratory served as the heat sink.

Pressure Measuring Equipment

The pressure measuring equipment consisted of a dead weight piston gage and screw pump manufactured by Ruska Instrument Corporation of Houston, Texas, and a quartz Bourdon tube gage. The Ruska piston gage is a dual range instrument (low range 6-2428 psig, high range 30-12140 psig). The Ruska gage was calibrated by comparison to a Ruska "plant master" gage which was calibrated by the National Bureau of Standards in Washington, D.C. The low range and high range pistons were reported to be accurate to one part in 10,000 at 25 °C. The effects of temperature and pressure on the piston areas were determined. The specifications and calibrations for the Ruska gage are shown in Appendix A.

A Ruska screw pump was used to generate pressure for the piston gage and oil system. The screw pump and attached Bourdon gage had a maximum working pressure of 15,000 psi. The screw pump came equipped with two Ruska needle valves. The screw pump was connected through one valve to the Ruska piston gage by a 3/16-inch stainless steel tube and through the other valve to the oil system.

The oil system consisted of a series of valves and 1/8-inch stainless steel tubing connecting, the DPI cell, pressure jacket of

the two bombs, screw pump, zeroing manometer for DPI cell, and Ruska piston gage. The valves were arranged so that any component of the system could be isolated. Also, provisions were made for attaching an isochoric PVT apparatus. The oil used in the system was purchased from Ruska.

The quartz Bourdon tube gage manufactured by Texas Instruments Incorporated of Dallas Texas (Model 141), was used as a barometer. The gage was calibrated by Texas Instruments accurate to 0.015% over a pressure range of 0 to 100 cm Hg. The calibration is shown in Appendix B.

Temperature Measuring Equipment

A four lead, platinum resistance thermometer (Leeds and Northrup, Model 8164) was placed in the center of the air thermostat between the two bombs. This thermometer was calibrated by the National Bureau of Standards (the calibration is shown in Appendix C).

A calibrated resistance bridge (see Appendix C) was used for measuring the resistance of the platinum thermometer. The bridge (Model 8069B, Type G-2 Mueller Bridge) was manufactured by Leeds and Northrup. The temperature of the bridge was maintained at 34.9 °C by an on-off controller.

A ballastic galvanometer with lamp and scale, manufactured by Leeds and Northrup, provided the needed sensitivity for the G-2 Mueller bridge. The galvanometer was mounted on a pedestal with a concrete base independent of the foundation and floor of the laboratory building. Using the ballastic galvanometer, the G-2 Mueller bridge is capable of measuring resistances to the nearest 0.0001 ohm.

Auxiliary Equipment

Gas Compressor

A hand-operated gas compressor with a maximum operating pressure of 15,000 psig was used for charging the bombs. The compressor (manufactured by Autoclave Engineers) consisted of a free-piston hone-fitted in a cylinder and hydraulic pump. The piston was fitted with two ring seals to minimize oil leakage. The pump forced oil into the cylinder below the piston compressing the gas above the piston. The gas compressor was connected to the Burnett apparatus and gas storage bottles as shown in Figure 4.

Vacuum System

The vacuum system consisted of a Welch vacuum pump, a diffusion pump, and a tilting McLeod gage. The vacuum system was connected to the Burnett apparatus and gas compressor as shown in Figure 4. The McLeod gage had a range of 0 to 5 mm Hg.

CHAPTER V

EXPERIMENTAL PROCEDURE

In this chapter, the procedures used in obtaining the experimental data are described. This description includes preliminary procedures, checking ice point resistance of the platinum thermometer and adjusting the temperature controller; preparations for a run, zeroing DPI cell and charging bombs with a gas sample; and the methods used in obtaining a data point. At the end of this chapter, some of the difficulties encountered during the experimental work are discussed.

Checking Ice Point Resistance

The resistance of the platinum thermometer at the ice point should be checked periodically, since the resistance can change with use. The resistance was checked by submersing the thermometer in an ice bath prepared by freezing distilled water with liquid nitrogen (see Appendix E for details). Ten measurements of the resistance were made during a 24 hr. period. The ice point resistances were corrected for barometric pressure and the submersion depth of the platinum thermometer. The results are shown in Appendix E.

Setting Temperature of Air Thermostat

The settings of the three modes of control (proportional band, rate, and reset) and the sensitivity of the D.C. null detector that would give the best control at the desired temperature were achieved by using the procedure outlined in this section.

The proportional band was adjusted starting with a wide band, with rate mode of zero and with reset of 0.03. The proportional band width was decreased by steps until an optimum value was attained. The proportional band should be made as small as possible. A too narrow band will cause the controller to "hunt". A proportional band of 40% was used for 25 °C. At 50 and 75 °C, the proportional band was 20% (the auxiliary bath was not used at 50 and 75 °C).

The proper value for the reset mode was determined by increasing it in steps. The reset (repeats/minute) should be made as large as possible. The proper value of reset should bring the temperature of the air thermostat back to the set point overshooting only one or two times after a small upset. The temperature will continually overshoot the setpoint if the reset is too large. The reset was 0.1 repeats/minute at 25 °C and 0.06 repeats/minute at 50 and 75 °C.

The proper value of the rate mode was determined by starting with a low value and increasing it by steps. If the rate mode causes the controlled variable to increase its oscillation about the setpoint, the rate mode should not be used. The rate mode was not used during this work.

Preparations for a Run

A run consisted of zeroing the DPI cell, charging bombs with a gas sample, and making the isothermal expansions. Three runs were made at each temperature (25, 50, and 75 °C) for each of the gases (two pure and four mixtures). An additional run at each isotherm was made for ethylene and the 20-80 methane-ethylene mixture.

Before changing to a different gas, the bombs, gas compressor, and connecting lines were evacuated to 50 microns Hg, flushed with the gas, and re-evacuated to 50 microns Hg.

The DPI cell readout was zeroed before each run. At the conclusion of the previous run, the gas remaining in the bombs was vented to the atmosphere and the pressure in the oil system was released. The Ruska piston gage was isolated from the oil system and the valve connecting the oil manometer to the system was opened. The Ruska screw pump was used to adjust the oil level in the manometer to the reference point. Minor adjustments were made over a two to three hour period allowing the oil system to stabilize. The reference point corresponded to the top of the DPI cell. There was 2 inches of oil above the diaphram of the DPI cell. Thus, the zero point of the cell was made with 2 inches of oil differential pressure across the DPI cell. The 2 inches of oil was accounted for when calculating the pressure of the gas sample.

The zero point changed from run to run. Usually the change was only one turn or less out of ten of the zeroing potentiometer. Also, the zero point was dependent on the temperature of the DPI cell.

The bombs were charged using the hand-operated gas compressor. After evacuating the bombs and gas compressor to 50 microns Hg, bomb V_1 of the expansion cell and gas compressor were filled with gas from the

gas storage bottle. The gas pressure was raised to the desired pressure, indicated by a Bourdon tube gage in the gas charging system. While charging the bomb V_1, the pressure on the oil side of the DPI cell was maintained at least 500 psig above the gas pressure using the Ruska screw pump. The jacket pressure of the bombs was set at approximately 0.8 of the gas pressure. The gas sample was allowed to set overnight before starting the isothermal expansions.

The gas compressor had a large enough volume for two or three charges without refilling.

Isothermal Expansions

The isothermal expansions consisted of making a series of expansions of the gas sample from bomb V_1 into bomb V_2 measuring the gas pressure, barometric pressure, and air thermostat temperature before each expansion.

With the DPI sensitivity set at three-fourths of maximum, a preliminary pressure measurement was made using the Ruska gage. The jacket pressure was set at 0.8024 of the gas pressure using the Ruska gage. The piston and weights were rotated at the preliminary pressure for 15 to 20 minutes to allow the gage to come to equilibrium. At the high pressures, the oil is heated by compression. This heat should be dissipated before making the pressure measurements.

Two pressure measurements were made during a 30 minute period, one with the piston and weights rotating clockwise and the other counterclock wise. The two pressure measurements served as a check for leaks and temperature changes. The barometric pressure, gage

temperature, and room temperature were noted during the pressure measurements.

During the 30 minute period, the temperature of the air thermostat was measured every 5 minutes using the platinum resistance thermometer and Mueller bridge. If the air thermostat was not near the desired temperature (within ±0.01 °C), the setpoint of the controller was reset. After allowing the air thermostat to equilibrate, the pressure measurements were made.

Before the first expansion, the pressure was measured with the expansion valve closed and a 50 micron vacuum in bomb V_2. The remaining pressure measurements before each expansion were made with the expansion valve open, less than 1/8 of a turn.

After the pressure measurements, the expansion valve was closed (except for the first pressure measurement) observing any change in pressure on the DPI readout. The change in volume of the expansion cell caused by closing the expansion valve was not detected by the DPI cell. Bomb V_2 was vented and evacuated to 50 microns Hg while observing the DPI readout for any pressure changes.

The expansion valve was opened slowly until the pressure in bomb V_1 started to decrease as indicated by the DPI readout. The pressure on the oil side of the DPI cell was maintained slightly higher than the gas pressure in bomb V_1. Care was exercised always to over pressure the DPI cell from the oil side. The expansion valve was opened in a series of steps. After allowing part of the gas to expand into bomb V_2, the expansion valve was opened further expanding more of the gas, opening the valve, expanding gas, etc. The steps were repeated until movement of the expansion valve ceased to cause a pressure decrease.

After completing the expansion, the jacket pressure was set approximately 0.8 of the gas pressure as measured by a Bourdon tube gage on the Ruska screw pump.

The gas in the bombs was allowed to reach thermal equilibrium with the air thermostat before making the subsequent pressure measurements. The time allowed for attaining thermal equilibrium after an expansion was determined by monitoring the gas pressure. Eight hours was required after the first expansion, 6 hours after the second, 4 hours after the third, fourth, and fifth, 2 hours after the sixth, and 1 hour for the remaining expansions. These long periods of time after each expansion to attain thermal equilibrium was due to the low heat capacity of air and the slow rate of heat transfer from the air to the bombs. The change in the length of these periods after each expansion was a result of the amount of cooling which occurred during each expansion. The gas sample was cooled less during each expansion as the pressure ratio decreased.

Some Experimental Difficulties

Before the pressure measurements were started, the bombs and gas charging system were pressure-tested to 12,000 psi. A liquid detergent was placed on the connections to detect leaks. This method worked well for relatively large leaks, but it was unsatisfactory for small leaks. The small leaks were eliminated by a trial-and-error procedure, tightening and retightening connections and pressure testing. For the final test, the bombs were filled with gas to 12,000 psi. The pressure was monitored for 8 hours using the Ruska gage. No loss in pressure was observed during this final test.

The most difficult problem encountered during the course of this work was trying to achieve ±0.01 °C or better temperature control in the air thermostat. Several factors were found that had an effect on the temperature control, e.g., blower speed variations, room temperature variations, setpoint stability, auxiliary-bath temperature control, and auxiliary-bath circulating pump variations.

The blower shaft had to be aligned properly to avoid drag which caused blower speed variations. Using a hysteresis motor with a properly aligned blower shaft cured this problem.

An auxiliary constant temperature bath and circulating pump was used during the 25 °C runs to provide cold water as a heat sink for the air thermostat. An induction motor was used to drive the circulating pump eliminating this variation. The auxiliary bath was controlled to ±0.05 °C. This method of providing a heat sink for the air thermostat worked satisfactorily for the 25 °C runs.

The Leeds and Northrup temperature control system (Figure 6) initially used a thermocouple as the sensing element. The original setpoint unit was basically a potentiometer. The difference between the emf from the thermocouple and the setpoint unit provided a measure of the deviation of the thermostat temperature from the setpoint. This differential emf was amplified by the D.C. null detector. The thermocouple and original setpoint unit proved to be unsatisfactory. The setpoint unit was not stable and was very sensitive to fluctuations in room temperature. The cycling of the laboratory air conditioner or opening of the laboratory door would cause a ±0.1 °C change in the setpoint temperature. In addition, the differential emf signal from the setpoint unit was very small, a few mircovolts, requiring maximum

sensitivity of the D.C. null detector. The electronic noise level of the D.C. null detector at maximum sensitivity was approximately a mircovolt and added to the instability of the temperature control system.

The thermocouple sensing element and setpoint unit were replaced by a 100-ohm platinum resistance thermometer and a resistance bridge. The new setpoint unit and sensing element provided an electrical signal much larger than the original setpoint unit and proved to be very stable. Also, the new setpoint unit was not as sensitive to room temperature changes as the old one.

Even with the new setpoint unit, the effects of room temperature changes were not eliminated. Variations in room temperature were reflected in the control of the air thermostat. The temperature of the air conditioned laboratory varied as much as 10 °F. Even opening the laboratory door resulted in an upset of the air thermostat. A constant temperature and controlled access laboratory would help to minimize this problem.

CHAPTER VI

PRESENTATION AND DISCUSSION OF EXPERIMENTAL DATA

In this chapter, the compressibility factors derived from the isothermal expansion data are presented. Compressibility factors were determined for methane, ethylene, and four mixtures (nominal composition of 80-20, 60-40, 40-60, 20-80 mole % methane and ethylene, respectively) at 25, 50, and 75 °C (77, 122, and 167 °F) and pressures to 12,000 psia. Also, compressibility factors for helium at 25, 50, and 75 °C were determined.

The compressibility factors were compared with values from the literature. The second and third virial coefficients for the Leiden form of the virial equation of state were calculated from the compressibility factors using the slope-intercept method adapted to a digital computer. The virial coefficients were compared with values from the literature. The virial coefficients as derived by the slope-intercept method were compared with those determined by fitting compressibility factors to the Leiden form of the virial equation of state.

The experimental compressibility factors were compared to the RK, BWR, and Edmister et al. GBWR equations of state. Then, the second and third virial coefficients calculated from the constants for the RK, BWR, and GBWR equations were compared to the experimental values.

The experimental second virial coefficients for methane and ethylene were used to determine the parameters for the 6-12 Lennard-Jones

intermolecular potential function. The experimental mixture data were used to check the combination rules for the Lennard-Jones parameters for calculating the interaction second virial coefficients (B_{12}).

Compressibility Data

The compressibility factors for methane, ethylene, and four of their mixtures are shown in Table IV. Included in Table IV are the experimental data, the temperature and the pressure measurements, and the nominal composition for each gas (see Appendix D for the detail compositions). The compressibility factors for helium are shown in Table V.

The derivation of the compressibility factors from the isothermal expansion data involved calculating the temperature from platinum resistance thermometer readings and the pressures from the Ruska piston gage data and the Texas Instruments barometer. The platinum resistance thermometer readings were used to calculate the corresponding temperatures from the calibration formula, Eq. (C-1) of Appendix C. Since the formula was not explicit in temperature, the calculations were done using an iteration procedure programed for a digital computer (see Appendix F for more details). The pressures were calculated from the Ruska piston gage data (loading on the piston, gage temperature, etc.) as recommended by Ruska and corrected for the zero shift with pressure of the DPI cell and the other appropriate corrections as shown in Appendix F. Barometric pressure was determined from Eq. (B-1) which was derived by curve-fitting the calibration data for the Texas Instruments gage (Appendix B). The calculations for the gage pressure

TABLE IV

COMPRESSIBILITY FACTOR DATA

Experimental Data			Calculated Data		
Temp. °C	Run No.	P psia	Z	$\underline{V}$ ft^3/lb-mole	$1/\underline{V}$ lb-mole/ft^3
			99.0% Methane		
25.00	3	11923.988	1.64216	0.7932	1.2608
		3109.296	0.83210	1.5413	0.6488
		1616.426	0.84059	2.9950	0.3339
		890.810	0.90018	5.8199	0.1718
		480.610	0.94375	11.309	0.0884
		254.139	0.96974	21.975	0.0455
		132.972	0.98596	42.703	0.0234
		68.932	0.99320	82.981	0.0120
		35.590	0.99646	161.25	0.0062
25.00	4	8992.208	1.35563	0.8682	1.1517
		2805.281	0.82181	1.6872	0.5927
		1491.430	0.84901	3.2785	0.3050
		820.342	0.90745	6.3708	0.1570
		441.167	0.94831	12.379	0.0808
		232.776	0.97230	24.056	0.0416
25.00	5	5931.589	1.05584	1.0252	0.9755
		2362.153	0.81706	1.9921	0.5020
		1286.617	0.86479	3.8710	0.2583
		704.404	0.92003	7.5222	0.1329
		376.785	0.95629	14.617	0.0684

TABLE IV (Continued)

Experimental Data			Calculated Data		
Temp. °C	Run No.	P psia	Z	$\underline{V}$ ft^3/lb-mole	$1/\underline{V}$ lb-mole/ft^3
25.00	5	198.069	0.97686	28.404	0.0352
		102.092	0.97842	55.194	0.0181
		53.357	0.99367	107.25	0.0093
		27.532	0.99634	208.41	0.0048
25.01	10	9164.631	1.37110	0.8616	1.1606
		2826.778	0.82170	1.6743	0.5972
		1501.010	0.84795	3.2536	0.3074
		826.092	0.90685	6.3224	0.1582
		444.578	0.94835	12.285	0.0814
		234.605	0.97247	23.873	0.0419
		122.389	0.98583	46.390	0.0216
		63.440	0.99297	90.146	0.0111
		32.760	0.99641	175.17	0.0057
50.00	61	11963.512	1.60088	0.8353	1.1972
		3463.214	0.89793	1.6184	0.6179
		1761.245	0.88481	3.1359	0.3189
		951.438	0.92613	6.0762	0.1646
		508.174	0.95845	11.773	0.0849
		267.560	0.97778	22.811	0.0438
		139.575	0.98831	44.199	0.0226

TABLE IV (Continued)

Experimental Data			Calculated Data		
Temp. °C	Run No.	P psia	Z	$\underline{V}$ ft^3/lb-mole	$1/\underline{V}$ lb-mole/ft^3
50.00	62	8846.949	1.32188	0.9327	1.0722
		3048.801	0.88266	1.8072	0.5534
		1588.284	0.89095	3.5016	0.2856
		857.587	0.93211	6.7846	0.1474
		456.823	0.96206	13.145	0.0761
		240.078	0.97965	25.471	0.0393
		125.126	0.98930	49.353	0.0203
50.00	63	5938.709	1.06768	1.1222	0.8911
		2508.558	0.87385	2.1744	0.4599
		1337.705	0.90290	4.2132	0.2373
		720.368	0.94210	8.1635	0.1225
		382.104	0.96825	15.817	0.0632
		200.238	0.98314	30.648	0.0326
		104.188	0.99118	59.383	0.0168
75.02	44	11843.775	1.55684	0.8840	1.1312
		3724.907	0.94753	1.7108	0.5845
		1867.391	0.91926	3.3107	0.3020
		992.904	0.94588	6.4069	0.1561
		525.466	0.96873	12.398	0.0807
		275.389	0.98249	23.994	0.0417
		143.365	0.98981	46.433	0.0215

TABLE IV (Continued)

Experimental Data			Calculated Data		
Temp. °C	Run No.	P psia	Z	$\underline{V}$ ft^3/lb-mole	$1/\underline{V}$ lb-mole/ft^3
75.02	45	8972.775	1.32142	0.9904	1.0096
		3266.659	0.93098	1.9167	0.5217
		1674.502	0.92353	3.7092	0.2696
		891.108	0.95109	7.1781	0.1393
		470.809	0.97244	13.891	0.0720
		246.423	0.98497	26.882	0.0372
		128.258	0.99209	52.022	0.0192
75.02	46	5962.806	1.08387	1.2225	0.8180
		2606.722	0.91695	2.3658	0.4227
		1368.692	0.93171	4.5782	0.2184
		727.712	0.95865	8.8598	0.1129
		383.242	0.97702	17.145	0.0583
		200.132	0.98735	33.179	0.0301
		104.046	0.99336	64.209	0.0156
			78.8% Methane		
24.99	11	11958.295	1.68028	0.8092	1.2357
		2763.771	0.75408	1.5714	0.6364
		1489.199	0.78900	3.0513	0.3277
		846.072	0.87043	5.9250	0.1688
		464.507	0.92794	11.505	0.0869
		247.867	0.96151	22.340	0.0448
		130.043	0.97955	43.381	0.0231
		67.608	0.98887	84.237	0.0119
		34.953	0.99274	163.57	0.0061

TABLE IV (Continued)

Experimental Data			Calculated Data		
Temp. °C	Run No.	P psia	Z	$\underline{V}$ ft^3/lb-mole	$1/\underline{V}$ lb-mole/ft^3
25.00	12	8860.415	1.35430	0.8803	1.1360
		2516.502	0.74690	1.7094	0.5850
		1387.678	0.79976	3.3192	0.3013
		785.944	0.87956	6.4453	0.1552
		429.578	0.93351	12.515	0.0799
		228.593	0.96459	24.302	0.0411
		119.745	0.98117	47.191	0.0212
		62.216	0.98990	91.635	0.0109
		32.182	0.99428	177.94	0.0056
25.00	13	5958.462	1.04258	1.0077	0.9923
		2197.718	0.74671	1.9568	0.5110
		1239.408	0.81771	3.7997	0.2632
		697.152	0.89313	7.3783	0.1355
		378.584	0.94179	14.327	0.0698
		200.644	0.96922	27.820	0.0359
		104.896	0.98392	54.023	0.0185
		54.438	0.99153	104.90	0.0095
50.00	68	11792.833	1.61922	0.8571	1.1667
		3137.596	0.83388	1.6590	0.6028
		1639.056	0.84317	3.2114	0.3114
		906.546	0.90266	6.2155	0.1609
		490.696	0.94572	12.031	0.0831
		260.143	0.97046	23.287	0.0429
		136.198	0.98345	45.073	0.0222

TABLE IV (Continued)

Experimental Data			Calculated Data		
Temp. °C	Run No.	P psia	Z	$\underline{V}$ $ft^3/lb\text{-}mole$	$1/\underline{V}$ $lb\text{-}mole/ft^3$
50.00	69	8795.817	1.32816	0.9426	1.0609
		2814.943	0.82273	1.8244	0.5481
		1505.039	0.85144	3.5314	0.2832
		830.972	0.90993	6.8353	0.1463
		448.297	0.95017	13.230	0.0756
		237.447	0.97413	25.609	0.0390
		124.133	0.98572	49.568	0.0202
50.00	70	5718.180	1.03061	1.1251	0.8888
		2347.104	0.81882	2.1777	0.4592
		1285.858	0.86829	4.2151	0.2372
		706.227	0.92306	8.1588	0.1226
		378.694	0.95805	15.792	0.0633
		199.561	0.97722	30.567	0.0327
		104.274	0.98834	59.166	0.0169
75.02	47	11991.894	1.60104	0.8979	1.1137
		3477.037	0.89743	1.7358	0.5761
		1774.702	0.88551	3.3557	0.2980
		961.334	0.92730	6.4873	0.1541
		514.382	0.95919	12.541	0.0799
		271.149	0.97748	24.245	0.0412
		141.563	0.98656	46.870	0.0213

TABLE IV (Continued)

Experimental Data			Calculated Data		
Temp. °C	Run No.	P psia	Z	$\underline{V}$ $ft^3/lb\text{-}mole$	$1/\underline{V}$ $lb\text{-}mole/ft^3$
75.01	48	8933.873	1.32776	0.9995	1.0005
		3073.772	0.88314	1.9323	0.5175
		1606.097	0.89208	3.7355	0.2677
		869.554	0.93370	7.2215	0.1385
		464.016	0.96321	13.960	0.0716
		244.345	0.98054	26.988	0.0371
		127.429	0.98857	52.174	0.0192
75.02	49	6056.924	1.07607	1.1948	0.8369
		2546.748	0.87468	2.3098	0.4329
		1361.572	0.90403	4.4654	0.2239
		735.151	0.94362	8.6325	0.1158
		390.607	0.96925	16.688	0.0599
		205.120	0.98397	32.262	0.0310
		106.919	0.99153	62.369	0.0160
			57.2% Methane		
25.00	14	11963.053	1.72144	0.8287	1.2066
		2360.099	0.65945	1.6092	0.6214
		1335.785	0.72476	3.1248	0.3200
		790.976	0.83335	6.0678	0.1648
		443.622	0.90757	11.783	0.0849
		238.835	0.94879	22.879	0.0437
		125.448	0.96770	44.427	0.0225
		64.838	0.97120	86.268	0.0116

TABLE IV (Continued)

Experimental Data			Calculated Data		
Temp. °C	Run No.	P psia	Z	$\underline{V}$ $ft^3/lb\text{-}mole$	$1/\underline{V}$ $lb\text{-}mole/ft^3$
25.00	15	8764.120	1.35676	0.8916	1.1216
		2173.041	0.65323	1.7313	0.5776
		1262.966	0.73722	3.3618	0.2975
		743.873	0.84316	6.5280	0.1532
		415.249	0.91395	12.676	0.0789
		223.299	0.95434	24.614	0.0406
		117.594	0.97590	47.796	0.0209
		61.252	0.98707	92.810	0.0108
25.00	16	6086.609	1.04486	0.9887	1.0115
		1972.015	0.65735	1.9198	0.5209
		1168.436	0.75631	3.7279	0.2682
		681.768	0.85691	7.2388	0.1381
		377.887	0.92228	14.056	0.0711
		202.353	0.95900	27.294	0.0366
		102.339	0.94179	53.000	0.0189
		55.330	0.98873	102.92	0.0097
50.00	71	11829.056	1.63883	0.8648	1.1563
		2774.326	0.74524	1.6768	0.5964
		1504.353	0.78351	3.2511	0.3076
		858.775	0.86722	6.3035	0.1586
		472.775	0.92611	12.222	0.0818
		252.944	0.96025	23.697	0.0422
		132.945	0.97856	45.946	0.0218

TABLE IV (Continued)

Experimental Data			Calculated Data		
Temp. °C	Run No.	P psia	Z	$\underline{V}$ ft^3/lb-mole	$1/\underline{V}$ lb-mole/ft^3
50.00	72	8721.667	1.31711	0.9427	1.0608
		2525.071	0.73935	1.8277	0.5471
		1400.905	0.79532	3.5438	0.2822
		796.568	0.87682	6.8710	0.1455
		436.657	0.93193	13.322	0.0751
		233.191	0.96496	25.830	0.0387
		122.623	0.98384	50.083	0.0200
50.00	73	5736.129	1.00185	1.0902	0.9172
		2185.909	0.74024	2.1139	0.4731
		1240.546	0.81453	4.0986	0.2440
		700.215	0.89142	7.9467	0.1258
		381.093	0.94066	15.408	0.0649
		202.313	0.96824	29.874	0.0335
		105.923	0.98288	57.923	0.0173
75.01	50	11931.076	1.60440	0.9044	1.1058
		3144.515	0.81910	1.7518	0.5708
		1650.334	0.83274	3.3935	0.2947
		916.623	0.89594	6.5735	0.1521
		497.431	0.94183	12.734	0.0785
		264.105	0.96866	24.666	0.0405
		138.371	0.98308	47.781	0.0209

TABLE IV (Continued)

Experimental Data			Calculated Data		
Temp. °C	Run No.	P psia	Z	$\underline{V}$ ft^3/lb-mole	$1/\underline{V}$ lb-mole/ft^3
75.01	51	8910.900	1.31543	0.9928	1.0073
		2829.470	0.80910	1.9231	0.5200
		1519.409	0.84164	3.7252	0.2684
		842.145	0.90363	7.2162	0.1386
		455.388	0.94653	13.978	0.0715
		241.209	0.97118	27.078	0.0369
		126.335	0.98533	52.452	0.0191
75.00	52	6012.788	1.03886	1.1619	0.8606
		2407.190	0.80565	2.2508	0.4443
		1322.768	0.85757	4.3600	0.2294
		729.485	0.91612	8.4458	0.1184
		392.181	0.95406	16.360	0.0611
		206.948	0.97522	31.692	0.0316
		108.183	0.98754	61.390	0.0163
			38.4% Methane		
25.00	17	11764.563	1.72791	0.8459	1.1810
		1955.775	0.55796	1.6431	0.6086
		1189.713	0.65927	3.1915	0.3133
		737.574	0.79390	6.1991	0.1613
		423.983	0.88644	12.041	0.0830
		231.381	0.93965	23.389	0.0428
		122.741	0.96820	45.430	0.0220
		64.201	0.98369	88.244	0.0113

TABLE IV (Continued)

Experimental Data			Calculated Data		
Temp. °C	Run No.	P psia	Z	$\underline{V}$ $ft^3/lb\text{-}mole$	$1/\underline{V}$ $lb\text{-}mole/ft^3$
25.00	18	8918.879	1.38610	0.8951	1.1172
		1846.074	0.55728	1.7386	0.5752
		1144.849	0.67129	3.3770	0.2961
		705.753	0.80381	6.5594	0.1525
		403.254	0.89211	12.741	0.0785
		219.371	0.94267	24.748	0.0404
		116.274	0.97051	48.071	0.0208
		60.767	0.98520	93.373	0.0107
25.00	19	5868.987	1.00677	0.9879	1.0122
		1693.070	0.56413	1.9190	0.5211
		1070.448	0.69280	3.7274	0.2683
		652.354	0.82019	7.2401	0.1381
		369.452	0.90225	14.063	0.0711
		199.936	0.94831	27.316	0.0366
		105.721	0.97400	53.059	0.0188
		55.127	0.98652	103.06	0.0097
50.00	74	11821.134	1.65670	0.8748	1.1431
		2421.685	0.65883	1.6982	0.5889
		1374.401	0.72584	3.2966	0.3033
		812.618	0.83307	6.3993	0.1563
		455.889	0.90725	12.422	0.0805
		245.982	0.95025	24.114	0.0415
		130.200	0.97637	46.810	0.0214

TABLE IV (Continued)

Experimental Data			Calculated Data		
Temp. °C	Run No.	P psia	Z	$\underline{V}$ $ft^3/lb\text{-}mole$	$1/\underline{V}$ $lb\text{-}mole/ft^3$
50.00	75	8901.203	1.33764	0.9381	1.0660
		2249.571	0.65624	1.8210	0.5492
		1303.366	0.73807	3.53807	0.2829
		766.600	0.84270	6.8619	0.1457
		427.879	0.91305	13.320	0.0751
		230.156	0.95338	25.857	0.0387
		121.269	0.97513	50.194	0.0199
50.01	76	5843.055	0.99260	1.0604	0.9430
		2002.557	0.66037	2.0585	0.4858
		1185.764	0.75906	3.9959	0.2502
		690.819	0.85844	7.7569	0.1289
		382.411	0.92246	15.058	0.0664
		205.197	0.96085	29.230	0.0342
		108.205	0.98356	56.741	0.0176
75.01	53	11998.476	1.63012	0.9137	1.0945
		2830.143	0.74540	1.7713	0.5646
		1534.264	0.78338	3.4338	0.2912
		875.862	0.86695	6.6568	0.1502
		482.517	0.92589	12.905	0.0775
		258.132	0.96023	25.017	0.0400
		135.893	0.97999	48.499	0.0206

TABLE IV (Continued)

Experimental Data			Calculated Data		
Temp. °C	Run No.	P psia	Z	$\underline{V}$ $ft^3/lb\text{-}mole$	$1/\underline{V}$ $lb\text{-}mole/ft^3$
75.01	54	8928.785	1.31883	0.9934	1.0067
		2580.997	0.73905	1.9257	0.5193
		1431.200	0.79446	3.7332	0.2679
		814.058	0.87603	7.2372	0.1382
		446.464	0.93140	14.030	0.0713
		238.165	0.96320	27.199	0.0368
		125.020	0.98018	52.727	0.0190
75.01	55	5977.800	1.01416	1.1410	0.8764
		2249.283	0.73977	2.2119	0.4521
		1275.179	0.81304	4.2880	0.2332
		720.162	0.89014	8.3126	0.1203
		392.228	0.93985	16.115	0.0621
		208.346	0.96782	31.240	0.0320
		109.122	0.98267	60.562	0.0165
			18.4% Methane		
25.00	20	11817.669	1.75251	0.8541	1.1708
		1509.396	0.43552	1.6618	0.6018
		1026.253	0.57615	3.2334	0.3093
		680.590	0.74343	6.2911	0.1590
		403.531	0.85765	12.241	0.0817
		223.449	0.92403	23.817	0.0420
		119.359	0.96037	46.340	0.0216
		62.677	0.98123	90.164	0.0111

TABLE IV (Continued)

Experimental Data			Calculated Data		
Temp. °C	Run No.	P psia	Z	$\underline{V}$ ft^3/lb-mole	$1/\underline{V}$ lb-mole/ft^3
25.01	21	8876.317	1.39174	0.9030	1.1074
		1446.426	0.44110	1.7564	0.5694
		998.388	0.59219	3.4162	0.2927
		655.320	0.75603	6.6444	0.1505
		385.729	0.86554	12.923	0.0774
		212.742	0.92849	25.136	0.0398
		113.587	0.96421	48.890	0.0205
		59.599	0.98401	95.090	0.0105
25.01	22	5933.063	1.00438	0.9750	1.0257
		1367.377	0.45039	1.8970	0.5271
		956.220	0.61282	3.6910	0.2709
		618.626	0.77139	7.1816	0.1392
		360.462	0.87455	13.973	0.0716
		197.728	0.93340	27.188	0.0368
		105.093	0.96527	52.900	0.0189
		54.992	0.98276	102.93	0.0097
25.00	23	2894.576	0.58434	1.1626	0.8601
		1233.868	0.48465	2.2622	0.4421
		862.717	0.65933	4.4015	0.2272
		540.493	0.80371	8.5640	0.1168
		308.773	0.89336	16.663	0.0600
		167.615	0.94357	32.421	0.0308
		88.679	0.97131	63.082	0.0158

TABLE IV (Continued)

Experimental Data			Calculated Data		
Temp. °C	Run No.	P psia	Z	$\underline{V}$ $ft^3/lb\text{-}mole$	$1/\underline{V}$ $lb\text{-}mole/ft^3$
50.00	77	11720.820	1.66823	0.8884	1.1256
		2005.647	0.55503	1.7274	0.5789
		1221.971	0.65748	3.3586	0.2977
		757.549	0.79250	6.5301	0.1531
		435.012	0.88481	12.696	0.0788
		237.259	0.93829	24.686	0.0405
		126.177	0.97019	47.996	0.0208
50.00	78	8949.172	1.34952	0.9413	1.0624
		1896.242	0.55597	1.8302	0.5464
		1176.042	0.67042	3.5584	0.2810
		723.956	0.80241	6.9186	0.1445
		413.350	0.89077	13.452	0.0743
		224.740	0.94166	26.154	0.0382
		119.008	0.96951	50.852	0.0197
50.01	79	5803.481	0.97207	1.0456	0.9564
		1732.272	0.56414	2.0329	0.4919
		1095.235	0.69349	3.9525	0.2530
		665.879	0.81977	7.6849	0.1301
		376.562	0.90136	14.942	0.0669
		203.627	0.94767	29.051	0.0344
		107.492	0.97266	56.484	0.0177

TABLE IV (Continued)

Experimental Data			Calculated Data		
Temp. °C	Run No.	P psia	Z	$\underline{V}$ $ft^3/lb\text{-}mole$	$1/\underline{V}$ $lb\text{-}mole/ft^3$
50.00	80	2866.280	0.61757	1.3449	0.7435
		1444.130	0.60497	2.6150	0.3824
		916.016	0.74610	5.0843	0.1967
		540.335	0.85569	9.8853	0.1012
		299.478	0.92211	19.220	0.0520
		160.164	0.95884	37.370	0.0268
		84.341	0.98171	72.658	0.0138
75.02	36	11607.333	1.61803	0.9375	1.0667
		2424.357	0.65593	1.8196	0.5496
		1384.376	0.72697	3.5317	0.2832
		818.485	0.83421	6.8547	0.1459
		459.023	0.90803	13.304	0.0752
		247.663	0.95090	25.822	0.0387
		130.715	0.97409	50.118	0.0200
		68.224	0.98677	97.274	0.0103
75.02	37	8953.383	1.33087	0.9997	1.0003
		2269.948	0.65489	1.9403	0.5154
		1348.992	0.75538	3.7660	0.2655
		775.808	0.84316	7.3094	0.1368
		433.004	0.91338	14.187	0.0705
		232.974	0.95383	27.535	0.0363
		122.773	0.97559	53.443	0.0187

TABLE IV (Continued)

Experimental Data			Calculated Data		
Temp. °C	Run No.	P psia	Z	$\underline{V}$ ft^3/lb-mole	$1/\underline{V}$ lb-mole/ft^3
75.02	38	5708.660	0.96797	1.1404	0.8769
		2006.552	0.66036	2.2133	0.4518
		1191.905	0.76134	4.2960	0.2328
		693.866	0.86023	8.3380	0.1199
		383.882	0.92372	16.183	0.0618
		205.467	0.95959	31.410	0.0318
		107.983	0.97882	60.964	0.0164
75.02	39	2962.640	0.68315	1.5508	0.6448
		1564.158	0.70003	3.0100	0.3322
		933.498	0.81088	5.8420	0.1712
		529.930	0.89343	11.399	0.0882
		288.083	0.94268	22.007	0.0454
		152.681	0.96970	42.714	0.0234
		79.845	0.98424	82.904	0.0121
			99.9% Ethylene		
25.00	6	11858.506	1.77797	0.8635	1.1581
		1091.035	0.31892	1.6834	0.5940
		870.467	0.49606	3.2821	0.3047
		623.854	0.69313	6.3987	0.1563
		382.474	0.82847	12.475	0.0802
		215.040	0.90812	24.321	0.0411
		115.714	0.95269	47.416	0.0211
		60.867	0.97701	92.443	0.0108
		31.699	0.99199	180.23	0.0055

TABLE IV (Continued)

Experimental Data			Calculated Data		
Temp. °C	Run No.	P psia	Z	$\underline{V}$ $ft^3/lb\text{-}mole$	$1/\underline{V}$ $lb\text{-}mole/ft^3$
25.00	7	8832.565	1.38200	0.9011	1.1097
		1064.389	0.32469	1.7568	0.5692
		856.693	0.50949	3.4251	0.2920
		606.616	0.70335	6.6776	0.1498
		369.174	0.83452	13.019	0.0768
		206.808	0.91142	25.381	0.0394
		111.073	0.95435	49.483	0.0202
		58.398	0.97823	96.473	0.0104
		30.373	0.99192	188.08	0.0053
25.00	8	5933.975	0.99100	0.9618	1.0397
		1034.292	0.33676	1.8752	0.5333
		836.047	0.53070	3.6558	0.2735
		581.367	0.71947	7.1274	0.1403
		349.878	0.84417	13.896	0.0720
		194.887	0.91673	27.091	0.0369
		104.373	0.95717	52.816	0.0189
		54.814	0.98003	102.97	0.0097
		28.496	0.99328	200.75	0.0050
25.00	9	2991.405	0.56840	1.0943	0.9138
		991.945	0.36746	2.1335	0.4687
		792.281	0.57220	4.1595	0.2404
		532.844	0.75027	8.1093	0.1233
		314.715	0.86395	15.810	0.0633

TABLE IV (Continued)

Experimental Data			Calculated Data		
Temp. °C	Run No.	P psia	Z	V ft^3/lb-mole	1/V lb-mole/ft^3
		173.611	0.92915	30.823	0.0324
		92.578	0.96596	60.093	0.0166
		48.511	0.98683	117.16	0.0085
50.00	64	11836.604	1.69633	0.8946	1.1178
		1615.373	0.45155	1.7449	0.5731
		1079.404	0.58852	3.4034	0.2938
		706.116	0.75092	6.6383	0.1506
		415.704	0.86228	12.948	0.0772
		229.335	0.92786	25.255	0.0396
		122.225	0.96453	49.260	0.0203
50.00	65	8922.033	1.34595	0.9417	1.0619
		1544.856	0.45457	1.8367	0.5444
		1049.123	0.60212	3.5826	0.2791
		679.997	0.76122	6.9878	0.1431
		397.730	0.86844	13.630	0.0734
		218.670	0.93129	26.584	0.0376
		116.362	0.96661	51.853	0.0193
50.00	66	5749.098	0.94867	1.0300	0.9703
		1448.005	0.46605	2.0091	0.4977
		996.823	0.62578	3.9187	0.2552
		635.957	0.77872	7.6435	0.1308
		367.959	0.87882	14.909	0.0671
		201.110	0.93687	29.079	0.0344
		107.034	0.97255	56.719	0.0176

TABLE IV (Continued)

Experimental Data			Calculated Data		
Temp. °C	Run No.	P psia	Z	$\underline{V}$ $ft^3/lb\text{-}mole$	$1/\underline{V}$ $lb\text{-}mole/ft^3$
50.00	67	2870.147	0.56974	1.2391	0.8070
		1296.717	0.50207	2.4169	0.4138
		890.282	0.67234	4.7141	0.2121
		550.570	0.81100	9.1948	0.1088
		312.405	0.89758	17.935	0.0558
		168.976	0.94695	34.981	0.0286
		89.408	0.97728	68.231	0.0147
75.02	40	11750.645	1.65200	0.9455	1.0576
		2075.015	0.56667	1.8366	0.5445
		1258.918	0.66783	3.5677	0.2803
		775.367	0.79898	6.9302	0.1443
		443.869	0.88848	13.462	0.0743
		241.871	0.94045	26.150	0.0382
		128.266	0.96878	50.796	0.0197
75.02	41	8782.963	1.31405	1.0062	0.9938
		1952.500	0.56744	1.9546	0.5116
		1206.355	0.68103	3.7968	0.2634
		737.823	0.80911	7.3752	0.1356
		419.921	0.89450	14.326	0.0698
		228.078	0.94376	27.829	0.0359
		120.731	0.97041	54.057	0.0185

TABLE IV (Continued)

Experimental Data			Calculated Data		
Temp. °C	Run No.	P psia	Z	$\underline{V}$ ft^3/lb-mole	$1/\underline{V}$ lb-mole/ft^3
75.02	42	5835.299	0.96578	1.1131	0.8984
		1790.150	0.57553	2.1622	0.4625
		1125.214	0.70270	4.2000	0.2381
		680.209	0.82516	8.1586	0.1226
		383.722	0.90422	15.848	0.0631
		207.355	0.94915	30.785	0.0325
		109.475	0.97341	59.800	0.0167
75.02	43	3020.494	0.63453	1.4128	0.7078
		1504.315	0.61386	2.7444	0.3644
		948.188	0.75160	5.3310	0.1876
		557.636	0.85863	10.356	0.0966
		308.857	0.92379	20.116	0.0497
		165.211	0.95988	39.075	0.0256

TABLE V

COMPRESSIBILITY FACTOR DATA FOR HELIUM

Experimental Data			Calculated Data		
Temp. °C	Run No.	P psia	Z	$\underline{V}$ $ft^3/lb\text{-}mole$	$1/\underline{V}$ $lb\text{-}mole/ft^3$
25.00	24	5264.456	1.16706	1.2768	0.78323
		2514.328	1.08148	2.4772	0.40368
		1247.166	1.04082	4.8064	0.20806
		630.371	1.02071	9.3255	0.10723
		321.638	1.01048	18.094	0.05527
		164.939	1.00540	35.106	0.02848
		84.796	1.00288	68.114	0.01468
25.00	25	5190.713	1.16521	1.2928	0.77349
		2480.986	1.08058	2.5084	0.39866
		1231.224	1.04046	4.8669	0.20547
		622.348	1.02041	9.4430	0.10590
		317.635	1.01047	18.322	0.05458
		162.876	1.00533	35.548	0.02813
		83.744	1.00291	68.973	0.01450
25.00	26	5289.379	1.16782	1.2716	0.78643
		2524.571	1.08147	2.4671	0.40533
		1252.269	1.04083	4.7868	0.20890
		632.920	1.02067	9.2876	0.10767
		322.975	1.01056	18.020	0.05549
		165.605	1.00536	34.964	0.02860
		85.099	1.00238	67.838	0.01474

TABLE V (Continued)

Experimental Data			Calculated Data		
Temp. °C	Run No.	P psia	Z	$\underline{V}$ ft^3/lb-mole	$1/\underline{V}$ lb-mole/ft^3
25.00	27	5258.182	1.16732	1.2786	0.78212
		2511.251	1.08169	2.4808	0.40310
		1245.552	1.04095	4.8132	0.20776
		629.443	1.02066	9.3389	0.10708
		321.222	1.01061	18.120	0.05519
		164.703	1.00539	35.156	0.02844
		84.642	1.00248	68.212	0.01466
25.00	28	5263.354	1.16796	1.2780	0.78248
		2513.434	1.08215	2.4796	0.40329
		1246.697	1.04145	4.8110	0.20786
		630.008	1.02112	9.3346	0.10713
		321.426	1.01081	18.111	0.05521
		164.804	1.00556	35.140	0.02846
		84.704	1.00277	68.181	0.01467
50.00	56	2375.242	1.07031	2.8129	0.35550
		1187.180	1.03543	5.4444	0.18367
		603.047	1.01803	10.538	0.09490
		308.866	1.00921	20.397	0.04903
		158.863	1.00469	39.478	0.02533

TABLE V (Continued)

Experimental Data			Calculated Data		
Temp. °C	Run No.	P psia	Z	$\underline{V}$ $ft^3/lb\text{-}mole$	$1/\underline{V}$ $lb\text{-}mole/ft^3$
50.00	57	2312.248	1.06895	2.8858	0.34652
		1156.466	1.03480	5.5856	0.17903
		587.660	1.01778	10.811	0.09250
		301.029	1.00911	20.925	0.04779
		154.831	1.00459	40.502	0.02469
50.00	58	2155.712	1.06451	3.0825	0.32441
		1080.304	1.03254	5.9662	0.16761
		549.531	1.01660	11.547	0.08660
		281.660	1.00853	22.351	0.04474
		144.911	1.00431	43.262	0.02311
50.00	59	2258.056	1.06745	2.9509	0.33888
		1130.103	1.03403	5.7116	0.17508
		574.467	1.01737	11.055	0.09046
		294.334	1.00892	21.397	0.04673
		151.399	1.00448	41.415	0.02415
50.00	60	2360.303	1.07045	2.8310	0.35323
		1179.617	1.03548	5.4795	0.18250
		599.207	1.01807	10.606	0.09429
		306.898	1.00925	20.528	0.04871
		157.847	1.00471	39.733	0.02517

TABLE V (Continued)

Experimental Data			Calculated Data		
Temp. °C	Run No.	P psia	Z	$\underline{V}$ $ft^3/lb\text{-}mole$	$1/\underline{V}$ $lb\text{-}mole/ft^3$
75.02	30	4615.196	1.13067	1.6476	0.60693
		2247.927	1.06735	3.1933	0.31316
		1120.420	1.03106	6.1890	0.16158
		569.539	1.01579	11.995	0.08337
		291.632	1.00808	23.248	0.04302
		149.803	1.00360	45.056	0.02219
75.01	31	4926.634	1.13293	1.5465	0.64661
		2391.203	1.06573	2.9974	0.33363
		1196.055	1.03314	5.8092	0.17214
		607.341	1.01677	11.259	0.08882
		310.842	1.00857	21.821	0.04583
		159.719	1.00439	42.292	0.02364
75.02	32	5115.142	1.13770	1.4958	0.66852
		2477.527	1.06799	2.8991	0.34493
		1237.976	1.03428	5.6188	0.17797
		628.379	1.01749	10.890	0.09183
		321.507	1.00897	21.106	0.04738
		165.171	1.00461	40.905	0.02445

TABLE V (Continued)

Experimental Data			Calculated Data		
Temp. °C	Run No.	P psia	Z	$\underline{V}$ ft^3/lb-mole	$1/\underline{V}$ lb-mole/ft^3
75.02	33	4891.454	1.13231	1.5568	0.64233
		2374.970	1.06552	3.0173	0.33142
		1188.300	1.03327	5.8479	0.17100
		603.386	1.01686	11.334	0.08823
		308.826	1.00869	21.966	0.04552
		158.669	1.00442	42.573	0.02348
75.02	34	4595.309	1.12350	1.6443	0.60817
		2239.400	1.06113	3.1868	0.31379
		1122.228	1.03062	6.1764	0.16191
		570.536	1.01550	11.970	0.08354
		292.165	1.00786	23.200	0.04310
		150.200	1.00421	44.965	0.02224
75.02	35	4991.313	1.13436	1.5285	0.65425
		2420.951	1.06636	2.9624	0.33757
		1210.565	1.03344	5.7414	0.17417
		614.687	1.01702	11.127	0.08987
		314.572	1.00873	21.566	0.04637
		161.616	1.00442	41.798	0.02392

and barometric pressure were done using a digital computer. The temperature data and absolute pressure data for each series of expansions are shown in Table IV.

The compressibility factors were calculated from the isothermal expansion data using the relationships previously shown, Eqs. (II-11), (II-12), and (II-13). Plots of the isothermal pressure ratios, such as shown in Figure 7, were made for each gas system. The data points below 150 psia were omitted because of the scatter due to the difficulty in measuring low pressures with the piston gage. As previously illustrated, Eq. (II-12) defined the cell constant N. The cell constant for each series of expansions was evaluated by curve-fitting the low pressure data (below 1500 psia in general, depending upon the gas system) using the following model:

$$P_{i-1}/P_i = a + bP_i + cP_i^2 + \ldots \qquad \text{(VI-1)}$$

The value of N corresponded to the intercept a in the above equation. The results of the curve-fit were checked graphically. The values of N used are shown in Appendix H.

The next step in calculating the compressibility data from the isothermal pressure measurements was to determine the value of the compressibility factor z_o corresponding to the pressure P_o before the first expansion. Plots of $N^i P_i$ versus P_i were prepared for each run. The zero intercept of such plots gave values of P_o/z_o as shown by Eq. (II-13). The value of P_o/z_o for each run was determined by curve-fitting the data using the following model:

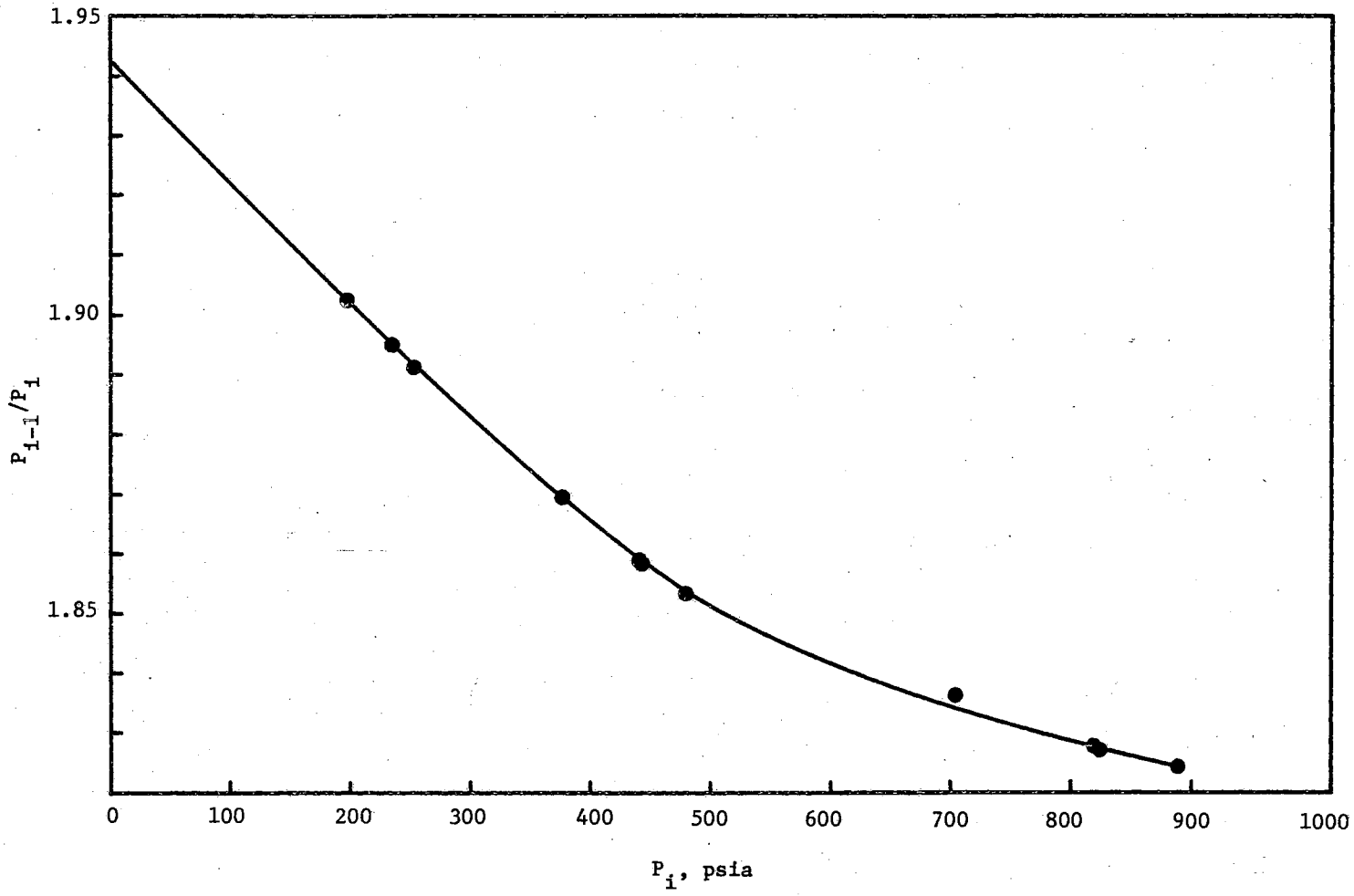

Figure 7. Isothermal Pressure Ratios for Methane 77 °F

$$N^{i}P_{i} = a + bP_{i} + cP_{i}^{2} + \ldots \qquad \text{(VI-2)}$$

Then, the value of P_o/z_o was used in Eq. (II-11) to calculate the compressibility factor for each pressure measurement.

During the course of deriving second virial coefficients by the slope-intercept method, a dependence of the slope on P_o/z_o was found. An example of this dependence is shown in Figure 8 for Run 3. The change in P_o/z_o shown in Figure 8 is ±0.1%. A value of P_o/z_o either too high or too low caused the plot of $(z-1)\underline{V}$ versus $1/\underline{V}$ to be non-linear at low densities. The plot should become linear as the density decreases. Rather than doing the adjustments graphically, the procedure was programed for a digital computer. The value of P_o/z_o was adjusted such that a minimum sum-of-squares was obtained when the compressibility and density data were fitted to the following model (see Appendix H):

$$(z-1)\underline{V} = B + C(1/\underline{V}) + D(1/\underline{V}^{2}) \qquad \text{(VI-3)}$$

The experimental compressibility factors for methane are compared with data by other investigators in Figure 9. Only a part of each investigator's data is shown. The experimental data were curve-fitted to the Leiden form of the virial equation of state (see section in this chapter on equations of state). The results of this fit are represented by the curves in Figure 9. The width of these curves gives the 95% confidence intervals for the experimental data. At the 95% confidence level, the compressibility factor data from the literature agree with the experimental values at 25 and 50 °C. Only the low pressure data at 75 °C fall within the 95% confidence interval. The

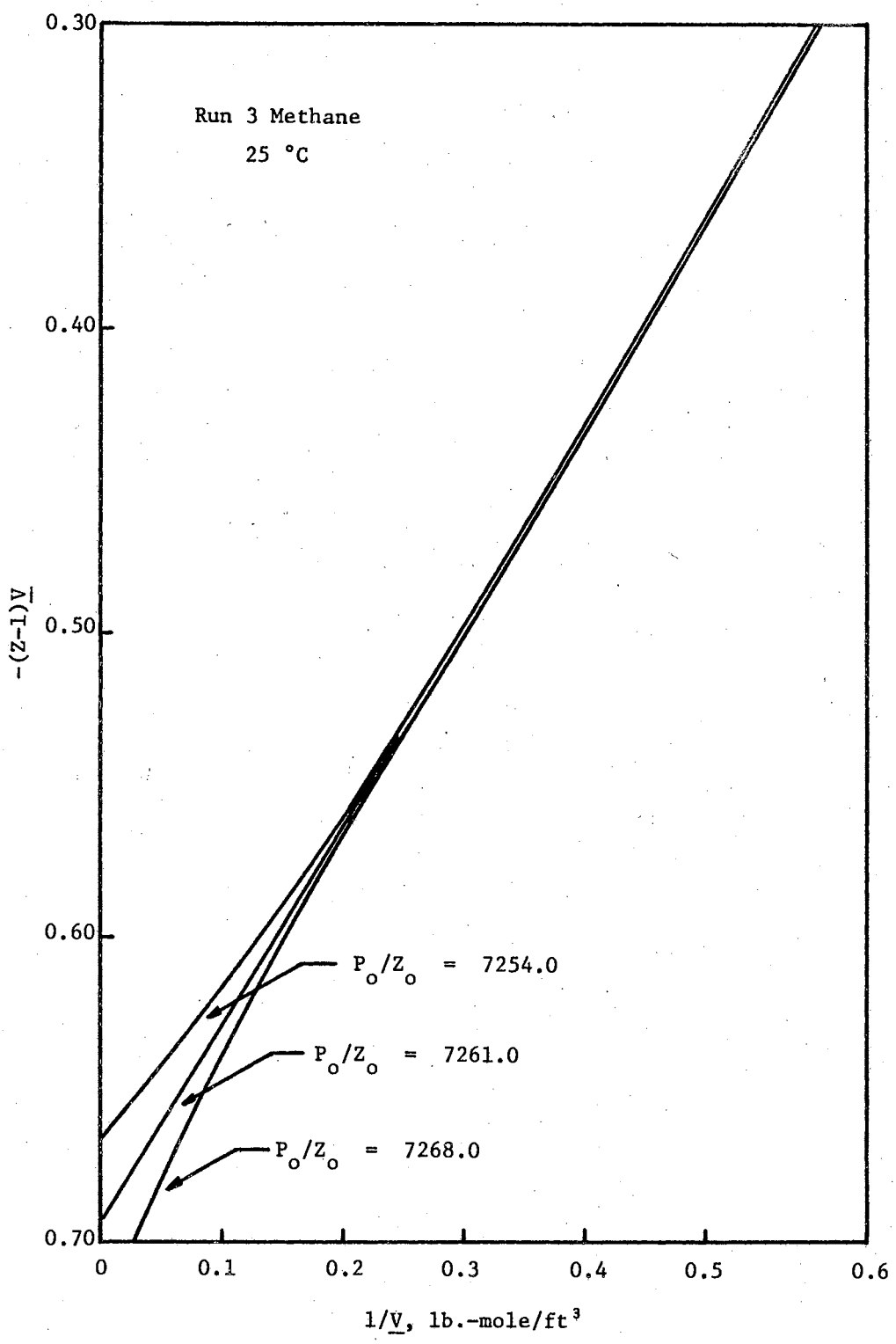

Figure 8. Effect of P_o/Z_o (Z-1)V

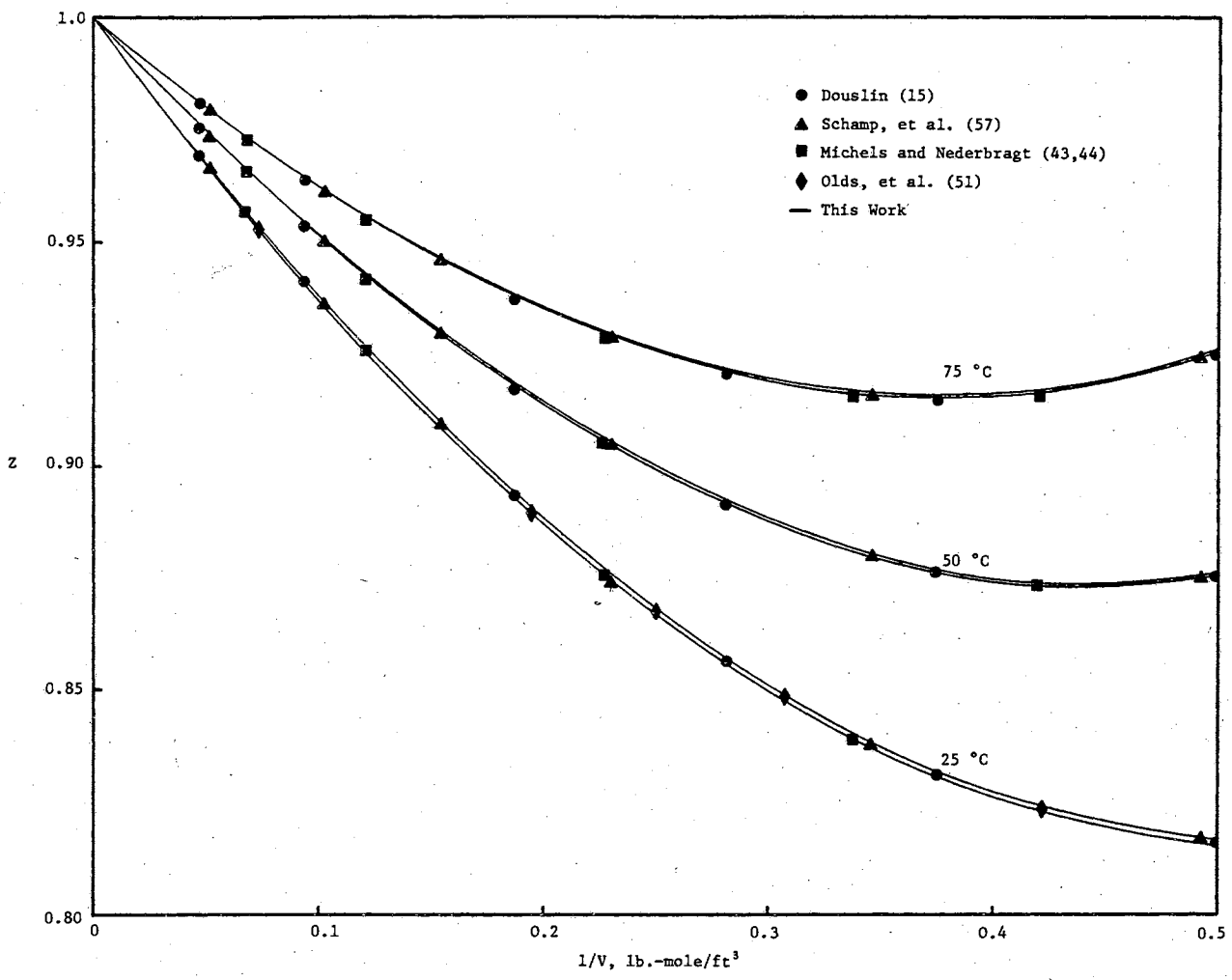

Figure 9. Methane Compressibility Factors

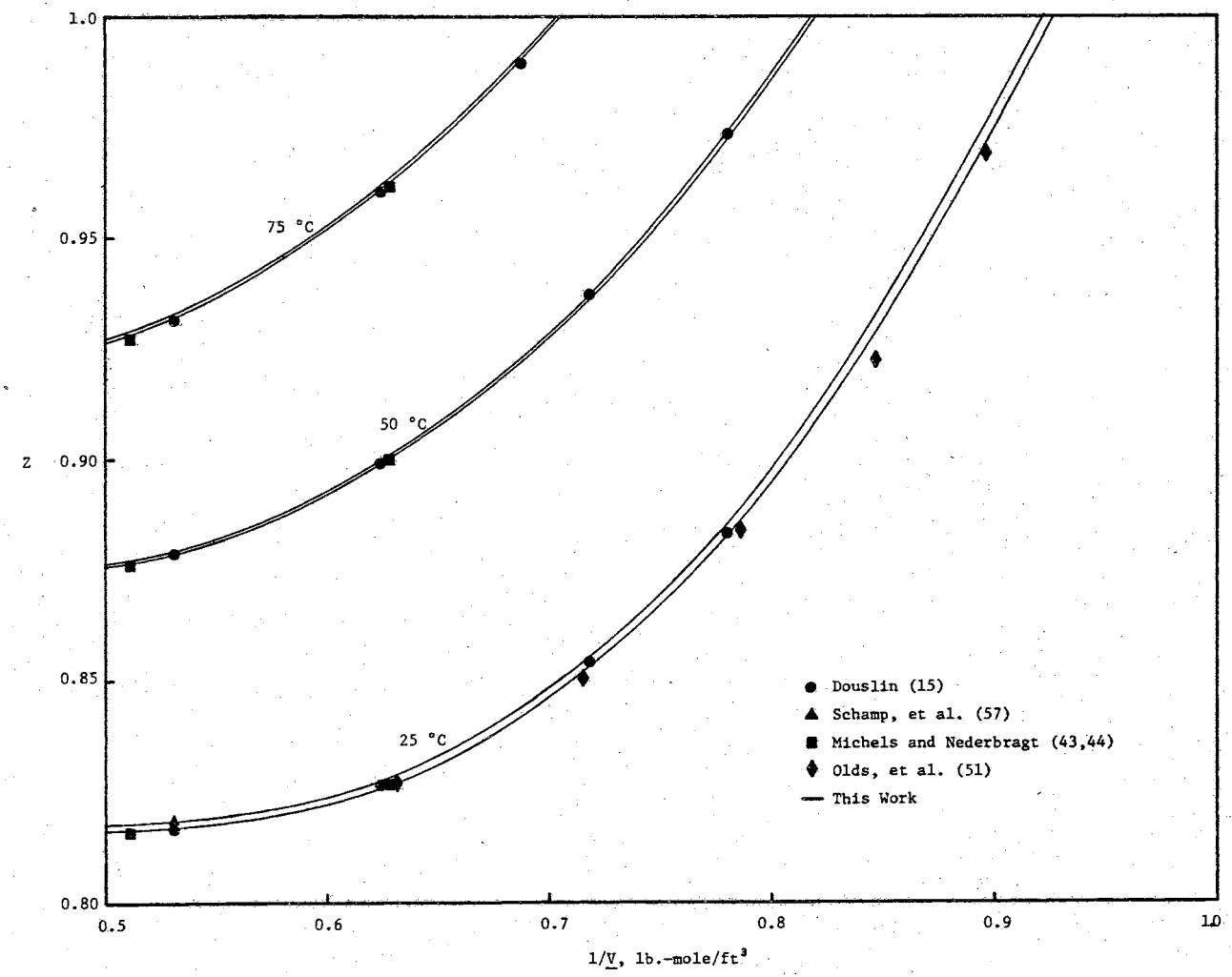

Figure 9. (Continued)

estimated errors at the 95% level for the experimental methane data are shown in Table VI.

The experimental compressibility factors for ethylene are compared with data by Michels and Geldermans (41) in Figure 10. The wide curves represent the experimental data at the 95% confidence level. The data of Michels and Geldermans fall within the confidence interval of the 25 °C experimental data. Only the low pressure data at 50 °C and 75 °C fall within the band. Also, the difference between the data increases with increasing pressure. This increasing divergence with pressure could be due to differences in the piston gages used for measuring pressure, the method of calculating the compressibility factors from the isothermal expansion data, and experimental errors.

A comparison of the Ruska piston gage and a Hart piston gage, which was the same make of piston gage used by Michels and Geldermans (41), made at Oklahoma State University showed that the disagreement between the two gages increased with increasing pressure. The difference at low pressures (below 1000 psi) was about two parts in 10,000 while the difference at 12,000 psi was five parts in 10,000.

In addition to the difference in the piston gages, the method of calculating the compressibility factors from the isothermal expansion data could contribute to the difference. The usual procedure for determining compressibility factors from Burnett's isothermal expansion method is to evaluate the cell constant N by using a gas such as helium. The pressure ratios for helium are linear over a relatively wide pressure range.

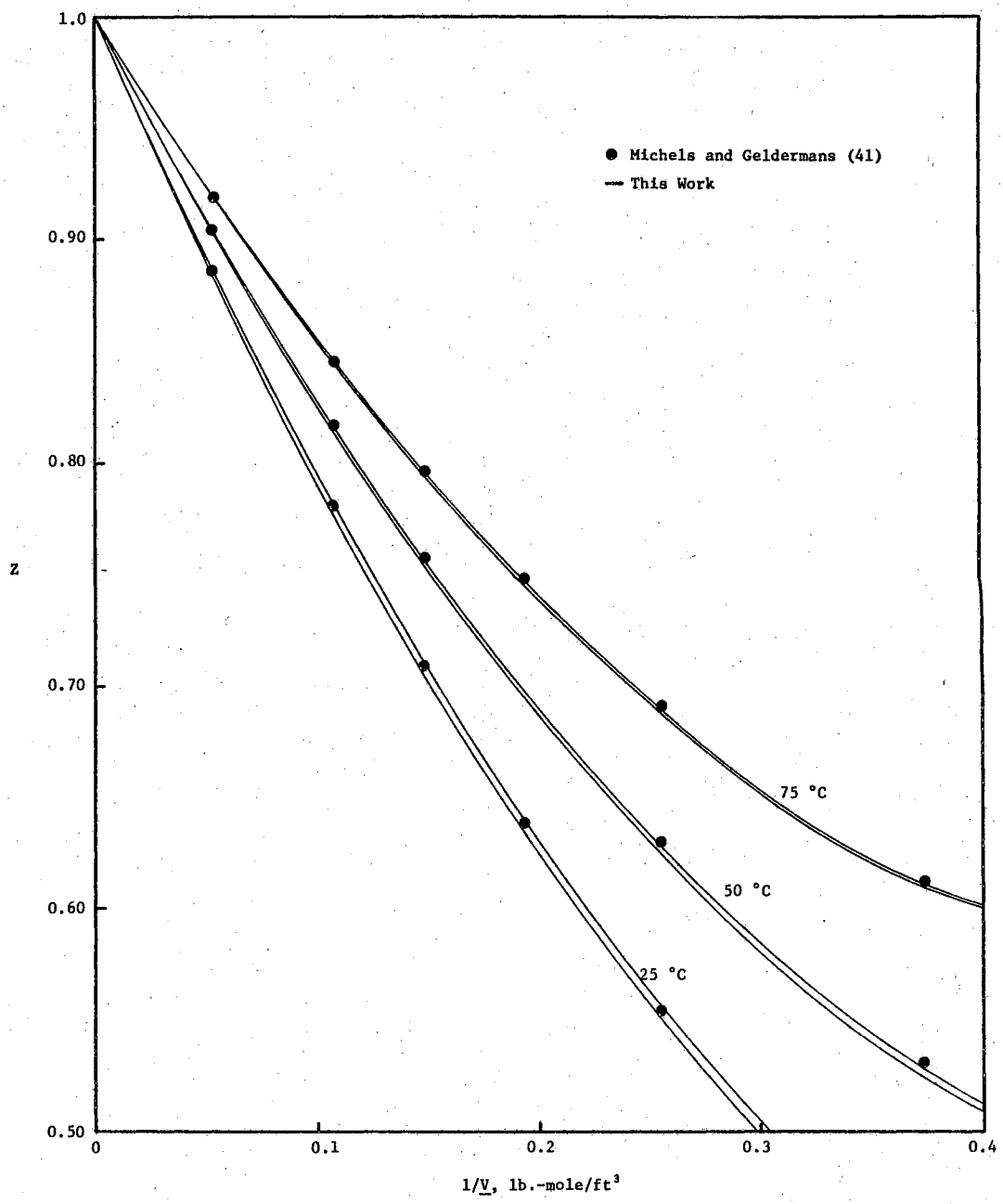

Figure 10. Ethylene Compressibility Factors

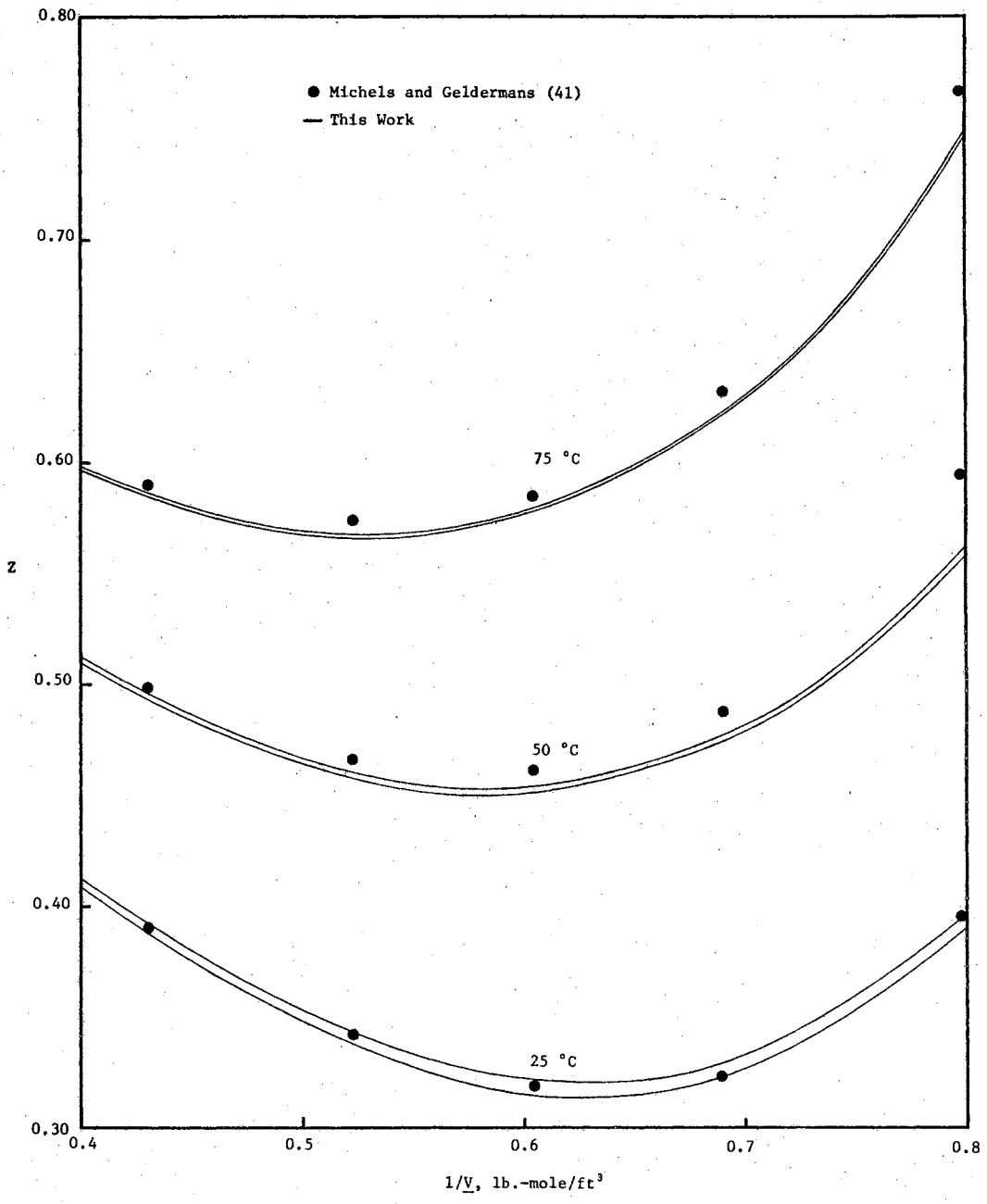

Figure 10. (Continued)

TABLE VI

ESTIMATED ERROR FOR EXPERIMENTAL COMPRESSIBILITY FACTORS AT 95% CONFIDENCE LEVEL

Estimated Error as % of z

Temperature °C	99% Methane	78.8% Methane	57.2% Methane	38.4% Methane	18.4% Methane	99.9% Ethylene
25	0.15	0.04	0.12	0.07	0.36	0.68
50	0.03	0.03	0.05	0.03	0.05	0.27
75	0.05	0.06	0.03	0.04	0.77	0.04

The helium data shown in Table V were obtained for the purpose of determining N. Shown in Figure 23, Appendix M, is a plot of the pressure ratios for helium at 25, 50, and 75 °C. The zero pressure intercept on this plot gives the value of N (see Table H-I). In principle, the value of N should not change with temperature; thus, the three lines should intersect at a common point. As shown, the lines do not intersect at a common point with the 50 °C line being much lower. It would appear that the 50 °C data were in error when compared to the other two. But, notice that several series of expansions were made at each temperature and that the data from each temperature were grouped together.

Rather than choosing a value of N based upon the helium data, the procedure presented previously in this section of using the pressure ratios to determine the value of N for each isotherm for each gas system was used. Again, the N values from the methane, ethylene, and the methane-ethylene mixture data should agree, but as shown in Table H-I and Figure 22, the N values varied. This procedure yielded methane compressibility data that compared favorably with literature data as shown previously in this section. The ethylene pressure ratio data had the most curvature of the gas systems studied and this curvature would make evaluation of N more uncertain than for the other systems.

For comparison, ethylene compressibility factors were calculated using the cell constant N determined from the helium data. These compressibility data are shown in Table M-I and are compared with data by Michels and Geldermans (41) in Figure 24 (Appendix M). The

25 and 50 °C data were moved further away from Michels and Geldermans' data. The 75 °C data moved closer to the data by Michels and Geldermans.

Apparently, using the cell constant N as determined from the helium pressure ratios instead of the N calculated from the ethylene pressure ratios does not solve the problem. For example, if the methane compressibility data were calculated from the isothermal expansion data using the helium cell constant, the resulting compressibility factors would not agree with the literature data. Since in principle, the helium, methane, and ethylene pressure ratios should yield the same value for the cell constant, the discrepancy is probably due to experimental errors. Then, the disagreement between the ethylene compressibility, shown in Table IV and Figure 10, and the data by Michels and Geldermans (41) was due to experimental errors and the subsequent treatment of the isothermal expansion data.

Virial Coefficients

The second and third virial coefficients for methane, ethylene, and four of their mixtures were derived from the compressibility factors using the slope-intercept method. The derivation of the second and third virial coefficients was done by a section of the program for calculating the compressibility factors from the isothermal expansion data.

The usual procedure for deriving virial coefficients using the slope-intercept method was adapted to a digital computer. Second virial coefficients are usually determined by plotting $(z-1)\underline{V}$ versus $1/\underline{V}$ and by extrapolating to zero density. The intercept on this plot is the second virial coefficient.

Next, the second virial coefficient is used to make a plot of $((z-1)\underline{V}-B)\underline{V}$ versus $1/\underline{V}$ for determining the third virial coefficient. This plot for the third coefficient should become linear at low densities. This linear relationship is very sensitive to the value of B used to make the plot. The value of B is usually adjusted so that the plot of $((z-1)\underline{V}-B)\underline{V}$ versus $1/\underline{V}$ is linear. Then, the third coefficient can be used to evaluate the fourth virial coefficient by making a similar plot and adjusting the value of C to give a linear relationship on this plot.

Instead of making the plots, extrapolating, and adjusting the values of B and C graphically, the extrapolating and adjustments were done on a digital computer using curve-fits. The trial value of B was determined from a curve-fit of the low density data using Eq. (VI-3). Then, the value of B was adjusted until a curve-fit using the following model gave a minimum sum-of-squares:

$$((z - 1)\underline{V} - B)\underline{V} = C + D/\underline{V} + E/\underline{V}^2 \qquad \text{(VI-4)}$$

The value of C from the above equation was adjusted in a similar manner using the following model:

$$(((z - 1)\underline{V} - B)\underline{V} - C)\underline{V} = D + E/\underline{V} + F/\underline{V}^2 \qquad \text{(VI-5)}$$

The above procedure was checked graphically. Also, the range of the low density data used in the curve-fits was determined graphically.

The second and third virial coefficients for methane, ethylene, and their mixtures are shown in Table VII with 95% confidence limits. The gases used in this investigation contained impurities; thus, the coefficients shown in Table VII apply only to these gases (see Appendix D for the compositions). The estimated per cent error for the second and third virial coefficients at the 95% confidence level are shown in Table VIII.

The second virial coefficients were corrected for the impurities using cross-coefficients from the literature and using an empirical correlation by Prausnitz (56) as modified by Huff and Reed (27). The corrected second virial coefficients are shown in Table IX. The error in the corrected second coefficients was not estimated, but they would be about the same as for the uncorrected values but larger. The corrections made for the impurities were in general within the estimated error for the uncorrected values.

The second virial coefficients for helium from this investigation are compared with other investigators in Table X. The data from this work agree closest with the data of Stroud, Miller, and Brandt (64), whose data were derived using the isothermal expansion method of Burnett. As shown by the values in Table X, there are variations among the investigators. For example at 25 °C, the highest value for the second virial coefficient is 12.80 cc per g-mole and the lowest 11.56 cc per g-mole.

The second virial coefficients for methane from this work are compared with other investigators in Figure 11. The values from

TABLE VII

EXPERIMENTAL VIRIAL COEFFICIENTS
WITH 95% CONFIDENCE LIMITS

Nominal Composition	Temperature °K	B cc/g-mole	C $(cc/g\text{-}mole)^2 \times 10^{-3}$
Methane	298.15	-42.88±1.5	2.392±0.80
	323.15	-33.22±1.0	1.785±0.40
	348.17	-26.54±1.1	1.958±0.50
Ethylene	298.15	-145.60±4.8	9.794±2.60
	323.15	-120.40±1.3	7.046±0.40
	348.16	-100.80±1.1	5.982±0.80
80-20 Methane-Ethylene	298.15	-55.39±1.3	2.680±0.60
	323.15	-43.74±0.5	2.152±0.20
	348.16	-34.07±1.1	1.714±0.40
60-40 Methane-Ethylene	298.15	-72.35±3.0	3.248±1.60
	323.15	-60.54±0.4	3.206±0.09
	348.16	-49.85±0.4	2.820±0.09
40-60 Methane-Ethylene	298.15	-90.96±1.5	4.100±0.90
	323.15	-77.47±0.1	4.310±0.08
	348.16	-64.30±0.2	3.667±0.07
20-80 Methane-Ethylene	298.15	-116.90±1.4	6.537±0.60
	323.15	-98.32±0.7	5.713±0.10
	348.17	-82.03±0.8	4.696±0.40

TABLE VIII

ESTIMATED PER CENT ERROR FOR EXPERIMENTAL VIRIAL COEFFICIENTS
AT 95% CONFIDENCE LEVEL

Temp. °C	99% Methane		78.8% Methane		57.2% Methane		38.4% Methane		18.4% Methane		99.9% Ethylene	
	B	C	B	C	B	C	B	C	B	C	B	C
25	3.4	32	2.3	22.0	4.1	48.0	1.7	22.0	1.2	9.2	3.3	27
50	3.1	24	1.2	7.9	0.6	2.7	0.1	1.9	0.7	3.4	1.1	58
75	4.1	26	3.4	22.0	0.9	3.4	0.4	1.0	1.0	8.4	1.1	14

TABLE IX

SECOND VIRIAL COEFFICIENTS CORRECTED FOR IMPURITIES

Nominal Composition	Temperature °K	B cc/g-mole
Methane	298.15	-41.57
	323.15	-32.04
	348.17	-25.49
Ethylene*	298.15	-145.60
	323.15	-120.40
	348.16	-100.80
80-20 Methane-Ethylene	298.15	-52.51
	323.15	-41.19
	348.16	-31.81
60-40 Methane-Ethylene	298.15	-70.29
	323.15	-58.74
	348.15	-48.28
40-60 Methane-Ethylene	298.15	-89.85
	323.15	-76.51
	348.16	-63.46
20-80 Methane-Ethylene*	298.15	-116.90
	323.15	-98.32
	348.17	-82.03

*No corrections made for these gases.

TABLE X

SECOND VIRIAL COEFFICIENTS FOR HELIUM

Source	B, cc/g-mole, Temperature, °C		
	25	50	75
Stroud, Miller, and Brandt (64)	11.79	11.72	11.69
Schneider and Duffie (59)	11.71	11.61	11.52
Holborn and Otto (59)	11.61	11.52	11.45
Wiebe, Gaddy, and Heins (68)	11.56	11.48	11.39
Michels and Wouters (47)	12.80	11.57	11.43
This work	11.89	11.80	11.71

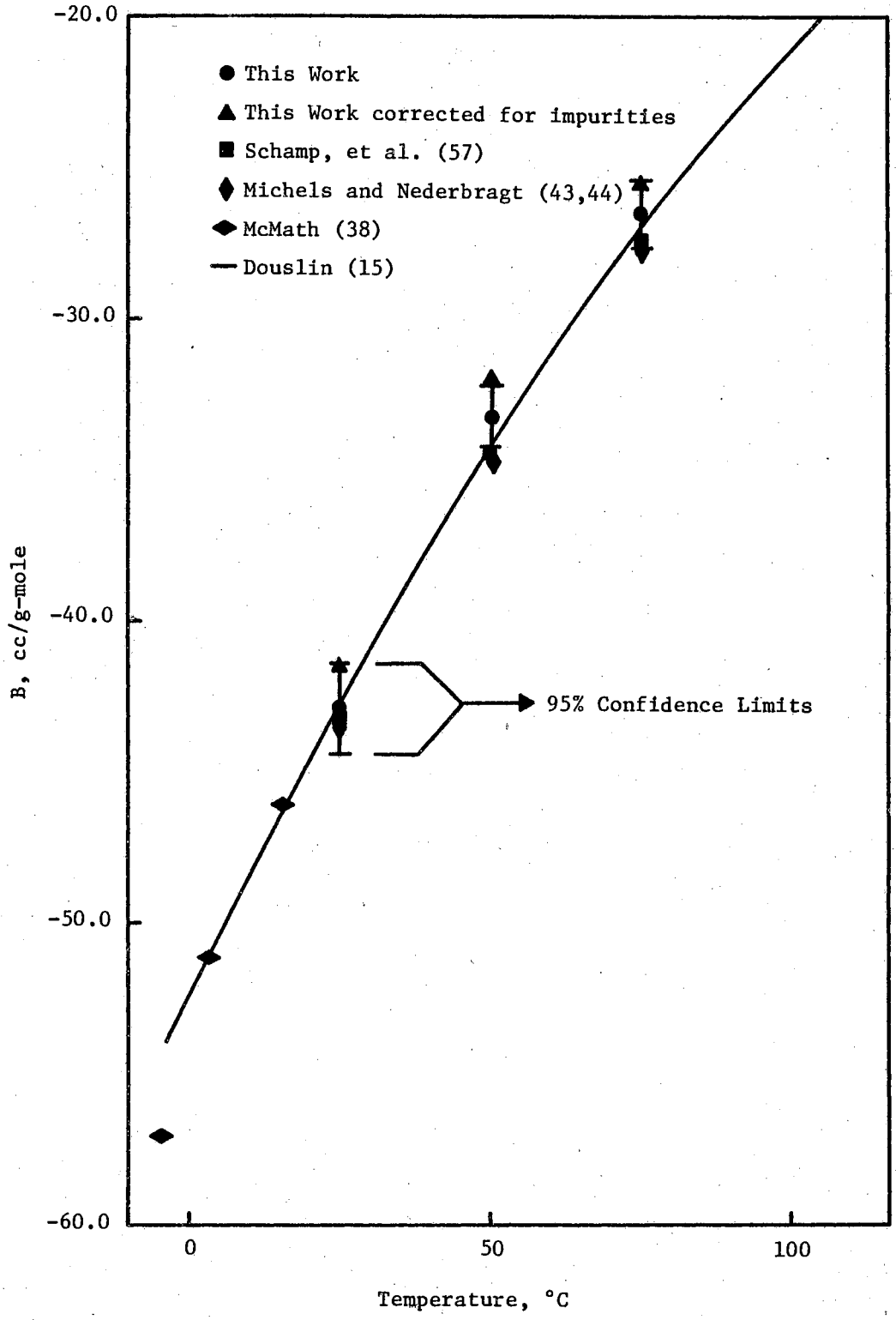

Figure 11. Second Virial Coefficients for Methane

Douslin (15) are represented by the curve; the other investigators' data are represented by the symbols shown in Figure 11. The values by Michels and Nederbragt (44) and Schamp et al. (57) agree closely and are lower than Douslin's data. The virial coefficients of Michels and Nederbragt and Schamp et al. were derived from compressibility data determined using the same type of apparatus and pressure measuring equipment. As shown, the uncorrected values from this work agreed within the estimated error with the other investigators at 25 and 75 °C. The values of Schamp et al. (57) and Michels and Nederbragt (43,44) at 50 °C fell outside the band.

The third virial coefficients for methane, with their 95% confidence limits, are compared with values from the literature in Figure 12. The variations among the investigators' data increased for the third virial coefficients as expected. The third virial coefficients from this work agreed within the estimated error with the other investigators shown in Figure 12 at 25 and 75 °C. The value at 50 °C barely agreed with Douslin's (15) data.

The second and third virial coefficients for ethylene are compared with literature values in Figures 13 and 14, respectively. The experimental second virial coefficient at 75 °C agreed with the value by Michels and Geldermans (41) and was lower than the data by Butcher and Dadson (7). The second virial coefficients from this work at 25 and 50° C were lower than either of the other investigators. The experimental third virial coefficients agreed within the estimated error at 50 and 75 °C with values by Butcher and Dadson (7).

The second virial coefficients corrected for impurities for the methane-ethylene mixtures are shown in Figure 15 (see Appendix G,

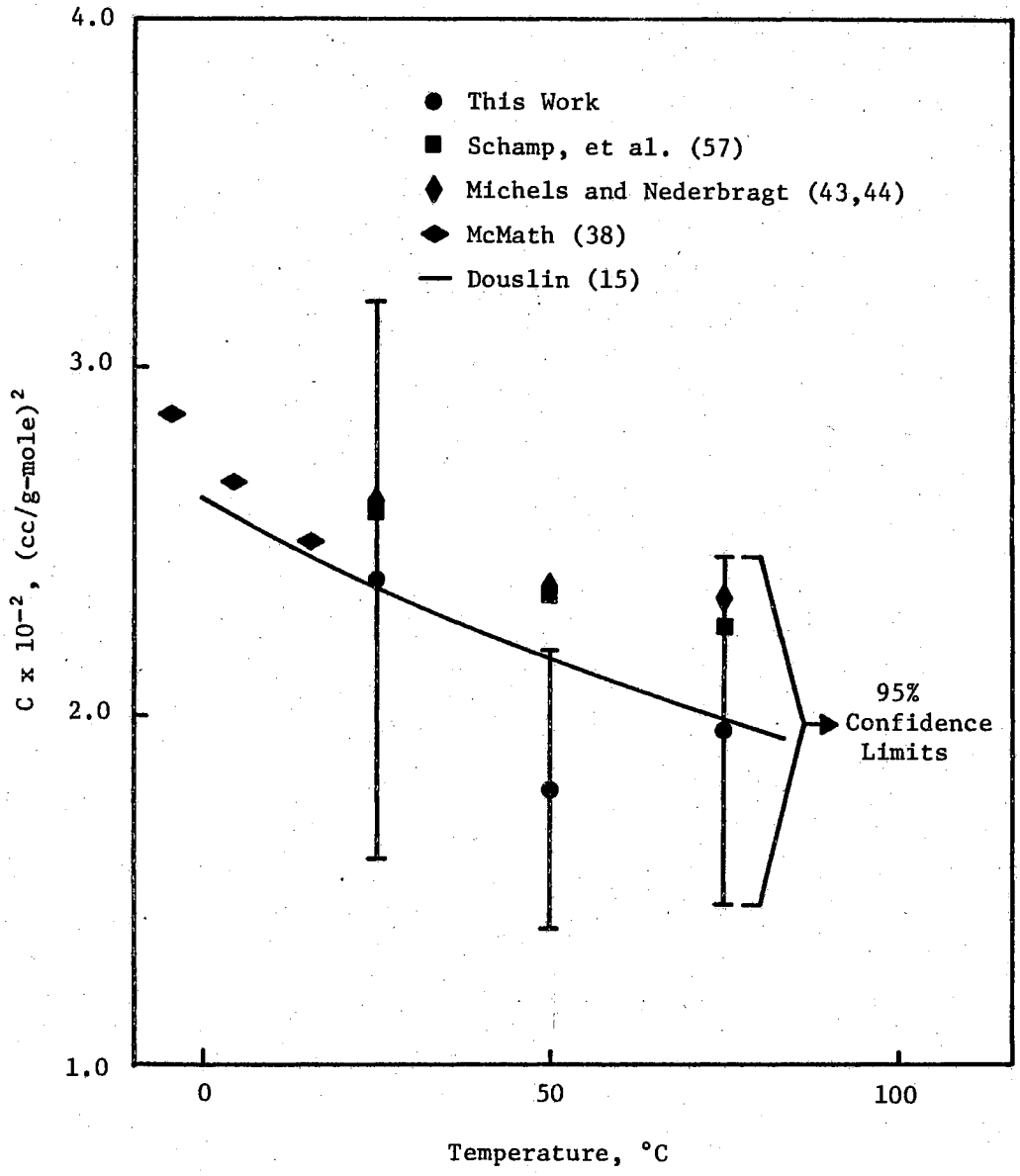

Figure 12. Third Virial Coefficients for Methane

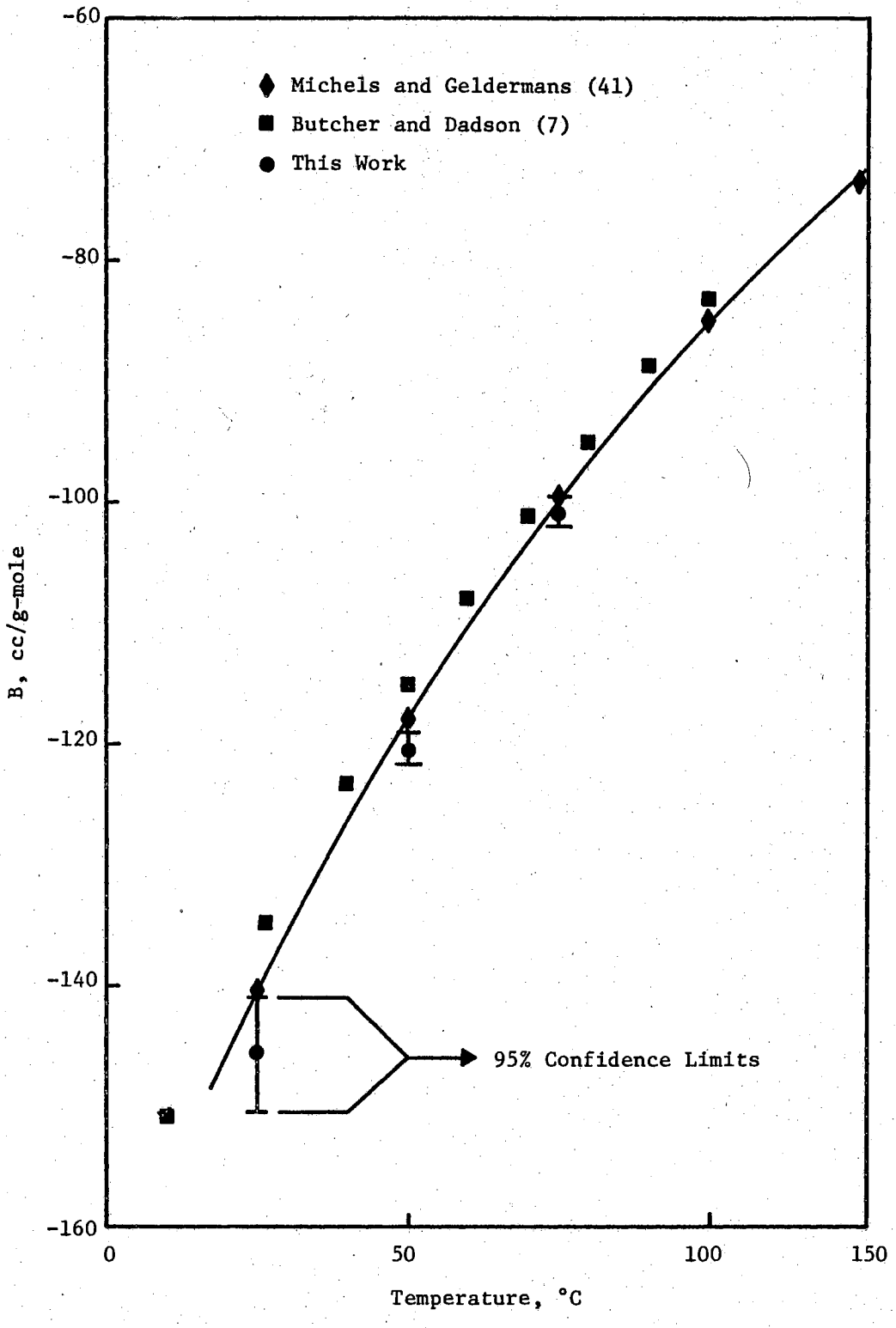

Figure 13. Second Virial Coefficients for Ethylene

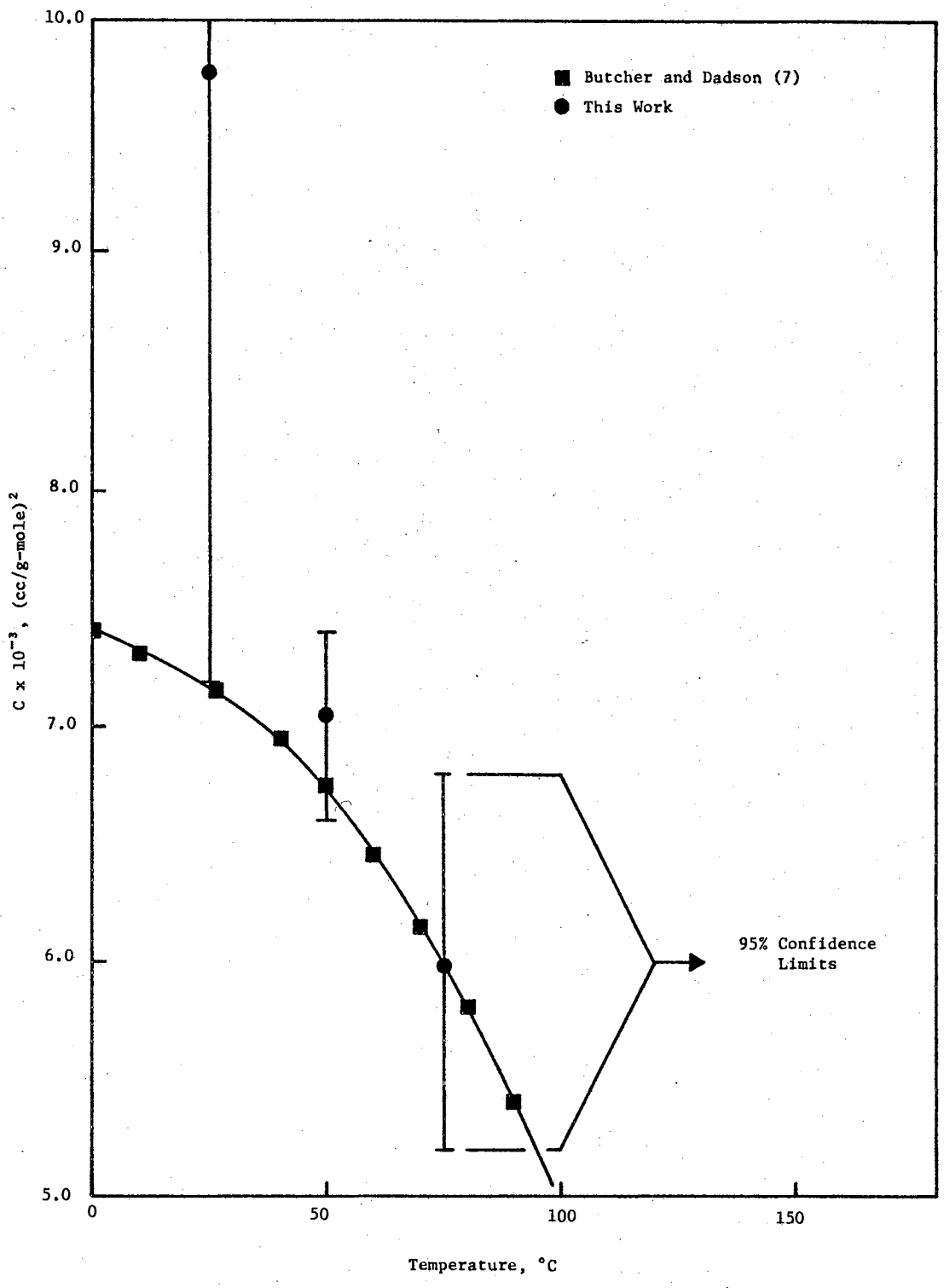

Figure 14. Third Virial Coefficients for Ethylene

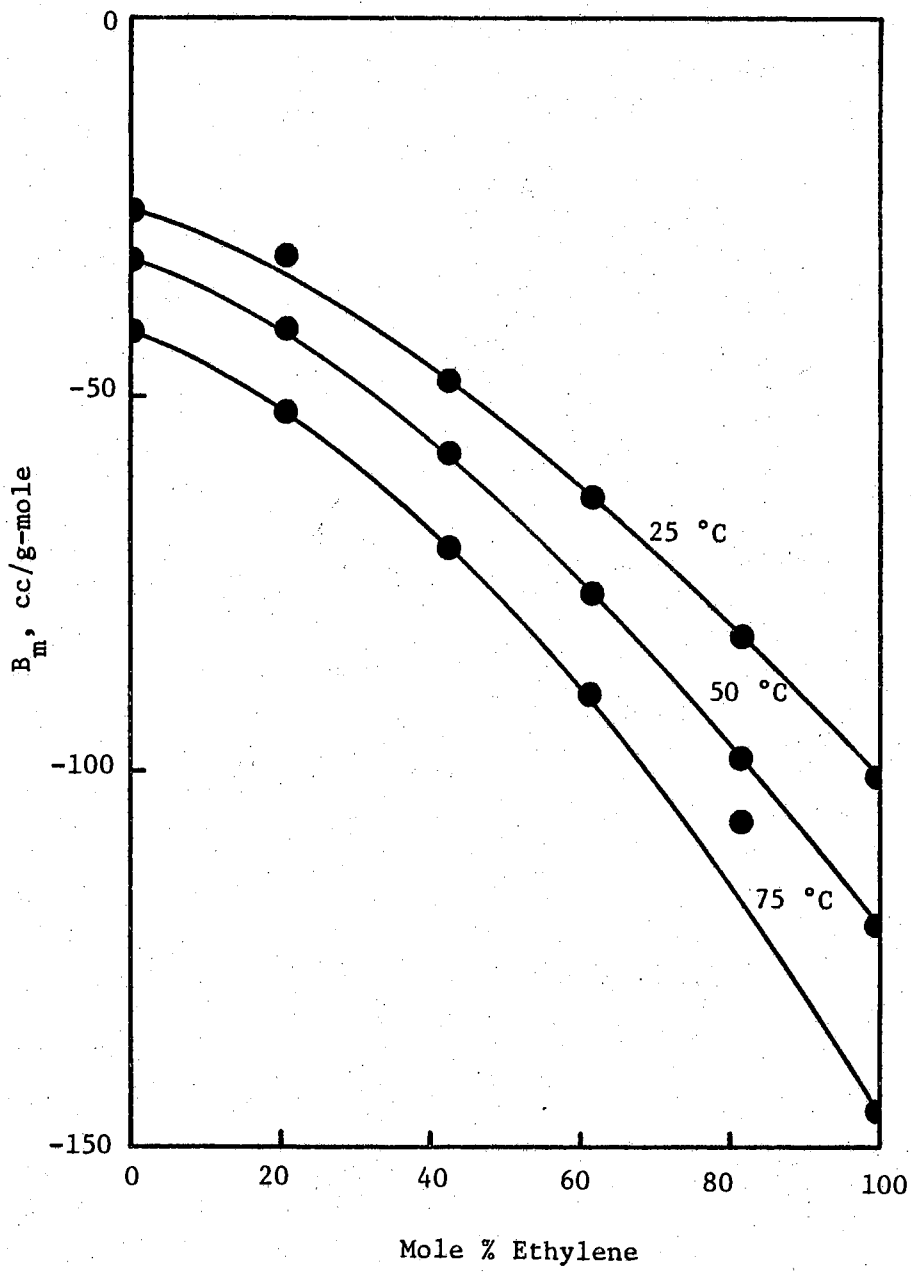

Figure 15. Mixture Second Virial Coefficients

Table G-V for the compositions). The coefficients were used to derive the cross-coefficients for methane-ethylene. For a binary mixture, the second virial coefficient is related to the pure component coefficients and the cross-coefficient by the following expression (23):

$$B_m = x_1^2 B_{11} + 2x_1x_2B_{12} + x_2^2 B_{22} \qquad \text{(III-24)}$$

The cross-coefficients, B_{12}, were determined by curve-fitting the data shown in Figure 15 and Table IX using Eq.(III-24)as the model. The resulting cross-coefficients are shown in Table XI and Figure 16. The estimated error based on the curve-fit was 1.1% at 25 °C, 5.5% at 50 °C, and 9.9% at 75 °C.

The experimental second virial coefficients and cross-coefficients were used to check combination rules for estimating mixture second virial coefficients for methane-ethylene binaries. The combination rules, presented in Chapter III, are shown below:

$$B_{12} = 1/2(B_{11} + B_{22}) \qquad \text{Linear} \qquad \text{(III-26)}$$

$$B_{12} = 1/4((B_{11})^{1/2} + (B_{22})^{1/2})^2 \qquad \text{Linear-square-root} \qquad \text{(III-28)}$$

$$B_{12} = (B_{11} B_{22})^{1/2} \qquad \text{Square root} \qquad \text{(III-29)}$$

$$B_{12} = ((B_{11})^{1/3} + (B_{22})^{1/3})^3/8 \qquad \text{Lorentz} \qquad \text{(III-31)}$$

The combination rules are compared with the experimental data in Tables XII, XIII, XIV, and XV. Three of the combination rules, linear-square-root, square root, and Lorentz, gave approximately the same results,

TABLE XI

CROSS COEFFICIENTS

Temperature °C	B_{12} cc/g-mole
25	-61.15
50	-53.99
75	-43.75

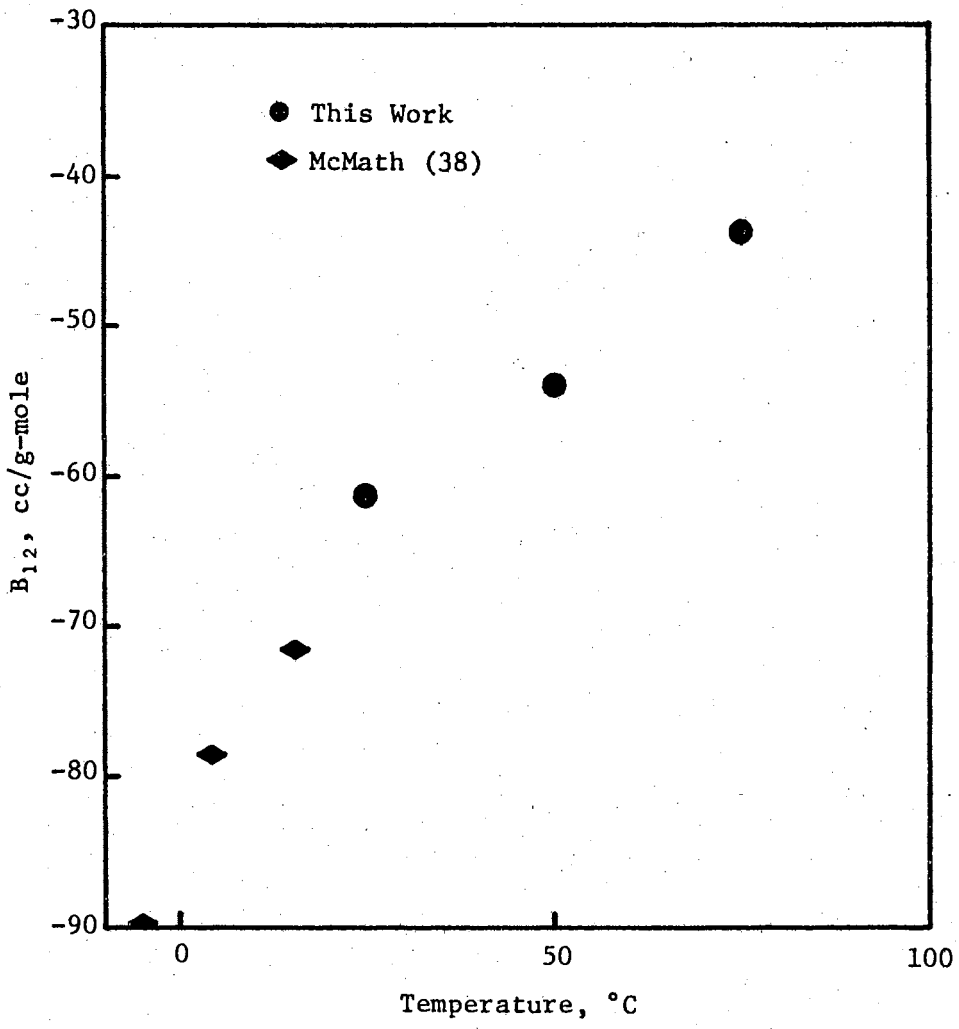

Figure 16. Cross-Coefficients for Methane-Ethylene System

TABLE XII

LINEAR COMBINATION

Units: cc/g-mole

Temp. °C	Mole Fraction Methane	Mole Fraction Ethylene	Experimental B_m	Experimental B_{12}	Linear B_m	Linear B_{12}	Difference $B_{mcal}-B_{mexp}$	Difference $B_{12cal}-B_{12exp}$
25	0.792	0.208	-52.51	-61.15	-63.20	-93.58	-10.69	-32.43
	0.574	0.426	-70.29		-85.89		-15.60	
	0.385	0.615	-89.85		-105.50		-15.65	
	0.184	0.816	-116.9		-126.50		-9.60	
							15.22	std. dev.
50	0.792	0.208	-41.19	-53.99	-50.41	-76.22	-9.22	-22.23
	0.574	0.426	-58.74		-69.68		-10.94	
	0.385	0.615	-76.51		-86.38		-9.87	
	0.184	0.816	-98.32		-104.10		-5.80	
							10.58	std. dev.
75	0.792	0.208	-31.81	-43.75	-41.15	-63.14	-9.34	-19.39
	0.574	0.426	-48.28		-57.57		-9.29	
	0.385	0.615	-63.46		-71.81		-8.35	
	0.184	0.816	-82.03		-86.94		-4.91	
							9.44	std. dev.

TABLE XIII

LINEAR SQUARE ROOT COMBINATION

Units: cc/g-mole

Temp. °C	Mole Fraction Methane	Mole Fraction Ethylene	Experimental B_m	Experimental B_{12}	Linear Square Root B_m	Linear Square Root B_{12}	Difference $B_{mcal}-B_{mexp}$	Difference $B_{12cal}-B_{12exp}$
25	0.792	0.208	-52.51	-61.15	-60.61	-85.69	-8.10	-24.54
	0.574	0.426	-70.29		-82.03		-11.74	
	0.385	0.615	-89.85		-101.80		-11.95	
	0.184	0.816	-116.90		-124.10		-7.20	
							11.52	std. dev.
50	0.792	0.208	-41.19	-53.74	-48.09	-69.16	-6.90	-15.17
	0.574	0.426	-58.74		-66.23		-7.49	
	0.385	0.615	-76.51		-83.04		-6.53	
	0.184	0.816	-98.32		-102.00		-3.70	
							7.30	std. dev.
75	0.792	0.208	-31.81	-43.75	-39.10	-56.92	-7.29	-13.17
	0.574	0.426	-48.28		-54.53		-6.05	
	0.385	0.615	-63.46		-68.86		-5.40	
	0.184	0.816	-82.03		-84.21		-2.18	
							6.50	std. dev.

TABLE XIV

SQUARE ROOT COMBINATION

Units: cc/g-mole

Temp. °C	Mole Fraction Methane	Mole Fraction Ethylene	Experimental B_m	Experimental B_{12}	Square Root B_m	Square Root B_{12}	Difference $B_{mcal}-B_{mexp}$	Difference $B_{12cal}-B_{12exp}$
25	0.792	0.208	-52.51	-61.15	-58.01	-77.80	-5.50	-16.65
	0.574	0.426	-70.29		-78.17		-7.88	
	0.385	0.615	-89.85		-98.07		-8.22	
	0.184	0.816	-116.90		-121.70		-4.80	
							7.81 std. dev.	
50	0.792	0.208	-41.19	-53.99	-45.77	-62.11	-4.58	-8.12
	0.574	0.426	-58.74		-62.78		-4.04	
	0.385	0.615	-76.51		-79.70		-3.19	
	0.184	0.816	-98.32		-99.90		-1.58	
							4.08 std. dev.	
75	0.792	0.208	-31.81	-43.75	-37.05	-50.69	-5.24	-6.94
	0.574	0.426	-48.28		-51.48		-3.20	
	0.385	0.615	-63.46		-65.91		-2.45	
	0.184	0.816	-82.03		-83.20		-1.17	
							3.87 std. dev.	

TABLE XV

LORENTZ COMBINATION

Units: cc/g-mole

Temp. °C	Mole Fraction Methane	Mole Fraction Ethylene	Experimental B_m	Experimental B_{12}	Lorentz B_m	Lorentz B_{12}	Difference $B_{mcal}-B_{mexp}$	Difference $B_{12cal}-B_{12exp}$
25	0.792	0.208	-52.51	-61.15	-59.40	-83.02	-6.89	-21.87
	0.574	0.426	-70.29		-80.74		-10.45	
	0.385	0.615	-89.85		-100.50		-10.65	
	0.184	0.816	-116.90		-123.8		-6.90	
							10.30	std. dev.
50	0.792	0.208	-41.19	-53.99	-47.31	-66.78	-6.12	-12.79
	0.574	0.426	-58.74		-65.07		-6.33	
	0.385	0.615	-76.51		-81.91		-5.40	
	0.184	0.816	-98.32		-101.30		-3.00	
							6.21	std. dev.
75	0.792	0.208	-31.81	-43.75	-38.41	-54.81	-6.60	-11.06
	0.574	0.426	-48.28		-53.50		-5.22	
	0.385	0.615	-63.46		-67.86		-4.40	
	0.184	0.816	-82.03		-84.44		-2.41	
							5.65	std. dev.

being better than the linear rule. The square root combination would be the best rule to use since it is the simplest of the three.

Equations of State

The experimental compressibility factors shown in Table IV were curve-fitted to the Leiden form of the virial equation of state, shown below:

$$z = A + B/\underline{V} + C/\underline{V}^2 + D/\underline{V}^3 + \ldots \qquad \text{(VI-6)}$$

The compressibility factors for pressures below 150 psia were not included in the curve-fit. Since the model used in the curve-fit is a theoretical model, the residual error is due to the choice of the number of coefficients in the model and experimental error. Hence, the number of coefficients in the model which gave the "best fit" was chosen such that the mean residual sum of squares (standard deviation for the fit) was a minimum. The coefficients, their standard deviations, the standard deviations for the fit, and the degrees of freedom are shown in Table XVI. The coefficients are for density units of lb.-mole per cubic foot.

The second and third virial coefficients derived from the slope-intercept method as described previously are compared with the coefficients from the curve-fit of the compressibility data in Table XVII. The 95% confidence limits are shown also in Table XVII. In general, the second virial coefficients derived by both methods gave

TABLE XVI

COEFFICIENTS FROM CURVE-FIT OF COMPRESSIBILITY FACTORS TO THE LEIDEN FORM OF THE VIRIAL EQUATION OF STATE

Density Units: lb-mole/ft^3

i	Coefficients	s_{bi}	s	d.f.
		Methane 25 °C		
1	0.9998004	0.00096	0.00086	17
2	-0.6841890	0.021		
3	0.6297567	0.14		
4	-0.1066659	0.41		
5	0.2851700	0.58		
6	-0.1741619	0.40		
7	0.1373626	0.11		
		Methane 50 °C		
1	1.0000830	0.00011	0.00016	15
2	-0.5357476	0.0027		
3	0.4867952	0.017		
4	0.2331225	0.039		
5	-0.02453715	0.038		
6	0.2636876	0.013		
		Methane 75 °C		
1	0.9997566	0.00032	0.00027	10
2	-0.4114680	0.0081		
3	0.3579997	0.063		
4	0.6263773	0.21		
5	-0.9872723	0.35		
6	0.9677234	0.28		
7	-0.2472527	0.083		

TABLE XVI (Continued)

i	Coefficients	s_{bi}	s	d.f.
		Ethylene 25 °C		
1	1.003008	0.0040	0.0029	16
2	-2.442701	0.096		
3	3.671667	0.71		
4	-5.860483	2.3		
5	9.673038	3.6		
6	-9.066705	2.8		
7	3.841122	0.8		
		Ethylene 50 °C		
1	1.001153	0.0022	0.0012	14
2	-1.955390	0.039		
3	1.934410	0.22		
4	0.3396489	0.49		
5	-2.440842	0.48		
6	2.176879	0.17		
		Ethylene 75 °C		
1	1.000299	0.00021	0.00021	19
2	-1.62423	0.0073		
3	1.621643	0.069		
4	0.008335	0.27		
5	-0.9184579	0.48		
6	0.8205693	0.41		
7	0.4367816	0.13		
		80-20 Methane-Ethylene 25 °C		
1	1.000335	0.00027	0.00023	12
2	-0.8959749	0.0056		
3	0.7384177	0.032		
4	0.1726574	0.069		
5	-0.3974254	0.063		
6	0.4374412	0.021		
		80-20 Methane-Ethylene 50 °C		
1	1.000191	0.00037	0.00017	9
2	-0.7027187	0.0063		
3	0.5411860	0.033		

TABLE XVI (Continued)

i	Coefficients	s_{bi}	s	d.f.
4	0.4197359	0.071		
5	-0.5137237	0.066		
6	0.4567650	0.022		
	80-20 Methane-Ethylene 75 °C			
1	1.000545	0.00068	0.00032	9
2	-0.5548790	0.012		
3	0.4706322	0.066		
4	0.4143606	0.15		
5	-0.3922206	0.15		
6	0.3885449	0.051		
	60-40 Methane-Ethylene 25 °C			
1	1.001576	0.00097	0.00061	9
2	-1.203773	0.022		
3	1.201754	0.17		
4	-0.6027667	0.62		
5	0.1992873	1.28		
6	1.366197	1.52		
7	-1.682892	0.95		
8	0.7407407	0.24		
	60-40 Methane-Ethylene 50 °C			
1	0.9995680	0.00086	0.00024	7
2	-0.9530783	0.017		
3	0.6233560	0.11		
4	1.131385	0.34		
5	-2.181761	0.50		
6	1.944805	0.37		
7	-0.4021739	0.10		
	60-40 Methane-Ethylene 75 °C			
1	1.000143	0.00040	0.00015	8
2	-0.8027822	0.0080		
3	0.7602824	0.053		
4	0.1189195	0.16		
5	-0.0284731	0.25		
6	0.07150422	0.19		
7	0.1782946	0.056		

TABLE XVI (Continued)

i	Coefficients	s_{bi}	s	d.f.
		40-60 Methane-Ethylene 25 °C		
1	1.000813	0.00042	0.00032	8
2	-1.480609	0.0090		
3	1.202449	0.051		
4	0.3837994	0.037		
5	-1.104405	0.26		
6	0.9528702	0.40		
7	-0.3657801	0.55		
8	0.9859571	0.34		
9	-0.9349593	0.38		
10	0.3333333	0.13		
		40-60 Methane-Ethylene 50 °C		
1	1.000113	0.00044	0.00014	7
2	-1.243214	0.0086		
3	1.107562	0.053		
4	0.0837558	0.15		
5	-0.047522	0.23		
6	-0.7122314	0.25		
7	1.335046	0.18		
8	-0.3928571	0.053		
		40-60 Methane-Ethylene 75 °C		
1	1.000892	0.00044	0.00018	6
2	-1.050767	0.0051		
3	1.100941	0.047		
4	-0.3786515	0.26		
5	0.9651010	0.59		
6	-1.538161	0.63		
7	1.657233	0.30		
8	-0.4575472	0.036		
		20-80 Methane-Ethylene 25 °C		
1	1.005993	0.0025	0.0016	12
2	-2.055623	0.062		
3	3.224266	0.46		
4	-4.953119	1.31		
5	4.723271	1.14		
6	1.876036	0.47		

TABLE XVI (Continued)

i	Coefficients	s_{bi}	s	d.f.
7	-2.804135	1.97		
8	-3.959789	1.27		
9	0.7476499	0.88		
10	6.832463	1.59		
11	-3.727273	0.72		
	20-80 Methane-Ethylene 50 °C			
1	1.000166	0.00022	0.00023	14
2	-1.574925	0.0036		
3	1.413852	0.027		
4	0.2478234	0.19		
5	-0.6061167	0.50		
6	-0.8044623	0.61		
7	2.156738	0.34		
8	-0.7267442	0.72		
	20-80 Methane-Ethylene 75 °C			
1	0.999286	0.0027	0.0037	17
2	-1.306775	0.049		
3	1.235946	0.098		
4	0.522916	1.13		
5	-2.261494	2.16		
6	2.751295	1.61		
7	-0.611091	0.38		

TABLE XVII

COMPARISON OF VIRIAL COEFFICIENTS DERIVED BY SLOPE-INTERCEPT METHOD AND CURVE-FITTING OF COMPRESSIBILITY DATA

Temperature °C	Slope-Intercept		Curve-Fit	
	B cc/g-mole	C x 10^{-3} $(cc/g\text{-}mole)^2$	B cc/g-mole	C x 10^{-3} $(cc/g\text{-}mole)^2$
		99% Methane		
25	-42.9±1.5	2.39±0.8	-42.7±2.3	2.45±0.9
50	-33.2±1.0	1.78±0.4	-33.5±0.3	1.90±0.1
75	-26.5±1.1	1.96±0.5	-25.7±0.9	1.40±0.4
		78.8% Methane		
25	-55.4±1.3	2.68±0.6	-55.9±0.6	2.88±0.2
50	-43.7±0.5	2.15±0.2	-43.9±0.7	2.11±0.2
75	-34.1±1.1	1.71±0.4	-34.6±1.4	1.83±0.5
		57.2% Methane		
25	-72.4±3.0	3.25±1.6	-75.2±2.6	4.70±1.2
50	-60.5±0.4	3.21±0.1	-59.5±2.1	2.43±0.8
75	-49.8±0.4	2.82±0.1	-50.1±0.9	2.96±0.4
		38.8% Methane		
25	-91.0±1.5	4.10±0.9	-92.4±1.0	4.69±0.4
50	-77.5±0.1	4.31±0.1	-77.6±1.0	4.32±0.4
75	-64.3±0.2	3.67±0.7	-65.6±0.6	4.29±0.4
		18.4% Methane		
25	-116.9±1.4	6.54±0.6	-128.3±3.9	12.60±3.2
50	-98.3±0.7	5.71±0.1	-98.3±0.4	5.51±0.2
75	-82.0±0.6	4.70±0.1	-81.6±5.2	4.82±0.7
		99.9% Ethylene		
25	-145.6±4.8	9.79±2.6	-152.5±6.0	14.30±4.9
50	-120.4±1.3	7.05±0.4	-122.0±2.4	7.50±1.5
75	-100.8±1.1	5.98±0.8	-101.5±0.8	6.32±0.5

the same values. Most of the third virial coefficients agreed; however, the disagreements were more numerous than for the second virial coefficients.

Three empirical equations of state, RK, BWR, and Edmister et al. generalized BWR (GBWR), were compared with the experimental compressibility factors.

The two constants in the RK equation were calculated for the pure components using Eq. (III-44). The mixture constants were determined using the combination rules shown in Chapter III, Eq. (III-46). The compressibility factors for each of the gases including the impurities were calculated.

The eight constants used in the BWR equation for the hydrocarbon components were those recommended by Benedict, Webb, and Rubin (4). The values for carbon dioxide were from Eakin and Ellington (17). The mixing rules for determining mixture constants shown in Chapter III, Eq. (III-34), were used including the linear and Lorentz combinations for B_o.

The constants for the Edmister et al. generalized BWR equation were calculated from the expressions derived by Edmister, Vairogs, and Klekers (19) shown in Chapter III, Eq. (III-40). The values of the accentric factors used in calculating the generalized constants were taken from Edmister, Vairogs, and Klekers (19) and Huff and Reed (27).

A summary of the comparison of the empirical equations of state with the experimental compressibility data are shown in Table XVIII. The compressibility factors are compared in detail in Appendix J.

As shown in Table XVIII, the standard deviations for the RK equation varied from 0.016 to 0.064 over the range of the experimental

TABLE XVIII

SUMMARY OF COMPARISON OF EMPIRICAL EQUATIONS OF STATE WITH EXPERIMENTAL COMPRESSIBILITY FACTORS

Temperature °C	s_{RK}	s_{BWR}[1/]	s_{BWR}[2/]	s_{GBWR}
		99.0% Methane		
25	0.021	0.076	0.068	0.075
50	0.023	0.062	0.062	0.064
75	0.024	0.052	0.051	0.056
		78.8% Methane		
25	0.031	0.127	0.128	0.123
50	0.035	0.105	0.105	0.108
75	0.037	0.089	0.090	0.095
		57.2% Methane		
25	0.037	0.179	0.180	0.176
50	0.025	0.137	0.138	0.138
75	0.026	0.100	0.112	0.115
		38.4% Methane		
25	0.031	0.227	0.228	0.222
50	0.016	0.174	0.199	0.171
75	0.021	0.142	0.143	0.146
		18.4% Methane		
25	0.021	0.288	0.288	0.256
50	0.019	0.217	0.218	0.185
75	0.021	0.178	0.179	0.179
		99.9% Ethylene		
25	0.064	0.334		0.334
50	0.054	0.260		0.241
75	0.022	0.221		0.216

[1/] Linear combination for B_{om}

[2/] Lorentz combination for B_{om}

data, temperatures of 25 to 75 °C, pressures of 150 to 12,000 psia, and six gases. The variations seemed to be ramdon with no dependence on composition or temperature except for the ethylene data.

Examination in detail of the comparison of the RK equation with the experimental data was more revealing than considering only the standards deviations shown in Table XVIII. The differences between the RK equation and the experimental compressibility factors for methane (99% methane) and ethylene are shown in Figures 17 and 18, respectively, as functions of density. If the RK equation was restricted to densities below 0.65 lb.-mole per cu. ft. (pressures below 3100 psia or reduced pressures below 4.6) for methane and below 0.5 lb.-mole per cu. ft. (pressures below 1000 psia or reduced pressures below 1.35) for ethylene, the RK compressibility factors would fall within ±0.02 of the experimental data.

The combination rules used to calculate the RK mixture constants worked well as shown by the summary of the standard deviations in Table XVIII. The comparison for the 20-80 methane-ethylene mixture shown in Figure 19 reflected the results for the other methane-ethylene mixtures. The RK equation and combination rules did a good job of predicting the mixture compressibility data below densities of 0.6 lb.-mole per cu. ft.

As shown in Table XVIII, the BWR and the GBWR did not do as good a job of predicting the experimental data as the simplier RK equation. Furthermore, when comparing the BWR and GBWR equations as shown in Appendix J and in Figures 20 and 21, these equations did not do as well as the RK equation at the lower densities. If the BWR and GBWR were restricted to densities below 0.25 lb.-mole per cu. ft. (pressures

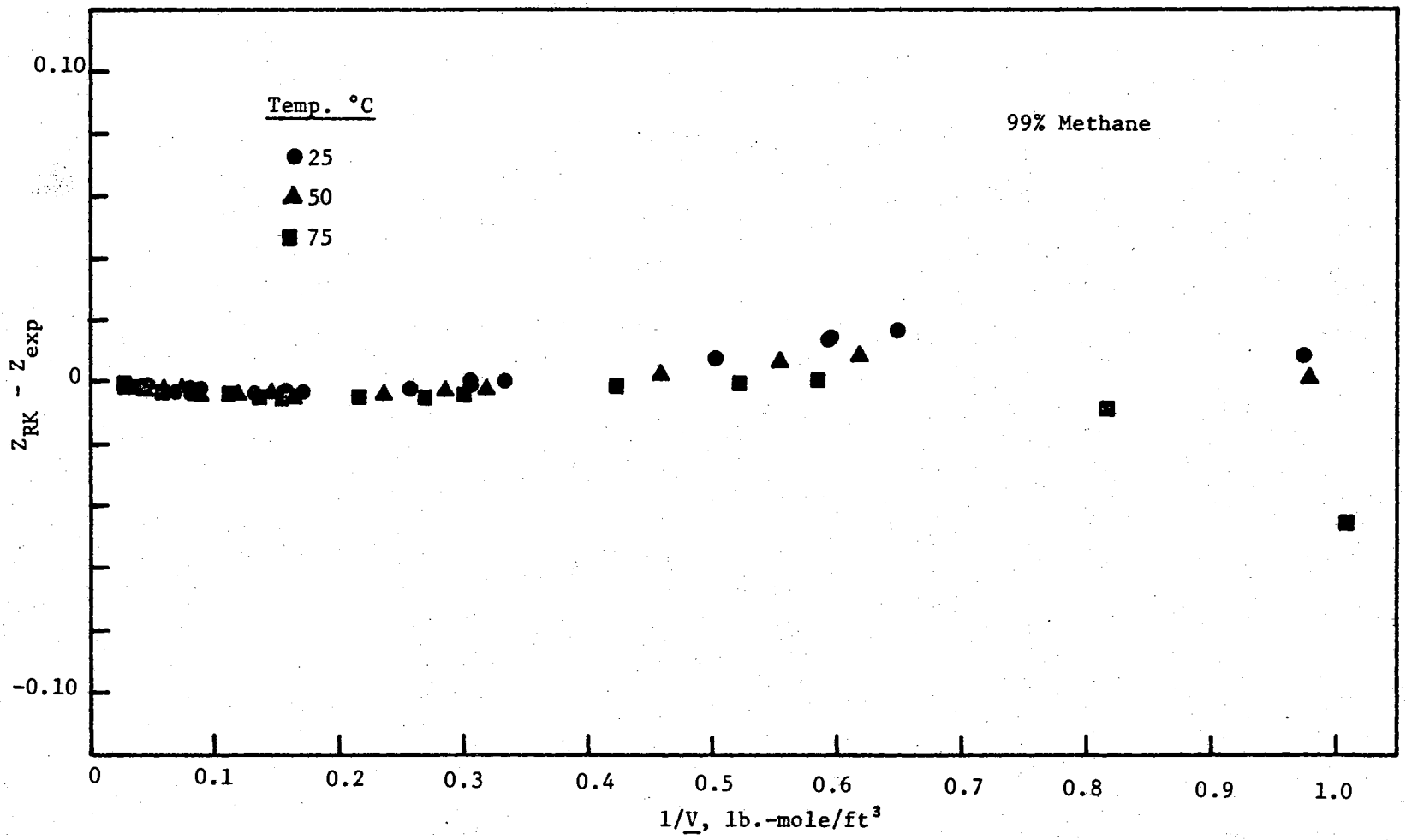

Figure 17. Comparison of Experimental Methane Compressibility Data with RK Equation of State

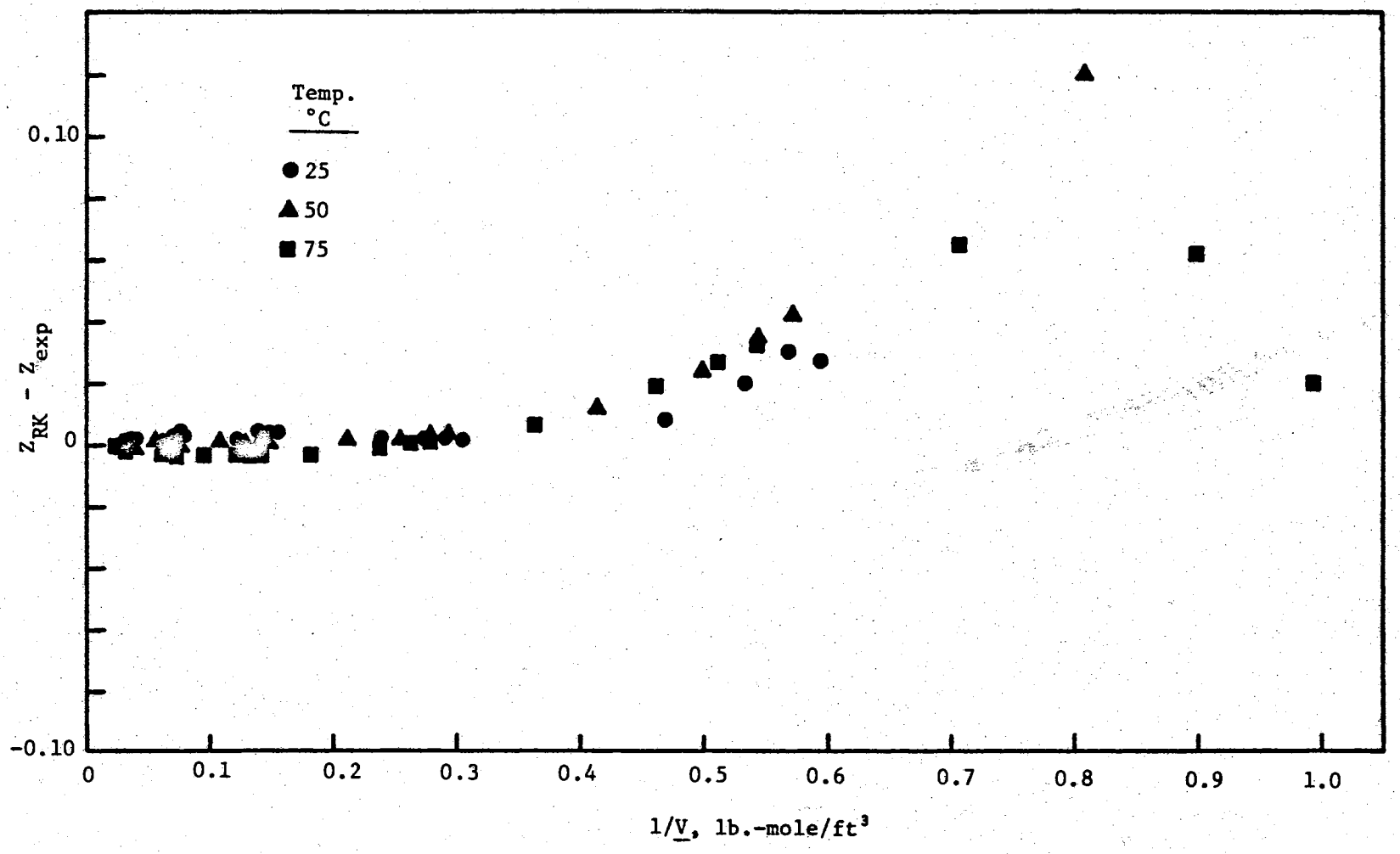

Figure 18. Comparison of Experimental Ethylene Compressibility Data with RK Equation of State

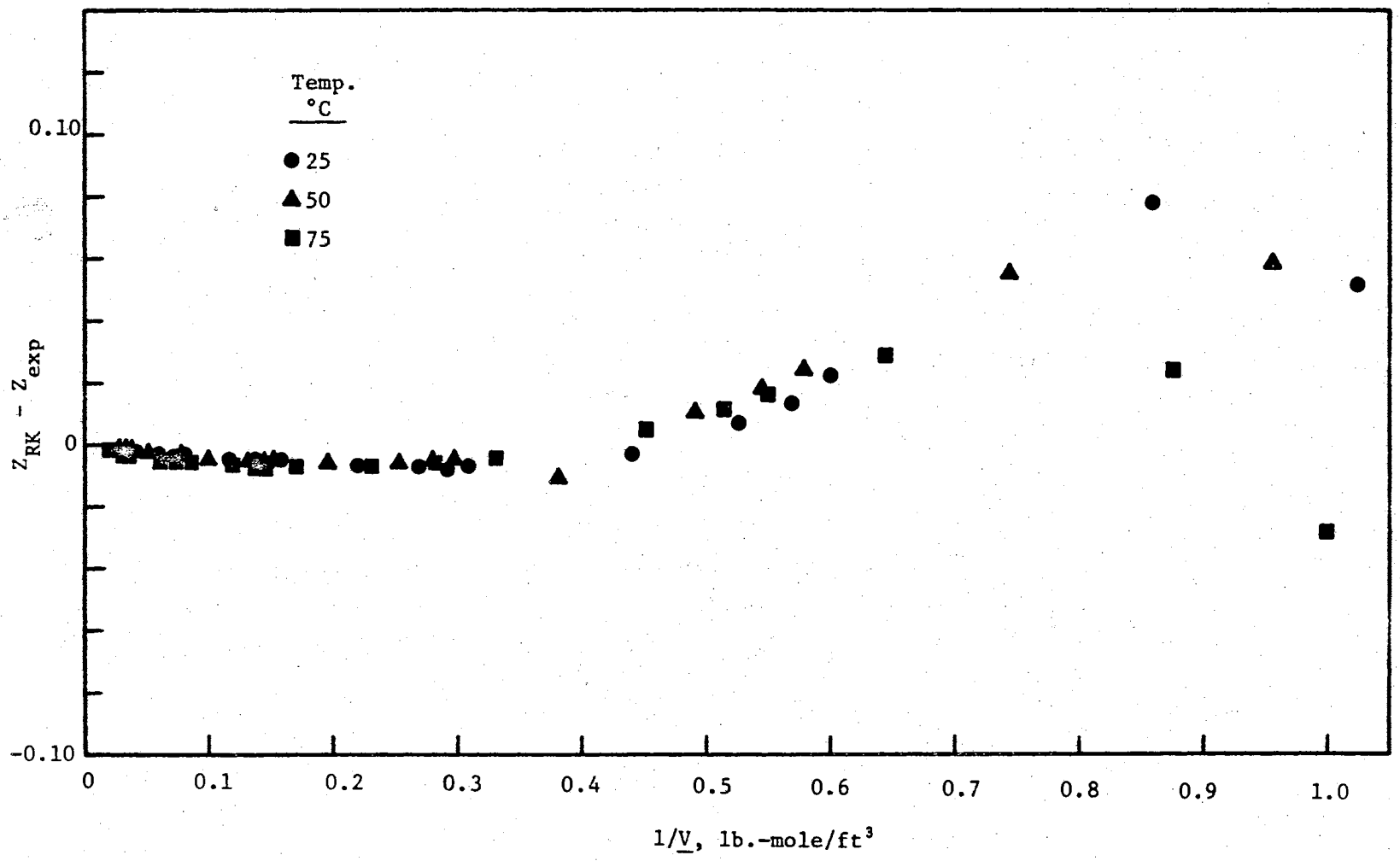

Figure 19. Comparison of 20-80 Methane-Ethylene Experimental Compressibility Data with RK Equation of State

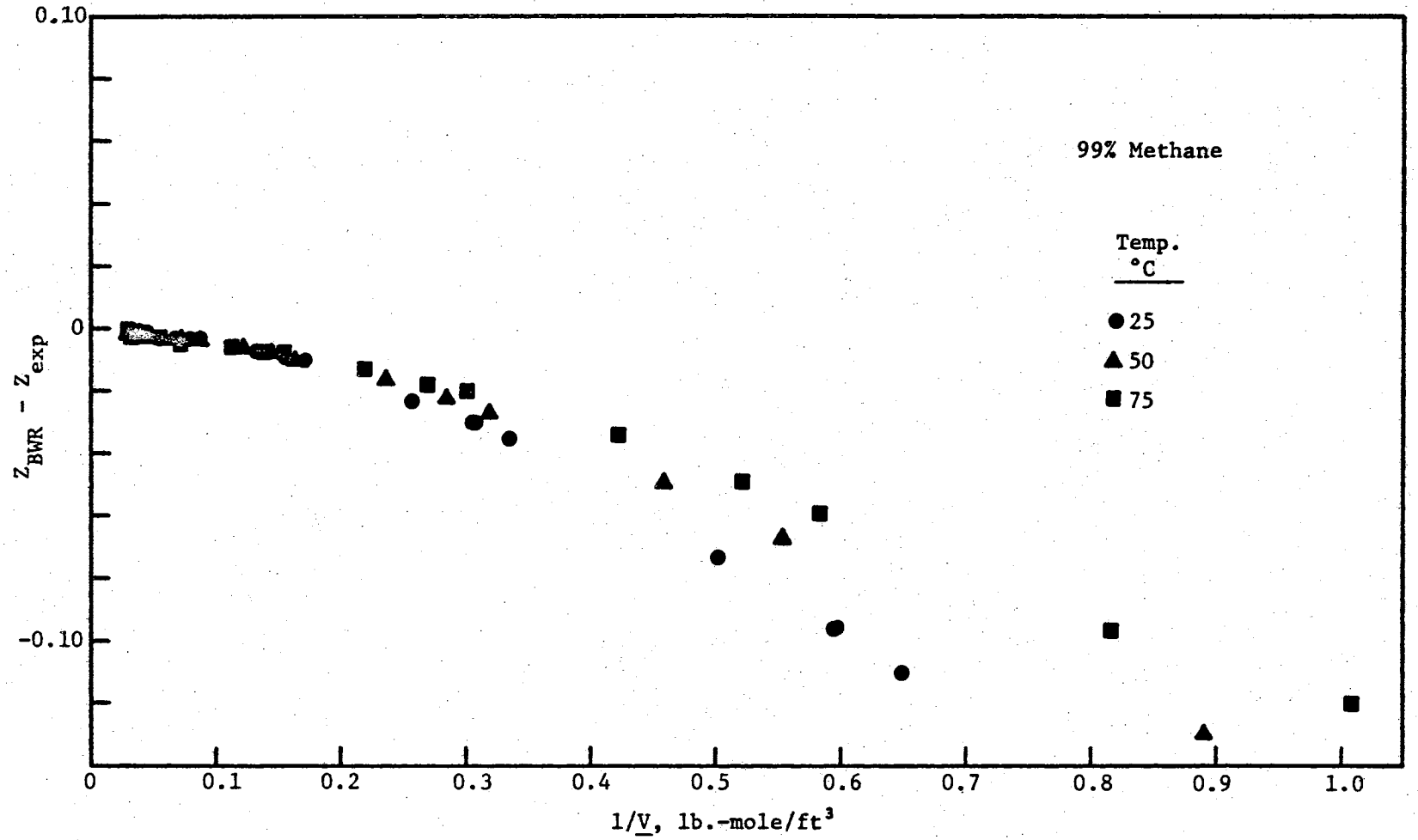

Figure 20. Comparison of Experimental Methane Compressibility Data with BWR Equation of State

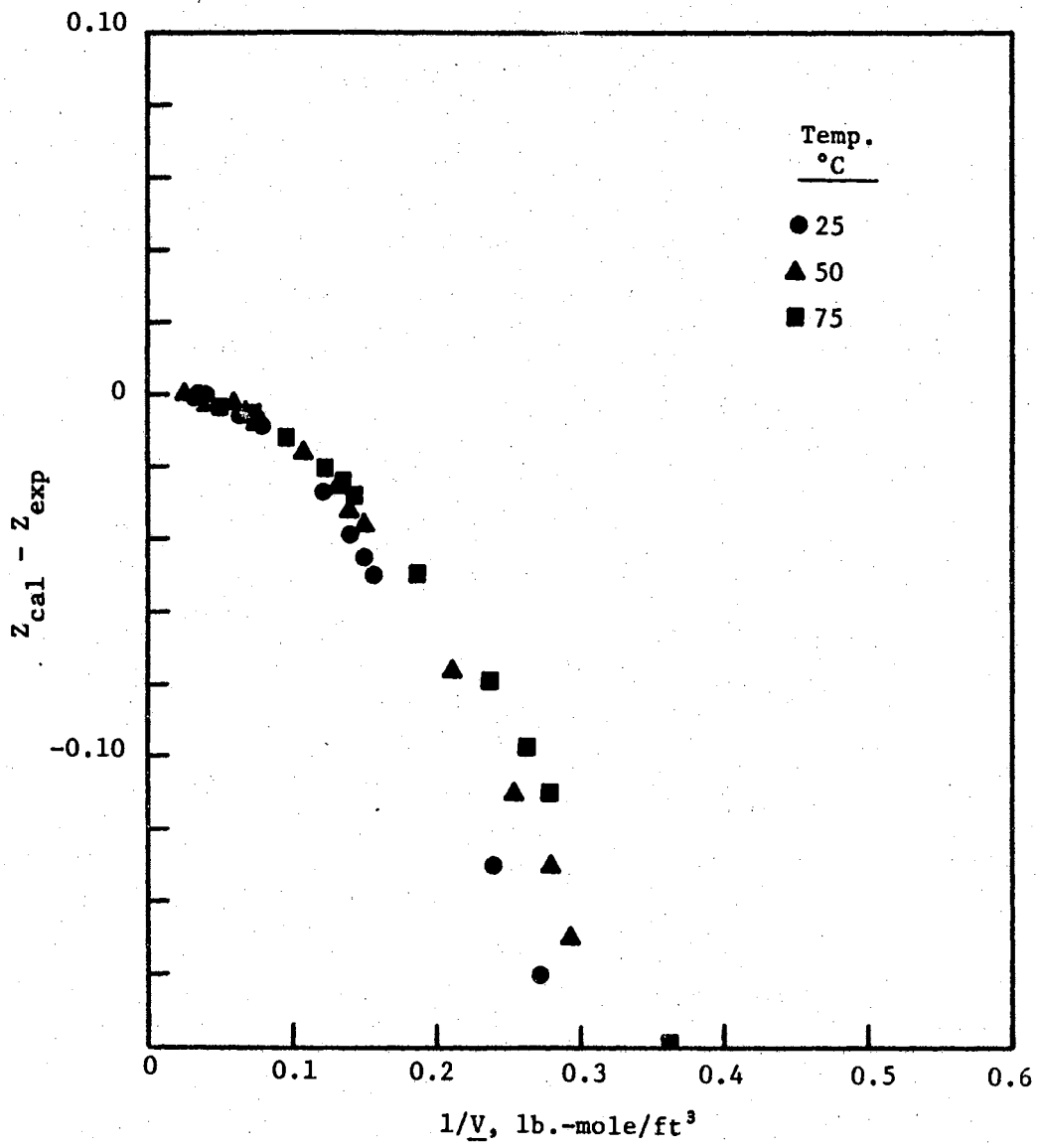

Figure 21. Comparison of Experimental Ethylene Compressibility Data with BWR Equation of State

below 1200 psia or reduced pressures of 1.8) for methane and below 0.12 lb.-mole per cu. ft. (pressures below 550 psia or reduced pressures below 0.74), their compressibility factors would fall within ±0.02 of the experimental data.

As shown in Table XVIII and in Appendix J, there was no difference between the BWR and the GBWR equations. Comparing the methane-ethylene mixtures with the BWR equations and combination rules was difficult since the BWR equations did not describe the experimental ethylene data very well or as well as the methane data. However, as shown in Table XVIII and in Appendix J, the linear combination rule for B_{om} worked as well as the Lorentz rule.

The second and third virial coefficients were calculated from the constants for the RK, BWR, and the Edmister et al. GBWR equations of state. The expressions for the second and third virial coefficients in terms of these three equations were presented in Chapter III. The expressions for the BWR and GBWR were:

$$B = B_o - A_o/(RT) - C_o/(RT^3) \qquad \text{(III-36)}$$

$$C = b - a/(RT) + c/(RT^3) \qquad \text{(III-37)}$$

The expressions for the RK equation were:

$$B = b - a/(RT^{1.5}) \qquad \text{(III-49)}$$

$$C = b^2 + ab/(RT^{1.5}) \qquad \text{(III-50)}$$

The results are shown in Table XIX and XX and are compared with the experimental values as derived by the slope-intercept and curve-fit methods.

In general, the second and third virial coefficients calculated from the constants for the RK, BWR, and the GBWR equations of state did not predict the experimental values within the estimated error of the experimental data. Considering that the RK equation has only two constants, the equation did a good job in predicting the second virial coefficient in comparison with the eight constant BWR equation.

The mixture data could provide an opportunity to check the combination rules for these three empirical equations. However as shown in the comparison with the experimental compressibility data, the equations inability to predict the pure component values made it difficult to draw conclusions.

The comparisons of the second and third virial coefficients based on the RK, BWR, and Edmister et al. GBWR equations of state indicated that improvements in these equations to predict compressibility data should be made in such a way as to improve their performance in predicting the second and third virial coefficients. No attempts were made as a part of this work to make improvements in these equations of state.

Lennard-Jones Potential Function

Lennard-Jones (32) proposed an intermolecular potential function for hard-sphere molecules. The potential function consisted of two terms: a term representing the attractive forces (first term) and a term representing the repulsive forces (second term). The potential

TABLE XIX

COMPARISON OF SECOND VIRIAL COEFFICIENTS

Units: cc/g-mole

Gas System	Slope-Intercept	Curve-Fit	BWR	Generalized BWR	RK
		25 °C			
Methane	-42.88±1.5	-42.70±2.30	-43.47	-44.72	-45.45
80-20	-55.39±1.3	-55.93±0.62	-56.42	-60.92	-61.04
60-40	-72.35±3.0	-75.20±2.60	-77.22	-77.04	-78.53
40-60	-90.96±1.5	-92.40±1.00	-93.95	-95.40	-97.89
20-80	-116.90±1.4	-128.30±3.90	-112.70	-116.10	-119.00
Ethylene	-145.60±4.8	-152.50±6.00	-123.60	-139.00	-142.10
		50 °C			
Methane	-33.22±1.0	-33.46±0.30	-35.41	-36.92	-36.89
80-20	-43.74±0.5	-43.87±0.71	-46.48	-50.96	-50.47
60-40	-60.54±0.4	-59.50±2.10	-64.88	-64.55	-65.74

TABLE XIX (Continued)

Gas System	Slope-Intercept	Curve-Fit	BWR	Generalized BWR	RK
40-60	-77.47±0.1	-77.60±1.00	-79.10	-79.97	-82.65
20-80	-93.32±0.7	-98.32±0.39	-94.02	-97.39	-101.20
Ethylene	-120.40±1.3	-122.10±2.40	-103.80	-116.70	-121.40
		75 °C			
Methane	-26.54±1.1	-25.69±0.90	-28.77	-30.49	-29.86
80-20	-34.07±1.1	-34.64±1.40	-38.37	-42.83	-41.78
60-40	-49.85±0.4	-50.12±0.93	-57.80	-54.40	-55.22
40-60	-64.30±0.2	-65.60±0.62	-67.05	-67.61	-70.17
20-80	-82.03±0.8	-81.60±5.20	-79.10	-82.47	-86.46
Ethylene	-100.80±1.1	-101.50±0.80	-87.96	-98.95	-104.30

TABLE XX

COMPARISON OF THIRD VIRIAL COEFFICIENTS

Units: $(cc/g\text{-}mole)^2 \times 10^{-3}$

Gas System	Slope-Intercept	Curve-Fit	BWR	Generalized BWR	RK
		25 °C			
Methane	2.39±0.80	2.45±0.87	3.16	3.17	3.11
80-20	2.68±0.60	2.88±0.21	4.51	4.55	3.95
60-40	3.25±1.60	4.70±1.20	6.58	6.68	4.93
40-60	4.10±0.90	4.69±0.37	9.61	9.85	5.52
20-80	6.54±0.60	12.60±3.20	13.93	14.40	6.69
Ethylene	9.79±2.60	14.30±4.90	19.92	20.80	8.85
		50 °C			
Methane	1.78±0.40	1.90±0.12	2.93	2.94	2.86
80-20	2.15±0.20	2.11±0.24	4.02	4.05	3.61

TABLE XX (Continued)

Gas System	Slope-Intercept	Curve-Fit	BWR	Generalized BWR	RK
60-40	3.21±0.09	2.43±0.81	5.65	5.74	4.50
40-60	4.31±0.08	4.32±0.40	8.02	8.23	5.52
20-80	5.71±0.07	5.51±0.19	11.38	11.79	6.69
Ethylene	7.05±0.40	7.50±1.50	16.03	16.75	8.02
		75 °C			
Methane	1.96±0.50	1.40±0.42	2.78	2.80	2.65
80-20	1.71±0.40	1.83±0.48	3.68	3.72	3.34
60-40	2.82±0.09	2.96±0.48	5.01	5.09	4.14
40-60	3.67±0.07	4.29±0.35	6.91	7.10	5.07
20-80	4.70±0.40	4.82±0.70	9.59	9.94	6.13
Ethylene	5.98±0.80	6.32±0.47	13.30	13.90	7.34

function expressed as a function of the intermolecular distance (r) is shown below:

$$\phi\ (r) \;=\; \lambda/r^{n} - \mu/r^{m} \qquad \text{(VI-7)}$$

The potential function is usually expressed in terms of σ where ϕ (σ = r) = 0 and the depth of the potential well ε, i.e., $\phi = \varepsilon$ where $d\phi/dr = 0$.

$$\phi\ (r) \;=\; \frac{m}{(n - m)} \left(\frac{n}{m}\right)^{\frac{n}{n-m}} \varepsilon\left[\left(\frac{\sigma}{r}\right)^{n} - \left(\frac{\sigma}{r}\right)^{m}\right] \qquad \text{(VI-8)}$$

Usually, an exponent of six for the repulsive term (m = 6) and an exponent of twelve for the attractive term (n = 12) works well for some simple gases.

The second virial coefficient shown below (23) as well as the others can be related to the intermolecular potential function.

$$B\ (T) \;=\; -\ \frac{2\pi\bar{N}}{3kT} \int_{0}^{\infty} r^{3}\ \frac{d\phi}{dr}\ e^{-\phi/(kT)}\ dr \qquad \text{(VI-9)}$$

The above expression has been integrated for the Lennard-Jones potential function (23). The resulting expression in terms of n and m is shown:

$$B\ (T) \;=\; -\ \frac{2\pi\bar{N}\sigma^{3}}{3} \left(\frac{3}{n}\right) \sum_{j=0}^{\infty} \frac{C_{nm}^{\gamma_j}}{j} \left(\frac{\varepsilon}{kT}\right)^{\gamma_j} \Gamma\left(\frac{jm - 3}{n}\right) \qquad \text{(VI-10)}$$

where $$\gamma_j \;=\; \frac{(n - m)j + 3}{n} \qquad \text{(VI-11)}$$

$$C_{nm} = \frac{m}{n - m} \left(\frac{n}{m}\right)^{\frac{n}{n - m}} \qquad \text{(VI-12)}$$

The parameters for the Lennard-Jones potential function can be determined from second virial coefficient data using Eq. (VI-10). Also, Eq. (VI-10) can be applied to second cross-coefficients (B_{ij}).

The pure component second virial coefficient data shown in Table IX and the cross coefficient data shown in Table XI were used to determine the parameters for the Lennard-Jones 6-12 potential function. The parameters were determined by a non-linear curve-fit of the second virial coefficient data. The non-linear curve-fit procedure is outlined in Appendix K. The resulting Lennard-Jones 6-12 parameters are shown in Table XXI with their 95% confidence intervals.

The second virial coefficients calculated from the Lennard-Jones 6-12 potential are compared with the experimental values in Table XXII. The Lennard-Jones 6-12 predicted the experimental second virial coefficients within the estimated error.

The Lennard-Jones parameters for pure components and mixtures can be used to check mixing rules for the cross parameters. The following rules are generally used for the Lennard-Jones function:

$$\sigma_{12} = \frac{\sigma_{11} + \sigma_{22}}{2} \qquad \text{(VI-13)}$$

$$\varepsilon_{12} = \sqrt{\varepsilon_{11}\, \varepsilon_{22}} \qquad \text{(VI-14)}$$

The confidence limits for the parameters shown in Table XXI were too wide for making comparisons of the experimental cross parameters with

TABLE XXI

LENNARD-JONES 6-12 PARAMETERS

Component	$\varepsilon \times 10^{13}$	$\sigma \times 10^{7}$
Methane	0.20±0.04	0.39±0.08
Ethylene	0.24±0.03	0.51±0.05
Methane-Ethylene	0.27±0.30	0.35±0.30

TABLE XXII

COMPARISON OF EXPERIMENTAL AND CALCULATED SECOND VIRIAL COEFFICIENTS

Lennard-Jones 6-12 Potential Function

Temperature °C	Experimental cc/g-mole	Calculated cc/g-mole	$B_{exp} - B_{cal}$
		Methane	
25	-41.57	-41.33	-0.23
50	-32.04	-32.56	0.52
75	-25.49	-25.21	-0.28
		Ethylene	
25	-145.60	-145.40	-0.20
50	-120.40	-120.90	0.50
75	-100.80	-100.50	-0.30
		Cross-coefficients Methane-Ethylene	
25	-61.15	-61.86	0.71
50	-53.99	-52.44	-1.55
75	-43.75	-44.58	0.83

the mixing rules. The Lennard-Jones parameters derived in this work were based upon only three data points (25, 50, 75 °C). A wider range of temperature with more data points are required to make a good check of the mixing rules as well as a better test of the Lennard-Jones potential function.

CHAPTER VII

CONCLUSIONS AND RECOMMENDATIONS

The three major objectives of this work were:

1. Design and assembly of an isothermal expansion ratio apparatus for the precise determination of compressibility factors of gases.

2. Use of this apparatus to obtain the compressibility factors for a binary gaseous system.

3. Comparison of the experimental compressibility factors and virial coefficient data with previous data and equations of state.

An isothermal expansion ratio apparatus was designed and assembled. This apparatus was used to obtain compressibility factors for methane, ethylene, and four of their binary mixtures. The compressibility factors and the derived second and third virial coefficients for methane and ethylene were compared with previous work. Combination rules for estimating mixture second virial coefficients for the methane-ethylene system were checked. Three empirical equations of state were compared with the experimental compressibility data. The experimental second and third virial coefficients were compared with coefficients derived from the empirical equations of state. In addition, the parameters for the Lennard-Jones 6-12 potential function were derived from the experimental second virial coefficients.

The conclusions and recommendations from this work are summarized in this section.

Apparatus

The isothermal expansion ratio apparatus was capable of providing precise data for determination of compressibility factors and virial coefficients. However, the apparatus at the School Chemical Engineering needs to be improved.

1. The temperature range of the air thermostat needs to be widened. Compressibility factors and virial coefficients over a wider temperature range provide a better basis for improving equations of state, testing intermolecular potential functions, or making other theoretical studies.

2. The temperature control of the air thermostat should be improved. During this work, temperature control of ±0.02 to ±0.01 °C was maintained.

3. The temperature of the air thermostat during this work was considered to be that of the gas in the bombs. The bombs should be modified so that the temperature of the gas sample could be measured directly.

4. The two high-pressure bombs were of equal and fixed volume. Another bomb with adjustable volume would improve the versatility of the apparatus. An adjustable volume would allow changing the cell constant N to obtain a desired spacing of the pressure measurements. The equal volume cells used in this investigation were not very suitable for high pressure work for the gases studied.

5. A general improvement of the laboratory facilities would aid in obtaining an apparatus that would be easier to operate and control, e.g., a constant temperature laboratory, a controlled access laboratory.

Experimental Data

1. The estimated error at the 95% confidence level for the experimental compressibility factors varied from 0.03 per cent to 0.68 per cent depending on the gas composition and temperature.

2. The experimental compressibility factors for methane and ethylene were compared with other investigators' data. The experimental methane data agreed within the estimated error at the 95% confidence level with other investigators' data at 25 and 50 °C, and only the low pressure data agreed at 75 °C. The experimental ethylene data agreed within the estimated error with data by Michels and Geldermans (41) at 25 °C, and only the low pressure data agreed at 50 and 75 °C.

3. Second and third virial coefficeints were derived from the experimental compressibility data using the slope-intercept method. In general, one order of accuracy was lost in deriving the second virial coefficient and two orders were lost in deriving the third virial coefficient from the compressibility data.

4. The experimental second and third virial coefficients for methane and ethylene were compared with literature values. The methane coefficients at 25 and 75 °C agreed within the estimated error with the literature values; the coefficients at 50 °C agreed with part of the literature values. Only the second virial coefficient for ethylene at 75 °C agreed with literature values within the estimated error. The third virial coefficients for ethylene at 50 and 75 °C agreed within the estimated error with data by Butcher and Dadson (7).

5. Of the four combination rules checked, the square root combination was the best in estimating second virial coefficients for binary mixtures of methane and ethylene from the pure component data.

6. The experimental compressibility factors were curve-fitted to a power series in density. The second and third virial coefficients determined by the curve-fit were compared with those derived by the slope-intercept method. In general, values of the second and third virial coefficients calculated using these two methods agreed within the estimated error at the 95% confidence level.

7. The RK, BWR, and Edmister et al. GBWR equations of state were compared with the experimental compressibility data. If the RK equation was restricted to densities from below 0.65 lb.-mole per cu. ft. (pressures below 3100 psia, reduced pressure 4.6) for methane to below 0.5 lb.-mole per cu. ft. (pressures below 1000 psia, reduced pressure 1.35) for ethylene, the RK compressibility factors would fall within ±0.02 of the experimental data. If the BWR and Edmister et al. GBWR were restricted to densities from below 0.25 lb.-mole per cu. ft. (pressures below 1200 psia, reduced pressure 1.8) for methane to below 0.12 lb.-mole per cu. ft. (pressures below 550 psia, reduced pressure 0.74) for ethylene, their compressibility factors would fall within ±0.02 of the experimental data.

8. Second and third virial coefficients were calculated from the constants for the RK, BWR, and Edmister et al. GBWR equations of state and compared to the experimental values. In general, the second and third virial coefficients based on these empirical equations of state did not predict the experimental values within the estimated error. The comparison of the three empirical equations of state with the experimental compressibility factors and virial coefficients showed that these equations need to be improved.

9. The experimental second virial coefficients were used to determine the parameters (σ,ε) for the Lennard-Jones 6-12 potential function and to check mixing rules for the cross parameters. The derived parameters were able to predict the values of the second virial coefficients within the estimated error. However, the estimated error for the parameters (σ,ε) were too large for testing the mixing rules.

SELECTED BIBLIOGRAPHY

1. Amagat, E. H., Annales de Chimie (5), 22, 353 (1881).

2. Bean, H. S., J. Research, National Bureau of Standards, 4 (1930).

3. Beattie, J. A., J. C. Huang, and M. Benedict, Proc. Am. Acad. Sci., 72, 137 (1938).

4. Benedict, M., G. B. Webb, and L. C. Rubin, Chem. Eng. Progr., 47, No. 8, 419 (1951).

5. Bloomer, O. T., Inst. Gas Tech. Res. Bul. 13, 12 pp. (1952).

6. Burnett, E. S., J. Appl. Mech. 3, A-136 (1936).

7. Butcher, E. G. and R. S. Dadson, Proc. Royal Soc. (London), Series A, 277, 448 (1964).

8. Canfield, Jr., F. B., Doctorate Thesis, Rice University, Houston, Texas (1962).

9. Canfield, F. B., T. W. Leland, and R. Kobayashi, Advan. Cry. Eng., 8, 146, Plenum Press, New York (1963).

10. Cattel, R. A. et al., U. S. Depart. Interior, Bur. Mines, R. I. 3501, 12 pp. (1940).

11. Ibid., R. I. 3616, 13 pp. (1942).

12. Cawood, W. and H. S. Patterson, J. Chem. Soc. (London), Part 1, 619 (1933).

13. Crain, R. W., Jr. and R. E. Sonntag, Advan. Cryog. Eng., 11, 379, Plenum Press, New York (1965).

14. Cook, D., Can. J. Chem., 35, 268 (1957).

15. Douslin, D. R., "Progress in International Research on Thermodynamics and Transport Properties", Papers of the Symposium on Thermophysical Properties, 2nd, Princeton, N. J., 135 pp. (1962).

16. Douslin, D. R., R. T. Moore, J. P. Dawson, and G. Waddington, J. Am. Chem. Soc., 80, 2031 (1958).

17. Eakin, B. E. and R. T. Ellington, Papers of the Symposium on Thermal Properties, Purdue University, Lafayette, Ind., 195 (1959).

18. Edmister, W. C., "Applied Hydrocarbon Thermodynamics", Gulf Publishing Co., Houston, Texas (1961).

19. Edmister, W. C., J. Vairogs, and A. J. Klekers, AIChE J., 14, 479 (1968).

20. Fruth, F. A. and T. T. H. Verschoyle, Proc. Royal Soc., 130A, 453 (1931).

21. Harper, R. C. and J. G. Miller, J. Chem. Phys., 27, 36 (1957).

22. Heichelheim, H. R., K. A. Kobe, I. H. Silberberg, and J. J. McKetta, J. Chem. Eng. Data, 7, 507 (1962).

23. Hirschfelder, J. C., C. F. Curtis, and R. B. Bird, "Molecular Theory of Gases and Liquids", John Wiley and Sons, Inc. (1954).

24. Hirth, L. J. and K. A. Kobe, J. Chem. Eng. Data, 6, 233 (1961).

25. Hoover, A. E., F. B. Canfield, R. Kobayashi, and T. W. Leland, Jr., J. Chem. Eng. Data, 9, 568 (1964).

26. Hoover, A. E., I. Nagata, T. W. Leland, Jr., and R. Kobayashi, J. Chem. Phys., 48, 2633 (1968).

27. Huff, J. A. and T. M. Reed, III, J. Chem. Eng. Data, 8, 306 (1963).

28. Kang, T. L., L. J. Hirth, K. A. Kobe, and J. J. McKetta, J. Chem. Eng. Data, 6, 220 (1961).

29. Keyes, F. G. and H. G. Burks, J. Am. Chem. Soc., 49, 1403 (1927).

30. Kramer, G. M. and J. G. Miller, J. Phys. Chem., 61, 785 (1957).

31. Kvalnes, H. M. and V. L. Gaddy, J. Am. Chem. Soc., 53, 394 (1931).

32. Lennard-Jones, J. E., Proc. Royal Soc. (London), 106A, 463 (1924).

33. Levelt, J. M. H., Doctorate Thesis, University of Amsterdam (1958).

34. MacCormack, K. E. and W. G. Schneider, J. Chem. Phys., 18, 1269 (1950).

35. Ibid., 19, 845 (1951).

36. Matthews, C. J. and C. O. Hurd, Trans. AIChE, 42, 55 (1946).

37. Masson, I. and L. G. F. Dolley, Proc. Royal Soc., 103A, 524 (1923).

38. McMath, Jr., H. G., Doctorate Thesis, Oklahoma State University, Stillwater, Oklahoma (1967).

39. Michels, A., B. Blaisse, and J. Hoogschagen, Physica, 9, 565 (1942).

40. Michels, A., J. DeGruyter, and F. Niesen, Physica, 3, 346 (1936).

41. Michels, A. and M. Geldermans, Physica, 9, 967 (1942).

42. Michels, A. and R. O. Gibson, Ann. Physik, 87, 850 (1928).

43. Michels, A. and G. W. Nederbragt, Physica 2, 1001 (1935).

44. Ibid., 3, 569 (1936).

45. Michels, A., T. Wassenaar, and T. N. Zwietering, Physica, 18, 67 (1952).

46. Michels, A., C. Michels, and H. Wouters, Proc. Royal Soc., 153A, 214 (1935).

47. Michels, A. and H. Wouters, Physica, 8, 923 (1941).

48. Mueller, W. H., Doctorate Thesis, Rice University, Houston, Texas (1959).

49. Mueller, W. H., T. W. Leland, Jr., and R. Kobayashi, AIChE J., 7, 267 (1961).

50. Nicholson, G. A. and W. G. Schneider, Can. J. Chem., 33, 589 (1955).

51. Olds, R. H., H. H. Reamer, B. H. Sage, and W. H. Lacey, Ind. Eng. Chem., 35, 922 (1943).

52. Ibid., 3, 569 (1936).

53. Pavlovich, N. V. and D. L. Timrot, Teploinergetike, 5, 69 (1958).

54. Pfefferle, W. C., Jr., J. A. Goff, and J. G. Miller, J. Chem. Phys., 23, 509 (1955).

55. Pfennig, H. W. and J. J. McKetta, Pet. Ref., 36, No. 11, 309 (1957).

56. Prausntiz, J. M., AIChE J., 5, 3 (1959).

57. Schamp, H. W., Jr., E. A. Mason, A. C. B. Richardson, and A. Attman, Phys. Fluids, 1, 329 (1958).

58. Schneider, W. G., Can. J. Res., 27B, 339 (1949).

59. Schneider, W. G. and J. A. H. Duffie, J. Chem. Phys., 17, 751 (1949).

60. Silberberg, I. H., K. A. Kobe, and J. J. McKetta, J. Chem. Eng. Data, 4, 314 (1959).

61. Ibid., 323 (1959).

62. Solbrig, C. W. and R. T. Ellington, Chem. Eng. Progr. Symp. Series, 59, No. 44, 127 (1963).

63. Stevens, A. B. and H. Vance, The Oil Weekly, 106, No. 1, 21 (1942).

64. Stroud, L., J. E. Miller, and L. W. Brandt, U. S. Depart. Interior, Bur. Mines, R. I. 5845, 11 pp. (1961).

65. Suh, K. W. and T. S. Storvick, AIChE J., 13, 231 (1967).

66. Vennix, A. J., Doctorate Thesis, Rice University, Houston, Texas (1966).

67. Walters, R. J., J. H. Tracht, E. B. Weinberger, and J. K. Rodgers, Chem. Eng. Prog., 50, 511 (1954).

68. Wiebe, R. V., L. Gaddy, and C. Heins, J. Am. Chem. Soc., 53, 1721 (1931).

69. Witonsky, R. J. and J. G. Miller, J. Am. Chem. Soc., 85, 282 (1963).

70. Whalley, E., Y. Lupien, and W. G. Schneider, Can. J. Chem., 31, 722 (1953).

71. Yntema, J. L. and W. G. Schneider, J. Chem. Phys., 18, 641 (1950).

72. York, R. and E. F. White, Trans. AIChE, 40, 227 (1944).

APPENDIX A

RUSKA PISTON GAGE

The Ruska gage (Model 2400 HL) is a dual-range instrument (low range 6-2428 psig, high range 30-12140 psig) using two piston-cylinder combinations. The gage was calibrated by comparison with a "plant master" gage (No. 7544) which was calibrated by National Bureau of Standards (NBS) to one part in 10,000 at 25 °C. The corrections for pressure distortion and thermal expansion of the plant master gage were also determined by NBS. The specifications for the Ruska gage are shown in Table A-I.

The loading for the Ruska piston gage is provided by a set of type 303 stainless steel "weights". The masses for each of the weights were measured by Ruska. The calibrations (see Table A-II) were reported to be accurate to one part in 50,000 for masses greater than 0.1 lb., one part in 20,000 for masses 0.01 to 0.1 lb., and one part in 10,000 for masses 0.001 to 0.01 lb.

TABLE A-I

RUSKA PISTON GAGE SPECIFICATIONS

Accuracy:	1:10,000
Resolution:	5:1,000,000
Low Range Piston-Cylinder (No. LC-142):	
Area @ 25 °C and 0 psig	0.130219 $in.^2$
Coefficient of thermal expansion	1.7×10^{-5} /°C
Coefficient of distortion	-5.4×10^{-8} /psi
High Range Piston-Cylinder (No. HC-133):	
Area @ 25 °C and 0 psig	0.0260416 $in.^2$
Coefficient of thermal expansion	1.7×10^{-5} /°C
Coefficient of distortion	-3.6×10^{-8}/psi

TABLE A-II

RUSKA MASS CALIBRATION

Designation	Nominal Pressure, psig		Apparent Mass versus Brass (M_A) lb.
	High Range	Low Range	
Low tare		6	0.78107
High tare	30		0.78107
A	1000	200	26.03509
B	1000	200	26.03537
C	1000	200	26.03571
D	1000	200	26.03570
E	1000	200	26.03536
F	1000	200	26.03592
G	1000	200	26.03603
H	1000	200	26.03558
I	1000	200	26.03568
J	1000	200	26.03608
K	1000	200	26.03568
L	500	100	13.01794
M	200	40	5.20714
N	200	40	5.20715
O	100	20	2.60359
P	50	10	1.30181
Q	20	4	0.52072
R	20	4	0.52074
S	10	2	0.26035
T	5	1	0.13020
U	2	0.4	0.05208
V	2	0.4	0.05209
W	1	0.2	0.02604
X	0.5	0.1	0.01302
$\overline{A}$	0.2	0.04	0.005203
$\overline{A}'$	0.2	0.04	0.005202
$\overline{B}$	0.1	0.02	0.002601
$\overline{C}$	0.05	0.01	0.001301
$\overline{D}$	0.02	0.004	0.000520
$\overline{D}'$	0.02	0.004	0.000521
$\overline{E}$	0.01	0.002	0.000260
$\overline{F}$	0.005	0.001	0.000130

APPENDIX B

TEXAS INSTRUMENTS QUARTZ PRESSURE GAGE

The Texas Instruments quartz gage (Model 141A) which was used to measure barometric pressure consisted of a low-hysteresis quartz Bourdon tube and a readout device.

The zero to 100 cm Hg quartz Bourdon tube was suspended in a glass cylinder. The top end of the Bourdon tube was evacuated and permanently sealed. A small mirror was attached to the bottom end of the Bourdon tube. The glass cylinder which was open to the atmosphere sat vertically in the readout device. As the barometric pressure changed, the Bourdon tube rotated. The amount of rotation was calibrated to measure pressure.

The readout device has an optical transducer mounted on a gear that travels concentrically around the Bourdon tube. Light reflected from the small mirror strikes a pair of balanced photocells which are connected to a microammeter. A closed-loop motor-driven servo-system automatically positions the gear so that the microammeter reads zero.

The Bourdon tube has a full scale rotation of 100 degrees. The amount of rotation is indicated on a dial. The dial reading is multiplied by a scale factor determined by calibration to give the measured pressure.

Texas Instruments calibrated the Bourdon tube against a 0.015% air-operated dead weight tester (its calibration traceable to NBS).

The calibration was made at a room temperature of 24 °C. A temperature correction factor was supplied with the pressure calibration. The calibration data were fitted to an empirical equation. The equation was:

$$P = 0.019336842\ [1 + 1.3 \times 10^{-4}\ (\frac{T - 32.0}{1.8} - 24.0)] \cdot$$
$$[0.03167 + 9.9358826\ R - 0.874314 \times 10^{-3}\ R^2 - 0.16175319 \times 10^{-5}\ R^3] \quad \text{(B-1)}$$

where P = psia

R = scale reading cm Hg

T = temperature at gage, °F

The first coefficient changes the units of the equation from mm Hg to psia. The second term corrects for temperature, and the third (a polynomial in R) resulted from the fit of the calibration data. The standard estimate of error for the fit and regression coefficients are shown below:

	Standard Estimate of Error
Fit	0.0047
Constant	0.0051
1st degree coefficient	0.0004
2nd degree coefficient	0.9×10^{-5}
3rd degree coefficient	0.5×10^{-7}

The standard estimate of error for pressures near 14.7 psia was 0.002.

APPENDIX C

PLATINUM RESISTANCE THERMOMETER AND MUELLER BRIDGE CALIBRATIONS

Platinum Resistance Thermometer

A four lead platinum resistance thermometer (Leeds and Northrup Model 8164, Serial No. 1612800) was used to measure temperatures. This thermometer was calibrated by NBS at the triple point of water, the steam point, the sulfur point and oxygen point. The calibration was made with 2 ma of current passing through the platinum resistance thermometer. This thermometer was certified by NBS as being a satisfactory standard for temperature on the International Practical Temperature Scale. The calibration was given in terms of the following formula:

$$t = \frac{R_t - R_o}{\alpha R_o} + \delta\left(\frac{t}{100} - 1\right)\frac{t}{100} + \beta\left(\frac{t}{100} - 1\right)\left(\frac{t}{100}\right)^3 \quad \text{(C-1)}$$

where t = °Celsius at outside surface of protective sheath

R_t = Resistance at $\underline{t}$ °C

R_o = Resistance at 0 °C

α = 0.003926375

δ = 1.49241

β = 0.11027 t below 0 °C

β = 0 t above 0 °C

R_o = 25.5446 abs ohms

Mueller Bridge

A Leeds and Northrup G-2 Mueller bridge was used to measure the resistance of the platinum thermometer. The bridge can measure a resistance from 0.0001 ohms to 111 ohms. The bridge has six dials in decades from 0.0001 to 100 ohms. The bridge was equipped with a switch to select either pair of leads from a four lead resistance thermometer. The average of the two readings (switch position R and N) gives the resistance of the thermometer independent of the resistance of the lead wires.

The Mueller bridge was calibrated by Leeds and Northrup. The results of the calibration are shown in Table C-I.

TABLE C-I

G-2 MUELLER BRIDGE CALIBRATION

(Serial No. 1550042)*

Reading	Correction, ohms	Reading	Correction, ohms
10 Dial		1 Dial	
0	0.0000	0	0.00000
10	0.0000	1	0.00001
20	0.0002	2	0.00002
20.5	0.0001	3	0.00002
30	0.0003	4	0.00002
40	0.0003	5	0.00003
50	0.0003	6	0.00004
60	0.0004	7	0.00005
70	0.0005	8	0.00006
80	0.0006	9	0.00006
90	0.0007	X	0.00006
X	0.0007		
0.1 Dial		0.01 Dial	
0.0	0.00000	0.00	0.00000
0.1	0.00000	0.01	0.00000
0.2	0.00000	0.02	0.00000
0.3	0.00001	0.03	0.00000
0.4	0.00001	0.04	0.00001
0.5	0.00002	0.05	0.00001
0.6	0.00002	0.06	0.00001
0.7	0.00002	0.07	0.00001
0.8	0.00002	0.08	0.00001
0.9	0.00003	0.09	0.00001
X	0.00003	X	0.00001

*Note: No correction for 0.001 and 0.0001 dial settings.

APPENDIX D

GAS COMPOSITIONS AND FUNDAMENTAL CONSTANTS

The six bottles of gases used in this study were donated by Phillips Petroleum Company of Bartlesville, Oklahoma. The donor analyzed the gases with a mass spectrometer and were reported to the nearest 0.1 mole per cent. A gas chromatographic analyses done at the School of Chemical Engineering confirmed Phillips' analyses. The composition of the gases are shown in Table D-I.

The value of the universal gas constant used in the calculations was 10.731496 $(psia\text{-}ft^3)/(lb\text{-}mole - °R)$.

The definition of the absolute temperature was expressed as $T(°K) = t(°C) + 273.15$. The expression for the Rankine scale was expressed as $T(°R) = t(°F) + 459.67$.

TABLE D-I

COMPOSITION OF GAS MIXTURES

(Phillips Petroleum Company Sample Transmittals No. 44043 through 44048)

Component	Mole %	Nominal Composition (Methane % - Ethylene %)	Cylinder Number
Methane	trace	0 - 100	MG-3943
Ethylene	99.9+		
Ethane	trace		
Total	100.0		
Methane	18.4	20 - 80	MG-4174
Ethylene	81.6		
Ethane	trace		
Propane	trace		
Total	100.0		
Methane	38.4	40 - 60	MG-1605
Ethylene	61.4		
Propane	0.2		
Ethane	trace		
Propylene	trace		
Total	100.0		
Methane	57.2	60 - 40	MG-576
Ethylene	42.4		
Propane	0.3		
Ethane	0.1		
Propylene	trace		
Total	100.0		
Methane	78.8	80 - 20	MG-4083
Ethylene	20.7		
Propane	0.4		
Ethane	0.1		
Propylene	trace		
Total	100.0		
Methane	99.0	100 - 0	MG-265
Nitrogen	0.6		
Propane	0.1		
Ethane	0.1		
Isobutane	trace		
Carbon Dioxide	0.2		
Total	100.0		

APPENDIX E

ICE POINT RESISTANCE OF PLATINUM THERMOMETER

The resistance of the platinum thermometer should be checked periodically since cycling the temperature of the thermometer can change its resistance. The resistance of the thermometer was checked before using it in this work.

By definition, the ice point of water (0 °C) is defined as ice and water in equilibrium saturated with air under a pressure of 760 mmHg. An ice bath was prepared keeping the above definition in mind. Ice was prepared from distilled water by spraying liquid nitrogen into a dewar of water that was stirred vigorously. The ice crystals were removed from the dewar and placed in another dewar containing the platinum resistance thermometer.

The first measurements were made after allowing the thermometer to stand in the ice bath for 4 hours. The ice bath was stirred before each measurement. More ice was added and another series of measurements were made the next morning. The barometric pressure and depth of submersion of the platinum resistance thermometer were noted.

The readings from the Mueller bridge were corrected using the calibration data (Appendix C). Also, the resistance measurements need to be corrected for barometric pressure and the submersion depth. The following expressions were used to determine these corrections (3).

Barometric Pressure

$$\Delta t_p = -1.3 \times 10^{-5} (P-760) \qquad \text{(E-1)}$$

Submersion

$$\Delta t_d = -0.072 \times 10^{-5} d \qquad \text{(E-2)}$$

where Δt_p = change in ice point due to pressure, °C

P = barometric pressure, mmHg

Δt_d = change due to depth of submersion

d = depth of submersion, mm

The barometric pressure varied from 736 to 737 mmHg and the platinum resistance thermometer was submersed 9 inches in the ice bath. The total temperature correction was 0.00015 °C. Approximately 0.0001Ω corresponds to 0.001 °C for a platinum 25 ohm resistance thermometer; hence, the correction to the resistance is very small (0.00001Ω) and can be neglected.

The results of ten measurements are summarized below:

Average Resistance $R_o = 25.5486\Omega$

Sample Deviation $s = 0.00009$

Confidence Limits for R_o

99% Level $25.5483 \leq R_o \leq 25.5488$

95% Level $25.5484 \leq R_o \leq 25.5487$

APPENDIX F

CALCULATION OF TEMPERATURE AND PRESSURE

In this appendix the procedures used for calculating temperatures from Mueller bridge resistance readings and the absolute pressure from the Ruska gage and Texas Instruments gage data are presented.

Temperature

During the pressure measurement, the temperature of the air thermostat was determined every 5 minutes using a platinum resistance thermometer and a Mueller bridge. Resistance readings from the Mueller bridge for the R and N positions were recorded. Readings were corrected using the Mueller bridge calibration (Appendix C). Temperature of the air thermostat was calculated from the resistances using the calibration formula shown in Appendix C and the value of R_o shown in Appendix E.

The calibration formula for calculating temperature is not explicit in temperature. Temperatures were calculated using an iteration procedure programmed for a digital computer (IBM 7040). The iteration procedure is described below using the following expressions:

$$R_t = \frac{R_N + R_R}{2} = \text{Average value of resistance}$$

$$t_c = \frac{R_t - R_o}{R_o} + f(t_a) \text{ Calibration formulae}$$

t_c = Calculated temperature

t_a = Assumed temperature

1. Assume a value for t_a.

2. Calculate t_c using calibration formula.

3. Compare t_c and t_a. If $\left|t_c - t_a\right| \leq 0.0001$, stop iteration; if not, let $t_a = t_c$ and repeat.

This iteration procedure worked well converging rapidly.

Pressure

Two pressure measurements were made after each expansion, one with the piston and weights rotating clockwise and the other counter-clockwise. The desired pressure in the lower chamber of the diaphragm cell was calculated based on the pressure at the Ruska gage reference level, barometric pressure, and various corrections.

The following expression related the desired pressure to the Ruska gage pressure and the corrections:

$$P = P_g - P_{oil} + P_{DPI} + P_b$$

where P_g = Pressure at reference level of Ruska gage, psig

P_{oil} = Pressure correction for head of oil on top of diaphragm when setting zero of DPI cell, psi

P_{DPI} = Pressure correction for zero shift of diaphragm with pressure, psi

P_b = Barometric pressure, psia

P = Pressure of gas in lower chamber of DPI cell, psia

The pressure at the Ruska gage reference level was calculated using the loading on the piston gage.

$$P_g = \frac{W}{A_E}$$

where W = Force on piston due to the "weights"

A_E = Effective area of piston

The force on the piston was determined using an approximate expression recommended by Ruska as being accurate to within one part per million.

$$W = \frac{g}{g_c}\left(1 = \frac{\rho_{AH}}{\rho_B}\right) M_A$$

where g = Acceleration due to gravity at Stillwater = $979.777 \frac{cm}{sec^2}$

g_c = Standard acceleration due to gravity = $980.665 \frac{cm}{sec^2}$

ρ_{AH} = Density of air at Houston = 0.0012 gm/cc

ρ_B = Density of brass

The effective area was calculated using the following equations:

$$A_{o,t} = A_o [1 + c(t - 25)]$$

$$A_E = A_{o,t} [1 + bP_N]$$

where A_o = Area of piston at 25 °C and 0 psig

c = Coefficient of thermal expansion

t = Temperature of Ruska piston gage

$A_{o,t}$ = Area of piston at t °C and 0 psig

b = Coefficient of pressure distortion

P_N = Nominal pressure

When the zero point of the DPI cell was set, the upper chamber pressure was higher than the lower chamber pressure by an amount equivalent to 2 inches of Ruska oil. Thus, the following expression was used to make this correction.

$$P_{oil} = 0.0022046 \times 16.3872\ h\ \rho_{oil}\ \frac{g}{g_c}$$

where h = Head of Oil = 2 inches

ρ_{oil} = Density of Ruska oil, g/cc

The coefficients in the above equation are conversion factors for changing units.

The zero point of the DPI cell changes with pressure. The following expression gives the correction as determined by calibration by Ruska.

$$P_{DPI} = P_g/S$$

where $S = 8/3 \times 10^5$

The expression for calculating the barometric pressure is shown in Appendix B.

The above calculational procedure was programmed for a digital computer. A sample calculation is shown below to illustrate the use of the equations. The data for the calculation are shown in Table F-I.

The correction for the head of oil:

$$\rho_{oil} = 0.85 \text{ g/cc}$$

$$P_{oil} = 0.0022046 \times 16.3872 \times 2 \times \frac{979.777}{980.665}$$

$$P_{oil} = 0.061 \text{ psi}$$

For the high range piston,

$$A_o = 0.026044$$

$$c = 1.7 \times 10^{-5}$$

$$b = -3.6 \times 10^{-8}$$

$$P_N = 3100$$

The effective area,

$$A_E = 0.026044\ [1 + 1.7 \times 10^{-5}(25.5 - 25)]\ [1 - 3.6 \times 10^{-8} \cdot (3100)]$$

$$A_E = 0.02604131 \text{ in.}^2$$

The load on the piston,

$$W = \frac{979.777}{980.665}\left(1 - \frac{0.0012}{8.4}\right) 80.68036$$

$$W = 80.595796 \text{ lb.}$$

and then

$$P_g = \frac{80.595796}{0.02604131}$$

$$P_g = 3094.921 \text{ psig}$$

The correction for the DPI zero shift:

$$P_{DPI} = 3094.921/(8/3 \times 10^5) \text{ psi}$$

$$P_{DPI} = 0.012 \text{ psi}$$

The pressure in the lower chamber of the DPI cell is:

$$P = 3094.921 - 0.061 + 0.012 + 14.422$$

$$P = 3109.294 \text{ psia}$$

TABLE F-I

DATA FOR PRESSURE CALCULATION

Run No. 3 First Expansion Weights	High Range Piston M_a, lb.
Hi tare	0.78107
A	26.03509
B	26.03537
C	26.03571
P	1.30181
S	0.26035
T	0.13020
U	0.05208
W	0.02604
X	0.01302
$\overline{A}$	0.005202
$\overline{B}$	0.002601
$\overline{C}$	0.001301
$\overline{D}$	0.000520
	M_a = 80.68036

t = 25.5 °C

P_b = 14.422

APPENDIX G

CORRECTING SECOND VIRIAL COEFFICIENTS FOR IMPURITIES

The gases used in this investigation contained small amounts of impurities (see Appendix D). The second virial data were corrected using the following equation relating the second-cross coefficients to the mixture second coefficients (23):

$$B_m = \sum_i^n \sum_j^n x_i x_j B_{ij} \qquad \text{(G-1)}$$

The cross-coefficient data for the impurities were taken from literature values as listed by Huff and Reed (27). Unavailable data were estimated using a correlation by Prausnitz (56) as modified by Huff and Reed (27).

Sample calculations for 25 °C data for methane and the 80-20 methane-ethylene mixture are shown to illustrate the procedure.

Methane

The composition of the methane used in this investigation is shown on next page.

TABLE G-I

COMPOSITION OF METHANE

i	Component	Mole %
1	Methane	99.0
2	Nitrogen	0.6
3	Ethane	0.1
4	Propane	0.1
5	Carbon Dioxide	0.2

Shown below in Table G-II are the terms in Eq. (G-I) for the methane mixture shown in Table G-I for 25 °C.

TABLE G-II

SECOND VIRIAL COEFFICIENTS FOR METHANE MIXTURE

	B_{ij}, cc/g-mole				
i \ j	1	2	3	4	5
1	B_{11}	-22.0	-92.0	-364	-244
2		-4.84	-46	-76.9	-44.1
3			-186.9	-270	-111
4				-359	-165
5					-124.6

All the values shown in Table G-II are literature values except B_{12}, B_{24}, and B_{34}. These three cross coefficients were estimated using Prausnitz's (56) correlation:

$$B_{ij} = \frac{V}{}_{cij} \; \theta \; (T/T_{cij}, \omega_{ij}) \qquad \text{(G-2)}$$

The mixing rules for the critical volume, critical temperature, and accentric factor were those recommended by Huff and Reed (27).

$$T_{cij} = \left(T_{cii}\, T_{cjj}\right)^{1/2} f_I\, f_s^6 \tag{G-3}$$

$$f_I = 2\left(I_i/I_j\right)^{1/2} / \left(1 + I_1/I_j\right) \tag{G-4}$$

$$f_s = 2\left(\underline{V}_{cii}/\underline{V}_{cjj}\right)^{1/6} \left[1 + \left(\underline{V}_{cii}/\underline{V}_{cjj}\right)^{1/3}\right] \tag{G-5}$$

$$\underline{V}_{cij} = \left[\frac{\underline{V}_{cii}^{1/3} + \underline{V}_{cjj}^{1/3}}{2}\right]^3 \tag{G-6}$$

$$\omega_{ij} = \frac{\omega_{ii} + \omega_{jj}}{2} \tag{G-7}$$

where T_c = Critical temperature

$\underline{V}_c$ = Critical volume

I = Ionization potential

ω = Accentric factor

For B_{12}

I_1	= 13.16	I_2	= 15.51
$\underline{V}_{c11}$	= 99.0 cc/g-mole	$\underline{V}_{c22}$	= 84.6 cc/g-mole
T_{c11}	= 191.1 °K	T_{c22}	= 126.2 °K
ω_{11}	= 0.010	ω_{22}	= 0.041

Then

$$f_I = 2(13.16/15.51)^{1/2} / (1 + 13.16/15.51) = 0.9966$$

$$f_s^6 = 2^6 (99/84.6) / [1 + (99/846)^{1/3}]^6 = 0.9979$$

$$T_{c12} = (191.1 \times 126.2)^{1/2} (0.9966) (0.9979) = 154.4$$

$$V_{c12} = \left[\frac{(99) + (84.6)^3}{2}\right]^3 = 91.6$$

$$\omega_{12} = 1/2 (0.01 + 0.04) = 0.0255$$

From Prausnitz (56):

$$\theta (1.93, 0.0255) = -0.240$$

$$B_{12} = 91.6 (-0.240) = -22.0 \text{ cc/g-mole}$$

For this calculation Eq. (G-1) becomes:

$$B_m = \sum_{i=1}^{5} \sum_{j=1}^{5} x_i x_j B_{ij}$$

Solve the previous equation for B_{11}.

$$B_{11} = \frac{B_m - \sum_i \sum_j x_i x_j B_{ij}}{x_{11}^2} \quad i \neq j \text{ for } i = 1$$

Substitute the values of B_{ij}'s from Table G-II into the above equation ($B_m = -42.88$ cc/g-mole).

$$B_{11} = \frac{-42.88 + 2.14}{0.9801} = -41.57$$

80-20 Methane-Ethylene

The composition of the 80-20 methane-ethylene mixture is shown below in Table G-III.

TABLE G-III

COMPOSITION 80-20 METHANE-ETHYLENE MIXTURE

i	Component	Mole %
1	Methane	78.8
2	Ethylene	20.7
3	Ethane	0.1
4	Propane	0.4

Shown below in Table G-IV are the terms for Eq. (G-1) for the 80-20 methane-ethylene mixture for 25 °C.

TABLE G-IV

SECOND VIRIAL COEFFICIENTS FOR 80-20 METHANE-ETHYLENE MIXTURE

	B_{ij}, cc/g-mole			
i \ j	1	2	3	4
1	B_{11}	B_{12}	-90	-364
2		B_{22}	-158	-224
3			-186.9	-270
4				-359

Using Eq. (G-1) the following expression can be written:

$$B_m = B'_m + \sum_i \sum_j x_i x_j B_{ij} \qquad i=3,4 \quad j=3,4 \tag{G-8}$$

where $$B'_m = x_1^2 B_{11} + 2x_1 x_2 B_{12} + x_2^2 B_{22} \tag{G-9}$$

The term B'_m is the desired term, corrected for the impurities. Solving Eq. (G-8) for B'_m gives:

$$B'_m = B_m - \sum_i \sum_j x_i x_j B_{ij} \qquad i=3,4 \quad j=3,4 \tag{G-10}$$

Substituting the values of the B_{ij}'s from Table G-IV gives ($B_m = -55.39$):

$$\sum_i \sum_j x_i x_j B_{ij} = -2.88 \qquad i=3,4 \quad j=3,4$$

$$B'_m = -55.39 + 2.88 = -52.51$$

The above second virial coefficient corresponds to a methane-ethylene mixture of the composition shown in Table G-V.

TABLE G-V

COMPOSITION OF MIXTURES CORRECTED FOR IMPURITIES

Nominal Composition		Mole %	
Methane	Ethylene	Methane	Ethylene
80	20	79.2	20.8
60	40	57.4	42.6
40	60	38.5	61.5
20	80	18.4	81.6

APPENDIX H

CALCULATION OF COMPRESSIBILITY FACTORS AND VIRIAL COEFFICIENTS

The calculation of the compressibility factors from the expansion data and the subsequent derivation of the virial coefficients from the compressibility data were done using a procedure programed for a digital computer. The procedure is outlined in this section.

The low pressure data from the isothermal expansions were curve-fitted to the following equation, using the number of coefficients that gave a minimum estimated error:

$$\frac{P_{i-1}}{P_i} = a_o + a_1 P_i + a_2 P_i^2 + \ldots \qquad \text{(H-1)}$$

Using Eq. (II-12), the following relationship is written:

$$N = a_o \qquad \text{(H-2)}$$

The resulting N's for each gas system are shown in Table H-I. These values of N should not be a function of composition since N is the ratio of the volume before an expansion to the volume after an expansion. The dependence on composition shown in Table H-I and Figure 22 were due probably at least in part to the procedure used in deriving N for each gas system at each isotherm. The cell constant N was derived

TABLE H-I

EXPANSION CELL CONSTANT

Gas System	N, Temperature, °C		
	25	50	75
Methane	1.9432	1.9362	1.9352
80-20	1.9418	1.9356	1.9332
60-40	1.9418	1.9389	1.9371
40-60	1.9424	1.9412	1.9386
20-80	1.9457	1.9443	1.9409
Ethylene	1.9496	1.9505	1.9425
Helium	1.94024	1.93554	1.93811

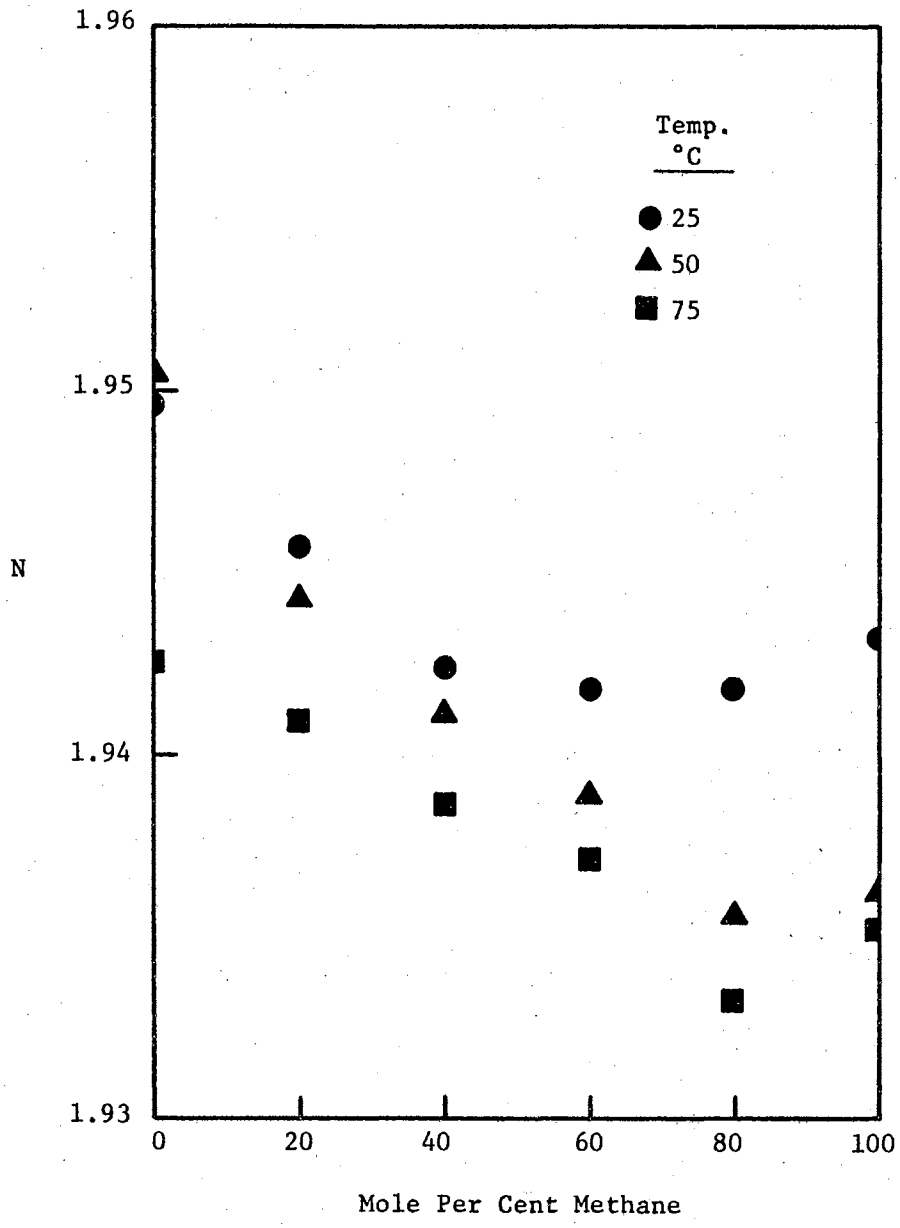

Figure 22. Expansion Cell Constant

by curve-fitting the low pressure expansion ratios. The pressure ratio plots for methane had less curvature at low pressures than for ethylene with their binaries being in between. In addition, pressure measurements below 150 psi with the piston gage were unreliable in general. Thus, these values of N reflected these difficulties.

The values of N for each gas system and the respective pressure data for each run were used to determine the initial value of the compressibility factor (z_o) for each run by curve-fitting using the following expression, using the number of coefficients that gave a minimum estimated error:

$$N^i P_i = b_o + b_1 P_i + b_2 P_i^2 + \ldots \qquad \text{(H-3)}$$

Using Eq. (II-13), the initial value of the compressibility factor is related to b_o in the above equation:

$$b_o = \frac{P_o}{Z_o} \qquad \text{(H-4)}$$

The cell constant, N, P_o/z_o, the pressure measurements, and temperature for each run were used as input data for a computer program written in Fortran IV for a 7040 IBM digital computer. The compressibility factors and the second and third virial coefficients were calculated using the following procedure:

1. Calculate compressibility factors from input data using following equation:

$$z_i = \frac{z_o}{P_o} N^i P_i$$

2. Calculate $(z_i - 1)\underline{V}_i = y_i$

where $\underline{V}_i = z_i RT/P_i$

Note that

$$(z_i - 1)\underline{V}_i = B + C/\underline{V}_i + D/\underline{V}_i^2 + \ldots$$

and

$$\text{Limit}_{P_i \to 0} \quad (z_i - 1)\underline{V}_i = B$$

3. Adjust P_o/z_o until a curve-fit of the low pressure data using the following model gives a minimum sum of squares:

$$y_i = \sum_i^k a_j \, (1/\underline{V}_i)^{j-1}$$

$$\sum_i^n (y_i - y_{cal})^2 = \text{minimum}$$

4. From the compressibility factors and B calculated in steps 1 through 3, calculate

$$y_i = ((z_i - 1)\underline{V}_i - B)\underline{V}_i$$

Note that

$$((z_i - 1)\underline{V}_i - B)\underline{V}_i = C + D/\underline{V}_i + E/\underline{V}_i^2 + \ldots$$

and

$$\text{Limit}_{P_i \to 0} \quad ((z_i - 1)\underline{V}_i - B)\underline{V}_i = C$$

5. Adjust the value of B until the curve-fit of the low pressure data using the following model gives a minimum sum of squares.

$$y_i = \sum_j^k a_j \, (1/\underline{V}_i)^{j-1}$$

6. The procedure outlined in steps 4 and 5 may be continued to calculate the third virial coefficient, the fourth, etc.

APPENDIX J

COMPARISON OF EQUATIONS OF STATE WITH EXPERIMENTAL COMPRESSIBILITY DATA

In this appendix, the compressibility factors calculated from the RK, BWR, and Edmister et al. GBWR are compared in detail with the experimental compressibility factors from Table IV in Table J-I.

TABLE J-I

COMPARISON OF EMPIRICAL EQUATIONS OF STATE WITH
EXPERIMENTAL COMPRESSIBILITY FACTORS

Temp. °C	1/V lb.-mole cu ft	z_{exp} [1]	z_{RK}	z_{BWR} [2]	z_{BWR} [3]	z_{GBWR}	Differences			
							$z_{RK}-z_{exp}$	z_{BWR} [2] $-z_{exp}$	z_{BWR} [3] $-z_{exp}$	$z_{GBWR}-z_{exp}$
				99.0% Methane						
25	1.2608	1.6422	1.5568	1.5196	1.5194	1.5451	-0.085	-0.12	-0.12	-0.097
	0.6488	0.8321	0.8490	0.7220	0.7219	0.7143	0.017	-0.11	-0.11	-0.12
	0.3339	0.8406	0.8411	0.8056	0.8055	0.8006	0.0005	-0.035	-0.035	-0.04
	0.1718	0.9002	0.8972	0.8897	0.8897	0.8870	-0.0030	-0.010	-0.010	-0.013
	0.0884	0.9438	0.9414	0.9406	0.9406	0.9392	-0.0023	-0.0031	-0.0031	-0.0045
	0.0455	0.9697	0.9683	0.9688	0.9688	0.9680	-0.0014	-0.0010	-0.0010	-0.0017
	1.1517	1.3556	1.3205	1.1953	1.1951	1.2069	-0.035	-0.16	-0.16	-0.15
	0.5927	0.8218	0.8353	0.7258	0.7258	0.7184	0.014	-0.096	-0.096	-0.10
	0.3050	0.8490	0.8482	0.8190	0.8190	0.8144	-0.0008	-0.030	-0.030	-0.035
	0.1570	0.9074	0.9043	0.8984	0.8984	0.8960	-0.0031	-0.0090	-0.0090	-0.011
	0.0808	0.9483	0.9460	0.9456	0.9456	0.9443	-0.0023	-0.0027	-0.0028	-0.0040
	0.0416	0.9723	0.9709	0.9714	0.9714	0.9707	-0.0014	-0.0008	-0.0009	-0.0016

[1] Experimental compressibility factors from Table IV.

[2] Based on linear combination for B_{om}.

[3] Based on Lorentz combination for B_{om}.

TABLE J-I (Continued)

Temp. °C	1/V lb.-mole cu. ft.	z_{exp} [1]	z_{RK}	z_{BWR} [2]	z_{BWR} [3]	z_{GBWR}	Differences $z_{RK}-z_{exp}$	z_{BWR} [2] $-z_{exp}$	z_{BWR} [3] $-z_{exp}$	$z_{GBWR}-z_{exp}$
25	0.9755	1.0558	1.0652	0.8827	0.8825	0.8813	0.0093	-0.17	-0.17	-0.17
	0.5020	0.8171	0.8250	0.7440	0.7439	0.7371	0.0080	-0.073	-0.073	-0.080
	0.2583	0.8648	0.8624	0.8422	0.8422	0.8383	-0.0024	-0.023	-0.023	-0.027
	0.1329	0.9200	0.9165	0.9129	0.9128	0.9107	-0.0035	-0.0072	-0.0072	-0.0093
	0.0684	0.9563	0.9536	0.9536	0.9536	0.9525	-0.0027	-0.0027	-0.0027	-0.0038
	0.0352	0.9769	0.9752	0.9757	0.9757	0.9751	-0.0017	-0.0011	-0.0011	-0.0017
	1.1606	1.3711	1.3370	1.2172	1.2172	1.2298	-0.034	-0.15	-0.15	-0.14
	0.5972	0.8217	0.8362	0.7254	0.7253	0.7178	0.015	-0.096	-0.096	-0.10
	0.3074	0.8480	0.8476	0.8179	0.8179	0.8133	-0.0004	-0.030	-0.030	-0.035
	0.1582	0.9068	0.9037	0.8977	0.8977	0.8952	-0.0031	-0.0091	-0.0092	-0.012
	0.0814	0.9484	0.9456	0.9452	0.9452	0.9439	-0.0027	-0.0032	-0.0032	-0.0045
	0.0419	0.9725	0.9707	0.9712	0.9712	0.9705	-0.0018	-0.0013	-0.0013	-0.0019
						std. dev.	0.021	0.076	0.068	0.075
50	1.1972	1.6001	1.5148	1.4792	1.4790	1.4883	-0.086	-0.12	-0.12	-0.11
	0.6179	0.8979	0.904	0.8175	0.8174	0.8069	0.0085	-0.080	-0.080	-0.091
	0.3189	0.8848	0.8827	0.8581	0.8581	0.8517	-0.0021	-0.027	-0.027	-0.033
	0.1646	0.9261	0.9216	0.9165	0.9165	0.9137	-0.0045	-0.0096	-0.0096	-0.013
	0.0849	0.9584	0.9547	0.9543	0.9543	0.9525	-0.0037	-0.0042	-0.0042	-0.0060
	0.0438	0.9778	0.9753	0.9757	0.9757	0.9748	-0.0024	-0.0021	-0.0021	-0.0030
	1.0722	1.3219	1.2866	1.1834	1.1832	1.1818	-0.035	-0.14	-0.14	-0.14
	0.5534	0.8827	0.8894	0.8156	0.8155	0.8056	0.0067	-0.067	-0.067	-0.077
	0.2856	0.8910	0.8883	0.8690	0.8690	0.8632	-0.0026	-0.022	-0.022	-0.028
	0.1474	0.9321	0.9280	0.9242	0.9242	0.9212	-0.0041	-0.0079	-0.0079	-0.011
	0.0761	0.9621	0.9590	0.9588	0.9588	0.9572	-0.0031	-0.0033	-0.0033	-0.0049
	0.0393	0.9797	0.9778	0.9782	0.9782	0.9773	-0.0019	-0.0015	-0.0015	-0.0023
	0.8911	1.0677	1.0692	0.9380	0.9378	0.9287	0.0015	-0.13	-0.13	-0.14

TABLE J-I (Continued)

Temp. °C	1/V lb.-mole cu. ft.	z_{exp} [1]	z_{RK}	z_{BWR} [2]	z_{BWR} [3]	z_{GBWR}	Differences $z_{RK}-z_{exp}$	z_{BWR} [2] $-z_{exp}$	z_{BWR} [3] $-z_{exp}$	$z_{GBWR}-z_{exp}$
50	0.4599	0.8739	0.8769	0.8245	0.8244	0.8157	0.0029	-0.049	-0.049	-0.058
	0.2373	0.9029	0.8991	0.8865	0.8864	0.8816	-0.0038	-0.016	-0.016	-0.021
	0.1225	0.9421	0.9380	0.9358	0.9358	0.9333	-0.0041	-0.0063	-0.0063	-0.0088
	0.0632	0.9682	0.9653	0.9654	0.9654	0.9641	-0.0029	-0.0028	-0.0028	-0.0042
	0.0326	0.9831	0.9814	0.9818	0.9818	0.9811	-0.0018	-0.0014	-0.0014	-0.0021
						std. dev.	0.023	0.062	0.062	0.064
75	1.1312	1.5568	1.4680	1.4404	1.4402	1.4380	-0.089	-0.12	-0.12	-0.12
	0.5845	0.9475	0.9486	0.8890	0.8889	0.8765	0.0010	-0.0010	-0.059	-0.071
	0.3020	0.9193	0.9153	0.8990	0.8990	0.8918	-0.0040	-0.020	-0.020	-0.027
	0.1561	0.9459	0.9412	0.9379	0.9379	0.9340	-0.0047	-0.0080	-0.0080	-0.012
	0.0807	0.9687	0.9656	0.9653	0.9653	0.9633	-0.0032	-0.0034	-0.0034	-0.0054
	0.0417	0.9825	0.9811	0.9814	0.9814	0.9803	-0.0014	-0.0011	-0.0011	-0.0021
	1.0096	1.3214	1.2761	1.2030	1.2028	1.1937	-0.045	-0.12	-0.12	-0.13
	0.5217	0.9310	0.9310	0.8819	0.8819	0.8704	0.0000	-0.049	-0.049	-0.061
	0.2696	0.9235	0.9186	0.9060	0.9059	0.8995	-0.0049	-0.018	-0.018	-0.024
	0.1393	0.9511	0.9460	0.9436	0.9436	0.9401	-0.0051	-0.0075	-0.0075	-0.011
	0.0720	0.9724	0.9689	0.9688	0.9688	0.9670	-0.0036	0.0037	-0.0037	-0.005
	0.0372	0.9850	0.9830	0.9833	0.9833	0.9824	-0.0019	-0.0016	-0.0017	-0.0026
	0.8180	1.0839	1.0760	0.9874	0.9872	0.9738	-0.0079	-0.096	-0.097	-0.11
	0.4227	0.9170	0.9154	0.8826	0.8825	0.8728	-0.0015	-0.034	-0.034	-0.044
	0.2184	0.9317	0.9267	0.9189	0.9189	0.9136	-0.0050	-0.013	-0.013	-0.018
	0.1129	0.9586	0.9543	0.9530	0.9530	0.9502	-0.0044	-0.0056	-0.0056	-0.0084
	0.0583	0.9770	0.9742	0.9744	0.9744	0.9729	-0.0028	-0.0026	-0.00027	-0.0041
	0.0301	0.9874	0.9861	0.9864	0.9864	0.9856	-0.0012	-0.0010	-0.0010	-0.0017
						std. dev.	0.024	0.052	0.051	0.056

TABLE J-I (Continued)

Temp. °C	1/V lb.-mole cu. ft.	z_{exp} [1]	z_{RK}	z_{BWR} [2]	z_{BWR} [3]	z_{GBWR}	Differences $z_{RK}-z_{exp}$	$z_{BWR}-z_{exp}$ [2]	$z_{BWR}-z_{exp}$ [3]	$z_{GBWR}-z_{exp}$
					78.8% Methane					
25	1.2357	1.6803	1.5726	1.5468	1.5444	1.5575	-0.11	-0.13	-0.14	-0.12
	0.6364	0.7541	0.7560	0.5516	0.5504	0.5503	0.0020	-0.20	-0.20	-0.20
	0.3277	0.7890	0.7766	0.7179	0.7173	0.7160	-0.012	-0.071	-0.072	-0.073
	0.1688	0.8704	0.8594	0.8463	0.8460	0.8450	-0.011	-0.024	-0.024	-0.025
	0.0869	0.9279	0.9206	0.9188	0.9186	0.9181	-0.0074	-0.0091	-0.0093	-0.0099
	0.0448	0.9615	0.9572	0.9577	0.9576	0.9572	-0.0043	-0.0039	-0.0039	-0.0043
	1.1360	1.3543	1.2998	1.1289	1.1267	1.1361	-0.055	-0.23	-0.23	-0.22
	0.5850	0.7469	0.7459	0.5670	0.5658	0.5653	-0.0013	-0.20	-0.18	-0.18
	0.3013	0.7998	0.7871	0.7380	0.7374	0.7361	-0.013	-0.062	-0.062	-0.064
	0.1552	0.8796	0.8687	0.8581	0.8578	0.8569	-0.011	-0.021	-0.022	-0.023
	0.0799	0.9335	0.9264	0.9252	0.9251	0.9245	-0.0071	-0.0083	-0.0085	-0.0090
	0.9923	1.0426	1.0348	0.7611	0.7592	0.7645	-0.0078	-0.28	-0.28	-0.28
	0.5110	0.7467	0.7408	0.5998	0.5986	0.5978	-0.0059	-0.15	-0.15	-0.15
	0.2632	0.8177	0.8045	0.7679	0.7674	0.7661	-0.013	-0.050	-0.050	-0.052
	0.1355	0.8931	0.8827	0.8753	0.8750	0.8742	-0.010	-0.018	-0.018	-0.019
	0.0698	0.9418	0.9350	0.9345	0.9343	0.9338	-0.0068	-0.0073	-0.0075	-0.0036
	0.0359	0.9692	0.9653	0.9659	0.9658	0.9656	-0.0039	-0.0033	-0.0034	-0.0036
						std. dev.	0.031	0.127	0.128	0.123
50	1.1667	1.6192	1.5003	1.4489	1.4466	1.4473	-0.12	-0.17	-0.17	-0.17
	0.6028	0.8339	0.8279	0.6830	0.6819	0.6771	-0.0060	-0.15	-0.15	-0.16
	0.3114	0.8432	0.8291	0.7890	0.7883	0.7850	-0.014	-0.054	-0.055	-0.058
	0.1609	0.9027	0.8903	0.8821	0.8817	0.8797	-0.012	-0.020	-0.021	-0.023
	0.0831	0.9457	0.9375	0.9368	0.9367	0.9355	-0.0082	-0.0089	-0.0091	-0.010

TABLE J-I (Continued)

Temp. °C	1/V lb.-mole cu. ft.	z_{exp} [1]	z_{RK}	z_{BWR} [2]	z_{BWR} [3]	z_{GBWR}	Differences $z_{RK}-z_{exp}$	$z_{BWR}-z_{exp}$ [2]	$z_{BWR}-z_{exp}$ [3]	$z_{GBWR}-z_{exp}$
50	0.0429	0.9705	0.9661	0.9668	0.9667	0.9661	-0.0044	-0.0037	-0.0038	-0.0044
	1.0609	1.3282	1.2643	1.1107	1.1086	1.1070	-0.064	-0.22	-0.22	-0.22
	0.5481	0.8227	0.8154	0.6919	0.6909	0.6861	-0.0073	-0.13	-0.13	-0.14
	0.2832	0.8514	0.8376	0.8051	0.8045	0.8013	-0.014	-0.046	-0.047	-0.050
	0.1463	0.9099	0.8983	0.8920	0.8917	0.8898	-0.012	-0.018	-0.018	-0.020
	0.0756	0.9502	0.9426	0.9423	0.9422	0.9412	-0.0076	-0.0078	-0.0078	-0.0090
	0.0390	0.9741	0.9690	0.9697	0.9696	0.9691	-0.0051	-0.0044	-0.0045	-0.0050
	0.8888	1.0306	1.0142	0.8023	0.8006	0.7968	-0.016	-0.23	-0.23	-0.23
	0.4592	0.8188	0.8083	0.7191	0.7182	0.7138	-0.011	-0.10	-0.10	-0.10
	0.2372	0.8683	0.8543	0.8326	0.8321	0.8293	-0.014	-0.036	-0.036	-0.039
	0.1226	0.9231	0.9;22	0.9085	0.9083	0.9067	-0.011	-0.015	-0.015	-0.016
	0.0633	0.9580	0.9512	0.9514	0.9513	0.9504	-0.0068	-0.0066	-0.0067	-0.0076
	0.0327	0.9772	0.9739	0.9746	0.9745	0.9740	-0.0034	-0.0027	-0.0027	-0.0032
							0.035	0.105	0.105	0.108
75	1.1137	1.6010	1.4731	1.4312	1.4290	1.4214	-0.13	-0.17	-0.17	-0.18
	0.5761	0.8974	0.8842	0.7818	0.7807	0.7728	-0.013	-0.12	-0.12	-0.12
	0.2980	0.8855	0.8697	0.8423	0.8417	0.8369	-0.016	-0.043	-0.044	-0.049
	0.1541	0.9273	0.9142	0.9092	0.9089	0.9061	-0.013	-0.018	-0.018	-0.021
	0.0799	0.9592	0.9506	0.9506	0.9605	0.9490	-0.0086	-0.0086	-0.0087	-0.010
	0.0412	0.9775	0.9731	0.9738	0.9737	0.9730	-0.0044	-0.0037	-0.0037	-0.0045
	1.0005	1.3278	1.2546	1.1349	1.1329	1.1243	-0.073	-0.19	-0.19	-0.20
	0.5175	0.8831	0.8693	0.7842	0.7832	0.7758	-0.014	-0.099	-0.10	-0.11
	0.2677	0.8921	0.8763	0.8548	0.8543	0.8499	-0.016	-0.037	-0.038	-0.042
	0.1385	0.9337	0.9211	0.9175	0.9172	0.9148	-0.013	-0.016	-0.016	-0.019
	0.0716	0.9632	0.9552	0.9554	0.9553	0.9540	-0.0080	-0.0078	-0.0079	-0.0093
	0.0371	0.9805	0.9757	0.9764	0.9764	0.9757	-0.0048	-0.0041	-0.0042	-0.0048
	0.8369	1.0761	1.0458	0.8930	0.8914	0.8823	-0.030	-0.18	-0.18	-0.19

TABLE J-I (Continued)

Temp. °C	1/V lb.-mole cu. ft.	z_{exp} [1]	z_{RK}	z_{BWR} [2]	z_{BWR} [3]	z_{GBWR}	Differences $z_{RK}-z_{exp}$	z_{BWR} [2] $-z_{exp}$	z_{BWR} [3] $-z_{exp}$	$z_{GBWR}-z_{exp}$
75	0.4329	0.8747	0.8594	0.7988	0.7979	0.7914	-0.015	-0.076	-0.077	-0.083
	0.2239	0.9040	0.8884	0.8744	0.8740	0.8702	-0.016	-0.030	-0.030	-0.034
	0.1158	0.9436	0.9318	0.9299	0.9297	0.9276	-0.011	-0.014	-0.014	-0.016
	0.0599	0.9692	0.9619	0.9624	0.9623	0.9612	-0.0074	-0.0068	-0.0069	-0.0080
	0.0310	0.9840	0.9795	0.9802	0.9801	0.9796	-0.0044	-0.0038	-0.0038	-0.0044
						std. dev.	0.037	0.089	0.090	0.095
					57.2% Methane					
25	1.2066	1.7214	1.5889	1.5436	1.5405	1.5319	-0.13	-0.18	-0.18	-0.19
	0.6214	0.6594	0.6547	0.3461	0.3445	0.3560	-0.0047	-0.31	-0.31	-0.30
	0.3200	0.7248	0.7073	0.6161	0.6153	0.6192	-0.018	-0.11	-0.11	-0.11
	0.1648	0.8334	0.8188	0.7970	0.7966	0.7979	-0.015	-0.036	-0.036	-0.035
	0.0849	0.9076	0.8984	0.8944	0.8941	0.8946	-0.0092	-0.013	-0.013	-0.013
	0.0437	0.9488	0.9454	0.9453	0.9452	0.9454	-0.0034	-0.0035	-0.0036	-0.0034
	1.1216	1.3568	1.2950	1.0586	1.0557	1.0582	-0.062	-0.30	-0.30	-0.30
	0.5776	0.6532	0.6478	0.3726	0.3711	0.3815	-0.0054	-0.28	-0.28	-0.27
	0.2975	0.7372	0.7200	0.6415	0.6408	0.6442	-0.017	-0.096	-0.096	-0.093
	0.1532	0.8432	0.8294	0.8110	0.8106	0.8118	-0.014	-0.032	-0.033	-0.031
	0.0789	0.9140	0.9049	0.9017	0.9015	0.9019	-0.0090	-0.012	-0.012	-0.012
	0.0406	0.9543	0.9491	0.9491	0.9490	0.9492	-0.0053	-0.0052	-0.0053	-0.0052
	1.0115	1.0449	1.0288	0.6476	0.6450	0.6557	-0.016	-0.40	-0.040	-0.39
	0.5209	0.6574	0.6466	0.4154	0.4141	0.4229	-0.011	-0.24	-0.24	-0.23
	0.2682	0.7563	0.7383	0.6750	0.6743	0.6771	-0.018	-0.081	-0.081	-0.079
	0.1381	0.8569	0.8437	0.8292	0.8289	0.8298	-0.013	-0.028	-0.028	-0.027
	0.0711	0.9223	0.9136	0.9113	0.9111	0.9114	-0.0087	-0.011	-0.011	-0.011

TABLE J-I (Continued)

Temp. °C	1/V lb.-mole cu. ft.	z_{exp} [1]	z_{RK}	z_{BWR} [2]	z_{BWR} [3]	z_{GBWR}	Differences $z_{RK}-z_{exp}$	$z_{BWR}-z_{exp}$ [2]	$z_{BWR}-z_{exp}$ [3]	$z_{GBWR}-z_{exp}$
25	0.0366	0.9590	0.9539	0.9541	0.9549	0.9541	-0.0051	-0.0049	-0.0050	-0.0049
						std. dev.	0.037	0.179	0.180	0.176
50	1.1563	1.6388	1.5532	1.4953	1.4923	1.4776	-0.086	-0.14	-0.15	-0.16
	0.5964	0.7452	0.7449	0.5179	0.5164	0.5204	-0.0003	-0.23	-0.23	-0.22
	0.3076	0.7835	0.7697	0.7051	0.7044	0.7048	-0.014	-0.078	-0.079	-0.079
	0.1586	0.8672	0.8552	0.8411	0.8407	0.8404	-0.012	-0.026	-0.026	-0.027
	0.0818	0.9261	0.9182	0.9164	0.9162	0.9159	-0.0079	-0.0097	-0.0099	-0.010
	0.0422	0.9602	0.9559	0.9565	0.9564	0.9562	-0.004	-0.0038	-0.0039	-0.0041
	1.0608	1.3171	1.2766	1.0638	1.0611	1.0562	-0.041	-0.25	-0.26	-0.26
	0.5471	0.7394	0.7349	0.5376	0.5362	0.5396	-0.0045	-0.20	-0.20	-0.20
	0.2822	0.7953	0.7809	0.7272	0.7265	0.7268	-0.014	-0.068	-0.069	-0.069
	0.1455	0.8768	0.8650	0.8537	0.8536	0.8530	-0.012	-0.023	-0.023	-0.024
	0.0751	0.9319	0.9244	0.9232	0.9230	0.9227	-0.0076	-0.0087	-0.0089	-0.0092
	0.0387	0.9650	0.9594	0.9600	0.9599	0.9597	-0.0056	-0.0049	-0.0050	-0.0052
	0.9172	1.0018	1.0018	0.6843	0.6819	0.6848	0.0000	-0.32	-0.32	-0.32
	0.4731	0.7402	0.7314	0.5791	0.5779	0.5802	0.0088	-0.16	-0.16	-0.16
	0.2440	0.8145	0.8003	0.7613	0.7607	0.7607	-0.014	-0.053	-0.054	-0.054
	0.2158	0.8914	0.8805	0.8729	0.8726	0.8722	-0.011	-0.019	-0.019	-0.019
	0.0649	0.9407	0.9338	0.9334	0.9333	0.9330	-0.0068	-0.0072	-0.0073	-0.0077
	0.0335	0.9682	0.9647	0.9654	0.9653	0.9651	-0.0036	-0.0028	-0.0029	-0.0031
						std. dev.	0.025	0.137	0.138	0.138
75	1.1058	1.6044	1.5147	1.4558	1.4530	1.4344	-0.090	-0.15	-0.15	-0.17
	0.5708	0.8191	0.8145	0.6492	0.6478	0.6466	-0.0046	-0.17	-0.17	-0.17
	0.2947	0.8327	0.8193	0.7743	0.7735	0.7717	-0.013	-0.058	-0.059	-0.061
	0.1521	0.8959	0.8844	0.8756	0.8753	0.8739	-0.012	-0.020	-0.020	-0.022

TABLE J-I (Continued)

Temp. °C	1/V lb.-mole cu. ft.	z_{exp} [1]	z_{RK}	z_{BWR} [2]	z_{BWR} [3]	z_{GBWR}	Differences $z_{RK}-z_{exp}$	$z_{BWR}-z_{exp}$ [2]	$z_{BWR}-z_{exp}$ [3]	$z_{GBWR}-z_{exp}$
75	0.0785	0.9418	0.9343	0.9339	0.9337	0.9328	-0.0076	-0.0080	-0.0082	-0.0090
	0.0405	0.9687	0.9644	0.9654	0.9652	0.9648	-0.0042	-0.0033	-0.0034	-0.0039
	1.0073	1.3154	1.2705	1.0955	1.0929	1.0827	-0.045	-0.22	-0.22	-0.23
	0.5200	0.8091	0.8024	0.6612	0.6599	0.6586	-0.0067	-0.15	-0.15	-0.15
	0.2684	0.8416	0.8282	0.7916	0.7910	0.7892	-0.013	-0.050	-0.051	-0.052
	0.1386	0.9036	0.8928	0.8861	0.8857	0.8844	-0.011	-0.018	-0.018	-0.019
	0.0715	0.9465	0.9396	0.9396	0.9394	0.9386	-0.0069	-0.0069	-0.0071	-0.0079
	0.0369	0.9712	0.9674	0.9684	0.9683	0.9679	-0.0037	-0.0028	-0.0029	-0.0033
	0.8606	1.0389	1.0284	0.7867	0.7844	0.7809	-0.010	-0.25	-0.25	-0.26
	0.4443	0.8056	0.7957	0.6901	0.6890	0.6875	-0.010	-0.12	-0.12	-0.12
	0.2294	0.8576	0.8440	0.8187	0.8181	0.8164	-0.014	-0.039	-0.039	-0.041
	0.1184	0.9161	0.9059	0.9019	0.9016	0.9004	-0.010	-0.014	-0.015	-0.016
	0.0611	0.9541	0.9477	0.9482	0.9480	0.9473	-0.0064	-0.0059	-0.0060	-0.0067
	0.0316	0.9752	0.9720	0.9729	0.9729	0.9725	-0.0032	-0.0023	-0.0024	-0.0027
						std. dev.	0.026	0.100	0.112	0.115
					38.4% Methane					
25	1.1819	1.7279	1.6139	1.5357	1.5329	1.4982	-0.11	-0.19	-0.20	-0.23
	0.6086	0.5580	0.5610	0.1404	0.1390	0.1633	-0.0030	-0.42	-0.42	-0.39
	0.3133	0.6593	0.6433	0.5163	0.5156	0.5249	-0.016	-0.14	-0.14	-0.13
	0.1613	0.7939	0.7816	0.7495	0.7491	0.7525	-0.012	-0.044	-0.045	-0.041
	0.0830	0.8864	0.8779	0.8710	0.8708	0.8722	-0.0085	-0.015	-0.016	-0.014
	0.0428	0.9396	0.9345	0.9336	0.9335	0.9341	-0.0051	-0.0061	-0.0062	-0.0056
	1.1172	1.3861	1.3338	1.0525	1.0498	1.0379	-0.052	-0.33	-0.34	-0.35
	0.5752	0.5573	0.5569	0.1712	0.1699	0.1926	-0.0004	-0.39	-0.39	-0.36
	0.2961	0.6713	0.6558	0.5423	0.5416	0.5501	-0.015	-0.13	-0.13	-0.12

TABLE J-I (Continued)

Temp. °C	1/V lb.-mole cu. ft.	z_{exp} [1]	z_{RK}	z_{BWR} [2]	z_{BWR} [3]	z_{GBWR}	Differences $z_{RK}-z_{exp}$	$z_{BWR}-z_{exp}$ [2]	$z_{BWR}-z_{exp}$ [3]	$z_{GBWR}-z_{exp}$
25	0.1525	0.8038	0.7916	0.7632	0.7628	0.7660	-0.012	-0.041	-0.041	-0.038
	0.0785	0.8921	0.8841	0.8780	0.8779	0.8792	-0.0080	-0.014	-0.014	-0.013
	0.0404	0.9427	0.9380	0.9372	0.9371	0.9377	-0.0047	-0.0055	-0.0056	-0.0050
	1.0122	1.0068	1.0125	0.5193	0.5169	0.5290	0.0058	-0.49	-0.49	-0.48
	0.5211	0.5641	0.5581	0.2300	0.2288	0.2488	-0.0060	-0.33	-0.34	-0.32
	0.2683	0.6928	0.6777	0.5846	0.5840	0.5913	-0.015	-0.11	-0.11	-0.10
	0.1381	0.8201	0.8083	0.7854	0.7851	0.7879	-0.011	-0.035	-0.035	-0.032
	0.0711	0.9022	0.8942	0.8895	0.8893	0.8905	-0.0081	-0.013	-0.013	-0.012
	0.0366	0.9483	0.9436	0.9431	0.9430	0.9435	-0.0047	-0.0052	-0.0053	-0.0048
						std. dev.	0.031	0.227	0.228	0.222
50	1.1431	1.6567	1.6070	1.5367	1.5339	1.4970	-0.050	-0.12	-0.12	-0.16
	0.5889	0.6588	0.6669	0.3501	0.3487	0.3625	-0.0081	-0.31	-0.31	-0.30
	0.3033	0.7258	0.7144	0.6223	0.6216	0.6262	-0.011	-0.10	-0.10	-0.10
	0.1563	0.8331	0.8227	0.8014	0.8010	0.8023	-0.010	-0.032	-0.032	-0.031
	0.0805	0.9072	0.9004	0.8969	0.8967	0.8971	-0.0069	-0.010	-0.011	-0.010
	0.0415	0.9502	0.9464	0.9467	0.9466	0.9467	-0.0038	-0.0036	-0.0037	-0.0034
	1.0660	1.3376	1.3235	1.0695	1.0670	1.0518	-0.014	-0.27	-0.27	-0.29
	0.5492	0.6562	0.6596	0.3760	0.3747	0.3873	0.0033	-0.28	-0.28	-0.27
	0.2829	0.7381	0.7261	0.6465	0.6458	0.6499	-0.012	-0.092	-0.092	-0.088
	0.1457	0.8427	0.8326	0.8146	0.8142	0.8154	-0.010	-0.028	-0.028	-0.027
	0.0751	0.9130	0.9065	0.9038	0.9036	0.9039	-0.0065	-0.0093	-0.0094	-0.0091
	0.0387	0.9534	0.9499	0.9503	0.9502	0.9503	-0.0035	-0.0031	-0.0032	-0.0031
	0.9430	0.9926	1.0150	0.5999	0.5977	0.6032	0.022	-0.39	-0.39	-0.39
	0.4858	0.6604	0.6577	0.4279	0.4268	0.4373	-0.0027	-0.23	-0.23	-0.22
	0.2502	0.7591	0.7471	0.6857	0.6851	0.6883	-0.012	-0.073	-0.074	-0.071
	0.1289	0.8584	0.8490	0.8357	0.8354	0.8363	-0.0094	-0.023	-0.023	-0.022

TABLE J-I (Continued)

Temp. °C	1/V lb.-mole cu. ft.	z_{exp} [1]	z_{RK}	z_{BWR} [2]	z_{BWR} [3]	z_{GBWR}	Differences $z_{RK}-z_{exp}$	z_{BWR} [2] $-z_{exp}$	z_{BWR} [3] $-z_{exp}$	$z_{GBWR}-z_{exp}$
50	0.0664	0.9225	0.9165	0.9148	0.9147	0.9149	-0.0059	-0.0076	-0.0078	-0.0075
	0.0342	0.9608	0.9555	0.9560	0.9559	0.9560	-0.0054	-0.0049	-0.0049	-0.0049
						std. dev.	0.016	0.174	0.199	0.185
75	1.0945	1.6301	1.5551	1.4738	1.4712	1.4366	-0.075	-0.16	-0.16	-0.19
	0.5646	0.7454	0.7487	0.5135	0.5122	0.5185	0.0033	-0.23	-0.23	-0.23
	0.2912	0.7834	0.7720	0.7066	0.7059	0.7072	-0.011	-0.077	-0.077	-0.076
	0.1502	0.8670	0.8565	0.8429	0.8425	0.8424	-0.010	-0.024	-0.024	-0.026
	0.0775	0.9259	0.9189	0.9176	0.9175	0.9171	-0.0070	-0.0083	-0.0084	-0.0088
	0.0400	0.9692	0.9562	0.9572	0.9571	0.9568	-0.0040	-0.0031	-0.0032	-0.0034
	1.0067	1.3188	1.2864	1.0542	1.0518	1.0362	-0.032	-0.26	-0.27	-0.28
	0.5193	0.7390	0.7387	0.5340	0.5327	0.5383	-0.0004	-0.21	-0.21	-0.20
	0.2679	0.7945	0.7828	0.7282	0.7276	0.7285	-0.012	-0.066	-0.067	-0.066
	0.1382	0.8760	0.8660	0.8551	0.8548	0.8545	-0.010	-0.021	-0.021	-0.021
	0.0713	0.9314	0.9249	0.9241	0.9240	0.9237	-0.0065	-0.0073	-0.0074	-0.0077
	0.0368	0.9632	0.9596	0.9606	0.9605	0.9603	-0.0036	-0.0026	-0.0027	-0.0029
	0.8764	1.0142	1.0186	0.6841	0.6820	0.6824	0.0045	-0.33	-0.33	-0.33
	0.4521	0.7398	0.7346	0.5750	0.5739	0.5782	-0.0052	-0.16	-0.16	-0.16
	0.2332	0.8130	0.8011	0.7611	0.7605	0.7610	-0.012	-0.052	-0.052	-0.052
	0.1203	0.8901	0.8806	0.8733	0.8730	0.8728	-0.0095	-0.017	-0.017	-0.017
	0.0621	0.9398	0.9338	0.9338	0.9337	0.9334	-0.0060	-0.0060	-0.0062	-0.0065
	0.0320	0.9678	0.9646	0.9656	0.9656	0.9654	-0.0032	-0.0022	-0.0023	-0.0024
						std. dev.	0.021	0.178	0.143	0.179

TABLE J-I (Continued)

Temp. °C	1/V lb.-mole cu. ft.	z_{exp} [1]	z_{RK}	z_{BWR} [2]	z_{BWR} [3]	z_{GBWR}	Differences $z_{RK}-z_{exp}$	z_{BWR} [2] $-z_{exp}$	z_{BWR} [3] $-z_{exp}$	$z_{GBWR}-z_{exp}$
					18.4% Methane					
25	1.1708	1.7525	1.7411	1.6737	1.6721	1.5917	-0.011	-0.079	-0.080	-0.16
	0.6018	0.4355	0.4573	-0.1122	-0.1131	-0.0719	-0.022	-0.55	-0.55	-0.51
	0.3093	0.5762	0.5696	0.3940	0.3935	0.4098	-0.0065	-0.18	-0.18	-0.17
	0.1590	0.7434	0.7383	0.6920	0.6918	0.6978	-0.0051	-0.051	-0.052	-0.046
	0.0817	0.8576	0.8542	0.8431	0.8430	0.8455	-0.0033	-0.015	-0.015	-0.012
	0.0420	0.9240	0.9221	0.9197	0.9197	0.9208	-0.0020	-0.0043	-0.0044	-0.0033
	1.1074	1.3917	1.3852	1.0461	1.0445	1.0071	-0.0065	-0.35	-0.35	-0.38
	0.5694	0.4411	0.4545	-0.0698	-0.0706	-0.0318	0.013	-0.51	-0.51	-0.47
	0.2927	0.5922	0.5846	0.4267	0.4263	0.4413	-0.0076	-0.17	-0.16	-0.15
	0.1505	0.7560	0.7500	0.7086	0.7084	0.7141	-0.0060	-0.047	-0.048	-0.042
	0.0774	0.8655	0.8614	0.8514	0.8513	0.8537	-0.0041	-0.014	-0.014	-0.012
	0.0398	0.9285	0.9260	0.9240	0.9239	0.9249	-0.0025	-0.0045	-0.0046	-0.-035
	1.0257	1.0044	1.0551	0.4662	0.4647	0.4676	0.051	-0.54	-0.54	-0.54
	0.5217	0.4504	0.4570	-0.0068	-0.0076	0.0278	0.0066	-0.46	-0.46	-0.42
	0.2709	0.6128	0.6057	0.4700	0.4696	0.4829	-0.0071	-0.14	-0.14	-0.13
	0.1392	0.7714	0.7660	0.7308	0.7306	0.7356	-0.0054	-0.041	-0.041	-0.036
	0.0716	0.8746	0.8710	0.8627	0.8626	0.8647	-0.0035	-0.012	-0.012	-0.0098
	0.0368	0.9334	0.9314	0.9297	0.9297	0.9306	-0.0020	-0.0037	-0.0037	-0.0028
	0.8601	0.5843	0.6625	-0.1178	-0.1191	-0.0775	0.078	-0.70	-0.70	-0.66
	0.4421	0.4846	0.4818	0.1391	0.1385	0.1662	-0.0028	-0.35	-0.35	-0.32
	0.2272	0.6593	0.6526	0.5569	0.5566	0.5668	-0.0067	-0.10	-0.11	-0.093
	0.1168	0.8037	0.7991	0.7748	0.7746	0.7786	-0.0046	-0.029	-0.029	-0.025
	0.0600	0.8934	0.8906	0.8850	0.8849	0.8866	-0.0028	-0.0083	-0.0084	-0.0067
	0.0308	0.9436	0.9421	0.9411	0.9411	0.9418	-0.0015	-0.0025	-0.0025	-0.0017
						std. dev.	0.021	0.288	0.288	0.256

TABLE J-I (Continued)

Temp. °C	1/V lb.-mole cu. ft.	z_{exp} [1]	z_{RK}	z_{BWR} [2]	z_{BWR} [3]	z_{GBWR}	Differences $z_{RK}-z_{exp}$	$z_{BWR}-z_{exp}$ [2]	$z_{BWR}-z_{exp}$ [3]	$z_{GBWR}-z_{exp}$
50	1.1256	1.6682	1.6701	1.5715	1.5700	1.5013	0.0019	-0.097	-0.098	-0.17
	0.5789	0.5550	0.5788	0.1492	0.1484	0.1748	0.024	-0.41	-0.41	-0.38
	0.2977	0.6575	0.6530	0.5259	0.5255	0.5351	-0.0045	-0.13	-0.13	-0.12
	0.1531	0.7925	0.7869	0.7561	0.7559	0.7590	-0.0056	-0.036	-0.037	-0.033
	0.0788	0.8848	0.8809	0.8749	0.8748	0.8759	-0.0039	-0.0099	-0.010	-0.0089
	0.0405	0.9383	0.9361	0.9357	0.9357	0.9361	-0.0022	-0.0025	-0.0026	-0.0022
	1.0624	1.3495	1.3754	1.0687	1.0672	1.0329	0.026	-0.28	-0.28	-0.32
	0.5464	0.5560	0.5737	0.1811	0.1803	0.2050	0.018	-0.37	-0.38	-0.35
	0.2810	0.6704	0.6652	0.5523	0.5519	0.5605	-0.0052	-0.12	-0.12	-0.11
	0.1445	0.8024	0.7969	0.7699	0.7697	0.7725	-0.0055	-0.033	-0.033	-0.030
	0.0743	0.8908	0.8870	0.8819	0.8818	0.8829	-0.0038	-0.0088	-0.0089	-0.0079
	0.0382	0.9417	0.9396	0.9394	0.9393	0.9397	-0.0021	-0.0023	-0.0024	-0.0019
	0.9564	0.9721	1.0302	0.5047	0.5034	0.5067	0.058	-0.47	-0.47	-0.47
	0.4919	0.5641	0.5738	0.2442	0.2435	0.2650	0.0096	-0.32	-0.32	-0.30
	0.2530	0.6935	0.6877	0.5966	0.5963	0.6035	-0.0058	-0.097	-0.097	-0.090
	0.1301	0.8198	0.8141	0.7929	0.7927	0.7951	-0.0056	-0.027	-0.027	-0.025
	0.0669	0.9014	0.8975	0.8937	0.8936	0.8945	-0.0039	-0.0076	-0.007	-0.0068
	0.0344	0.9477	0.9454	0.9454	0.9454	0.9457	-0.0023	-0.0023	-0.0023	-0.0019
	0.7435	0.6176	0.6726	0.0930	0.0920	0.1216	0.055	-0.52	-0.53	-0.50
	0.3824	0.6050	0.6039	0.3960	0.3955	0.4100	-0.0011	-0.21	-0.21	-0.19
	0.1967	0.7461	0.7399	0.6864	0.6862	0.6909	-0.0062	-0.060	-0.060	-0.055
	0.1012	0.8557	0.8507	0.8392	0.8390	0.8407	-0.0050	-0.017	-0.017	-0.015
	0.0520	0.9221	0.9190	0.9174	0.9174	0.9180	-0.0031	-0.0047	-0.0047	-0.0041
	0.0268	0.9588	0.9572	0.9576	0.9575	0.9578	-0.0016	-0.0013	-0.0013	-0.0010
						std. dev.	0.019	0.217	0.218	0.185

TABLE J-I (Continued)

Temp. °C	1/V lb.-mole cu. ft.	z_{exp} [1]	z_{RK}	z_{BWR} [2]	z_{BWR} [3]	z_{GBWR}	Differences $z_{RK}-z_{exp}$	$z_{BWR}-z_{exp}$ [2]	$z_{BWR}-z_{exp}$ [3]	$z_{GBWR}-z_{exp}$
75	1.0667	1.6180	1.5473	1.3947	1.3932	1.3412	-0.071	-0.22	-0.22	-0.28
	0.5496	0.6559	0.6723	0.3543	0.3535	0.3692	0.016	-0.30	-0.30	-0.29
	0.2832	0.7270	0.7212	0.6316	0.6312	0.6361	-0.0057	-0.095	-0.096	-0.091
	0.1459	0.8342	0.8273	0.8076	0.8074	0.8085	-0.0069	-0.027	-0.027	-0.026
	0.0752	0.9080	0.9030	0.9004	0.9003	0.9005	-0.0050	-0.0076	-0.0077	-0.0075
	0.0387	0.9509	0.9479	0.9486	0.9485	0.9485	-0.0030	-0.0023	-0.0024	-0.0024
	1.0003	1.3309	1.3034	0.9978	0.9964	0.9708	-0.028	-0.33	-0.33	-0.36
	0.5154	0.6549	0.6661	0.3798	0.3791	0.3935	0.011	-0.28	-0.28	-0.26
	0.2655	0.7554	0.7319	0.6536	0.6533	0.6576	-0.024	-0.10	-0.10	-0.098
	0.1368	0.8432	0.8362	0.8194	0.8192	0.8202	-0.0070	-0.024	-0.024	-0.023
	0.0705	0.9134	0.9085	0.9066	0.9065	0.9067	-0.0048	-0.0068	-0.0069	-0.0067
	0.0363	0.9538	0.9510	0.9516	0.9517	0.9517	-0.0029	-0.0020	-0.0021	-0.0021
	0.8769	0.9680	0.9920	0.5400	0.5388	0.5428	0.024	-0.43	-0.43	-0.43
	0.4518	0.6604	0.6648	0.4378	0.4371	0.4490	0.0045	-0.22	-0.22	-0.21
	0.2328	0.7613	0.7540	0.6952	0.6949	0.6981	-0.0074	-0.066	-0.066	-0.063
	0.1199	0.8602	0.8534	0.8415	0.8414	0.8421	-0.0069	-0.019	-0.019	-0.018
	0.0618	0.9237	0.9190	0.9181	0.9180	0.9181	-0.0047	-0.0057	-0.0057	-0.0056
	0.0318	0.9596	0.9568	0.9577	0.9577	0.9577	-0.0028	-0.0019	-0.0019	-0.0019
	0.6448	0.6832	0.7124	0.3129	0.3120	0.3298	0.024	-0.37	-0.37	-0.35
	0.3322	0.7000	0.6963	0.5713	0.5709	0.5776	-0.0038	-0.13	-0.13	-0.12
	0.1712	0.8109	0.8037	0.7746	0.7744	0.7761	-0.0072	-0.036	-0.037	-0.035
	0.0882	0.8934	0.8885	0.8838	0.8837	0.8841	-0.0049	-0.0096	-0.0097	-0.0094
	0.0454	0.9427	0.9393	0.9397	0.9396	0.9397	-0.0034	-0.0030	-0.0031	-0.0030
	0.0234	0.9697	0.9679	0.9689	0.9689	0.9688	-0.0018	-0.0008	-0.0008	-0.0009
						std. dev.	0.021	0.178	0.179	0.179

TABLE J-I (Continued)

Temp. °C	1/V lb.-mole cu. ft.	z_{exp} [1]	z_{RK}	z_{BWR} [2]	z_{GBWR}	Differences $z_{RK}-z_{exp}$	Differences $z_{BWR}-z_{exp}$	Differences $z_{GBWR}-z_{exp}$
				99.9% Ethylene				
25	1.1581	1.7780	1.9018	1.8396	1.7010	0.12	0.62	-0.077
	0.5940	0.3189	0.3560	-0.3745	-0.3142	0.037	-0.69	-0.63
	0.3047	0.4961	0.4981	0.2695	0.2933	0.0020	-0.23	-0.20
	0.1563	0.6931	0.6966	0.6346	0.6434	0.0035	-0.059	-0.050
	0.0802	0.8285	0.8316	0.8155	0.8191	0.0035	-0.013	-0.0093
	0.0411	0.9081	0.9102	0.9062	0.9078	0.0020	-0.0019	-0.0003
	1.1097	1.3820	1.5418	1.2102	1.1267	0.16	-0.17	-0.26
	0.5692	0.3247	0.3543	-0.3320	-0.2744	0.030	-0.66	-0.60
	0.2920	0.5095	0.5118	0.3011	0.3234	0.0023	-0.21	-0.19
	0.1498	0.7034	0.7073	0.6503	0.6586	0.0039	-0.053	-0.045
	0.0768	0.8345	0.8381	0.8234	0.8268	0.0036	-0.011	-0.0077
	0.0394	0.9114	0.9138	0.9101	0.9117	0.0023	-0.0013	-0.0002
	1.0397	0.9910	1.1560	0.5148	0.4921	0.16	-0.48	-0.50
	0.5333	0.3368	0.3569	-0.2637	-0.2103	0.020	-0.60	-0.55
	0.2735	0.5307	0.5328	0.3469	0.3670	0.0021	-0.18	-0.16
	0.1403	0.7195	0.7230	0.6730	0.6806	0.0036	-0.046	-0.039
	0.0720	0.8442	0.8476	0.8347	0.8378	0.0034	-0.0095	-0.0063
	0.0369	0.9167	0.9190	0.9159	0.9173	0.0023	-0.0009	0.0005
	0.9138	0.5684	0.7200	-0.2233	-0.1818	0.15	-0.79	-0.75
	0.4687	0.3675	0.3757	-0.1257	-0.0807	0.0082	-0.49	-0.45
	0.2404	0.5722	0.5738	0.4289	0.4455	0.0016	-0.14	-0.13
	0.1233	0.7503	0.7522	0.7136	0.7199	0.0020	-0.037	-0.030
	0.0633	0.8640	0.8649	0.8550	0.8557	0.0009	-0.0090	-0.0063
	0.0324	0.9292	0.9285	0.9261	0.9273	-0.0007	-0.0030	-0.0018
					std. dev.	0.064	0.334	0.334

TABLE J-I (Continued)

Temp. °C	1/V lb.-mole cu. ft.	z_{exp} [1]	z_{RK}	z_{BWR} [2]	z_{GBWR}	Differences $z_{RK}-z_{exp}$	Differences $z_{BWR}-z_{exp}$	Differences $z_{GBWR}-z_{exp}$
50	1.1178	1.6963	1.8119	1.7208	1.6050	0.11	0.24	-0.091
	0.5731	0.4516	0.4935	-0.0640	-0.0640	-0.2305	-0.52	-0.47
	0.2938	0.5885	0.5918	0.4248	0.4400	0.0033	-0.16	-0.15
	0.1506	0.7509	0.7514	0.7096	0.7147	0.0005	-0.041	-0.036
	0.0772	0.8623	0.8617	0.8527	0.8546	-0.0006	-0.0096	-0.0077
	0.0396	0.9279	0.9262	0.9249	0.9257	-0.0017	-0.0029	-0.0022
	1.0619	1.3460	1.4739	1.1385	1.0729	0.13	-0.21	-0.27
	0.5444	0.4546	0.4895	-0.2609	0.0126	0.035	-0.48	-0.44
	0.2791	0.6021	0.6049	0.4541	0.4680	0.0028	-0.15	-0.13
	0.1431	0.7612	0.7618	0.7244	0.7291	0.0006	-0.037	-0.032
	0.0734	0.8684	0.8681	0.8602	0.8619	-0.0004	-0.0083	-0.0065
	0.0376	0.9313	0.9297	0.9287	0.9294	-0.0016	-0.0026	-0.0019
	0.9703	0.9487	1.0845	0.4713	0.4628	0.14	-0.48	-0.49
	0.4977	0.4660	0.4903	0.0447	0.0792	0.024	-0.42	-0.39
	0.2552	0.6258	0.6278	0.5019	0.5139	0.0020	-0.12	-0.11
	0.1308	0.7787	0.7792	0.7485	0.7526	0.0005	-0.030	-0.026
	0.0671	0.8788	0.8786	0.8723	0.8738	-0.0002	-0.0065	-0.0050
	0.0344	0.9369	0.9355	0.9349	0.9355	-0.0014	-0.0020	-0.0014
	0.8070	0.5697	0.6881	-0.0867	-0.0475	0.12	-0.65	-0.62
	0.4138	0.5021	0.5137	0.1919	0.2182	0.012	-0.31	-0.28
	0.2121	0.6723	0.6740	0.5878	0.5966	0.0017	-0.084	-0.076
	0.1088	0.8110	0.8119	0.7916	0.7947	0.0009	-0.019	-0.016
	0.0558	0.8976	0.8978	0.8940	0.8952	0.0002	-0.0036	-0.0024
	0.0286	0.9470	0.9461	0.9459	0.9464	-0.0009	-0.0011	-0.0005
					std. dev.	0.054	0.260	0.241

TABLE J-I (Continued)

Temp. °C	1/V lb.-mole cu. ft.	z_{exp} [1]	z_{RK}	z_{BWR} [2]	z_{GBWR}	Differences $z_{RK}-z_{exp}$	Differences $z_{BWR}-z_{exp}$	Differences $z_{GBWR}-z_{exp}$
75	1.0576	1.6520	1.6243	1.4409	1.3598	-0.028	-0.21	-0.29
	0.5445	0.5667	0.5999	0.1825	0.2092	0.033	-0.38	-0.36
	0.2803	0.6678	0.6688	0.5489	0.5579	0.0010	-0.12	-0.11
	0.1443	0.7990	0.7963	0.7687	0.7712	-0.0027	-0.030	-0.028
	0.0743	0.8885	0.8860	0.8816	0.8822	-0.0025	-0.0070	-0.0063
	0.0382	0.9404	0.9388	0.9391	0.9394	-0.0017	-0.0013	-0.0011
	0.9938	1.3140	1.3340	0.9556	0.9155	0.020	-0.36	-0.40
	0.5116	0.5674	0.5946	0.2169	0.2417	0.027	-0.35	-0.33
	0.2634	0.6810	0.6814	0.5760	0.5840	0.0004	-0.11	-0.097
	0.1356	0.8091	0.8065	0.7827	0.7850	-0.0026	-0.026	-0.024
	0.0698	0.8945	0.8923	0.8886	0.8893	-0.0022	-0.0059	-0.0052
	0.0359	0.9438	0.9423	0.9428	0.9430	-0.0014	-0.0009	-0.0007
	0.7078	0.6345	0.6991	0.1190	0.1495	0.065	-0.51	-0.49
	0.3644	0.6139	0.6205	0.4171	0.4316	0.0066	-0.20	-0.18
	0.1876	0.7516	0.7491	0.6986	0.7028	-0.0025	-0.053	-0.049
	0.0966	0.8586	0.8556	0.8457	0.8469	-0.0030	-0.013	-0.012
	0.0497	0.9238	0.9215	0.9208	0.9212	-0.0023	-0.0030	-0.0026
	0.0256	0.9599	0.9584	0.9593	0.9594	-0.0014	-0.0006	-0.0005
	0.8984	0.9658	1.0279	0.4746	0.4747	0.062	-0.49	-0.49
	0.4625	0.5755	0.5944	0.2769	0.2984	0.019	-0.30	-0.28
	0.2381	0.7027	0.7019	0.6168	0.6234	-0.0008	-0.086	-0.079
	0.1226	0.8252	0.8223	0.8038	0.8056	-0.0028	-0.021	-0.020
	0.0631	0.9042	0.9019	0.8994	0.8999	-0.0023	-0.0048	-0.0043
	0.0325	0.9492	0.9477	0.9483	0.9485	-0.0015	-0.0008	-0.0007
					std. dev.	0.022	0.221	0.216

APPENDIX K

LENNARD-JONES POTENTIAL FUNCTION

The second virial coefficient in terms of the Lennard-Jones potential function was presented in Chapter VI, Eq. (VI-10). The parameters in the potential function (n, m,σ,ε) can be evaluated by curve-fitting second virial coefficient data.

Using Eq. (VI-10) as the model, the values of the parameters are determined such that the following expression is minimized:

$$Y = \sum_{i}^{n} (B_i - \hat{B}_i)^2 = \text{minimum} \qquad \text{(K-1)}$$

where $\hat{B}_i$ is defined by Eq. (VI-10) and B_i's are observed values for the second virial coefficient.

The values of n, m,σ, and ε that minimize Y are determined by solving the following equations, simultaneously:

$$\frac{\partial Y}{\partial n} = 0 \qquad \frac{\partial Y}{\partial m} = 0$$

$$\frac{\partial Y}{\partial \sigma} = 0 \qquad \frac{\partial Y}{\partial \varepsilon} = 0 \qquad \text{(K-2)}$$

The above equations are non-linear in the parameters. The four equations can be linearized by expanding in a first order Taylor series.

$$F_j = F_{oj} + \sum_j^4 \left(\frac{\partial F}{\partial x_j}\right)_{x_j = x_{oj}} \Delta x_j = 0 \qquad \text{(K-3)}$$

$$j = 1,2,3,4$$

where the subscript j refers to the parameters (n,m,σ,ε) and Eq. (K-2).

The following steps were used to solve Eqs. (K-3) for the values of the parameters that minimize Y.

1. Assume initial values for x_j's.
2. Calculate Y_{old}.
3. Set-up the four linearized equations, Eq. (K-3).
4. Solve the linearized equations for new values of x_j's.
5. Let $x_j = x_{j\ old} + t(x_{j\ new} - x_{j\ old})$.
6. Calculate $Y = Y(t)$ for $-1.75 \leq t \leq 1.5$.
7. Determine value of t that minimizes Y(t).
8. Calculate $x_j = x_{j\ old} + t_{min.}\ (x_{j\ new} - x_{j\ old})$ and $Y = Y(t_{min.})$.
9. Compare Y_{old} and $Y(t_{min.})$.
10. Repeat steps 1 through 9 until Y does not change.

The above procedure was program for a digital computer.

APPENDIX L

EXPRESSING PRESSURE RATIOS IN TERMS OF THE BERLIN VIRIAL EQUATION OF STATE

The ratio of the pressure before the j^{th} expansion to the pressure after the j^{th} expansion (P_{j-1}/P_j) for the isothermal expansion ratio method can be expressed in terms of the Berlin virial equation of state. Before the j^{th} expansion, the state of the gas in bomb V_1 (see Figure 1) is described by the following Berlin virial equation of state:

$$P_{j-1}\frac{V_1}{n_{j-1}} = A' + B'P_{j-1} + C'P_{j-1}^2 + \ldots \qquad \text{(L-1)}$$

where n_{j-1} = number of moles of gas.

After the j^{th} expansion, the gas in bombs V_1 and V_2 is characterized by the following equation of state:

$$P_j\left[\frac{V_1 + V_2}{n_{j-1}}\right] = A' + B'P_j + C'P_j^2 + \ldots \qquad \text{(L-2)}$$

Eliminating n_{j-1} between Eqs. (L-1) and (L-2) gives:

$$\frac{P_{j-1}}{P_j}\,\frac{V_1}{V_1 + V_2} = \frac{A' + B'P_{j-1} + C'P_{j-1}^2 + \ldots}{A' + B'P_j + C'P_j^2 + \ldots} \qquad \text{(L-3)}$$

Substituting Eq. (II-8) into Eq. (L-3) gives:

$$\frac{P_{j-1}}{P_j} = N \frac{[A' + B'P_{j-1} + C'P_{j-1}^2 + \ldots]}{A' + B'P_j + C'P_j^2 + \ldots} \tag{L-4}$$

Rearranging Eq. (L-4) gives:

$$P_{j-1} [A' + B'P_j + C'P_j^2 + \ldots] = N P_j [A' + B'P_{j-1} + C'P_{j-1}^2 + \ldots] \tag{L-5}$$

or

$$P_{j-1} A' + P_{j-1} [B'P_j + C'P_j^2 + \ldots] = N P_j A' + N P_j [B'P_{j-1} + C'P_{j-1}^2 + \ldots] \tag{L-6}$$

Transposing terms,

$$P_{j-1} A' = N P_j A' + N P_j [B'P_{j-1} + C'P_{j-1}^2 + \ldots] - P_{j-1} [B'P_j + C'P_j^2 + \ldots] \tag{L-7}$$

Dividing by $P_j A'$,

$$\frac{P_{j-1}}{P_j} = N + \frac{N}{A'} [B'P_{j-1} + C'P_{j-1}^2 + \ldots] - \frac{P_{j-1}}{P_j A'} [B'P_j + C'P_j^2 + \ldots] \tag{L-8}$$

Regrouping,

$$\frac{P_{j-1}}{P_j} = N + N \frac{B'}{A'} P_{j-1} + N \frac{C'}{A'} P_{j-1}^2 + \ldots - \frac{B'}{A'} P_{j-1} - \frac{C'}{A} P_{j-1} P_j - \ldots \tag{L-9}$$

Collecting terms and factoring,

$$\frac{P_{j-1}}{P_j} = N + (N-1)\frac{B'}{A'}P_{j-1} + \left[N - \frac{P_j}{P_{j-1}}\right]\frac{C'}{A'}P_{j-1}^2 + \ldots \qquad \text{(L-10)}$$

The above equation is Eq. (III-1).

APPENDIX M

ETHYLENE COMPRESSIBILITY DATA CALCULATED FROM HELIUM CELL CONSTANTS

In this appendix, the ethylene compressibility data calculated from the isothermal expansion data using cell constants determined from helium isothermal expansions are shown in Table M-I and compared with data by Michels and Geldermans (41) in Figure 24. Also, a plot of the helium pressure ratios used to evaluate the cell constant is shown in Figure 23.

TABLE M-I

COMPRESSIBILITY FACTORS FOR ETHYLENE BASED UPON CELL CONSTANT DETERMINED FROM HELIUM PRESSURE RATIO DATA

Experimental Data			Calculated Data	
Temp. °C	Run No.	P psia	Z	$1/\underline{V}$ lb.-mole/ft^3
				N = 1.94024
25.00	6	11858.506	1.83059	1.1248
		1091.035	0.32678	0.5797
		870.467	0.50585	0.2988
		623.854	0.70341	0.1540
		382.474	0.83673	0.0794
		215.040	0.91276	0.0409
		115.714	0.95298	0.0211
		60.867	0.97260	0.0109
		31.699	0.98278	0.0056
25.00	7	8832.565	1.42314	1.0776
		1064.389	0.33275	0.5554
		856.693	0.51963	0.2863
		606.616	0.71391	0.1475
		369.174	0.84297	0.0760
		206.808	0.91623	0.0392
		111.073	0.95478	0.0202
		58.398	0.97397	0.0104
		30.373	0.98286	0.0054
25.00	8	5933.975	1.02063	1.0095
		1034.292	0.34516	0.5203
		836.047	0.54133	0.2682
		581.367	0.73036	0.1382
		349.878	0.85283	0.0712
		194.887	0.92169	0.0367
		104.373	0.95773	0.0189
		54.814	0.97590	0.0098
		28.496	0.98434	0.0050
25.00	9	2991.405	0.58339	0.8903
		991.945	0.37534	0.4589
		792.281	0.58166	0.2365
		532.844	0.75901	0.1219
		314.715	0.86980	0.0628

TABLE M-I (Continued)

Experimental Data			Calculated Data	
Temp. °C	Run No.	P psia	Z	$1/\underline{V}$ lb.-mole/ft^3
25.00	9	173.611	0.93097	0.0324
		92.578	0.96321	0.0167
		48.511	0.97930	0.0086
				N = 1.93554
50.00	64	11836.604	1.77024	1.0712
		1615.373	0.46761	0.5534
		1079.404	0.60477	0.2859
		706.116	0.76575	0.1477
		415.704	0.87256	0.0763
		229.335	0.93172	0.0394
		122.225	0.96112	0.0204
50.00	65	8922.033	1.40465	1.0176
		1544.856	0.47075	0.5257
		1049.123	0.61878	0.2716
		679.997	0.77628	0.1403
		397.730	0.87882	0.0725
		218.670	0.93520	0.0375
		116.362	0.96323	0.0194
50.00	66	5749.098	0.99047	0.9299
		1448.005	0.48285	0.4804
		996.823	0.64338	0.2482
		635.957	0.79447	0.1282
		367.959	0.88972	0.0662
		201.110	0.94121	0.0342
		107.034	0.96957	0.0177
50.00	67	2870.147	0.59520	0.7725
		1296.717	0.52049	0.3991
		890.282	0.69166	0.2062
		550.570	0.82791	0.1065
		312.405	0.90926	0.0550
		168.976	0.95192	0.0284
		89.408	0.97488	0.0147

TABLE M-I (Continued)

Experimental Data			Calculated Data	
Temp. °C	Run No.	P psia	Z	$1/\underline{V}$ lb.-mole/ft^3
				N = 1.93811
75.01	40	11750.645	1.67422	1.0436
		2075.015	0.57299	0.5385
		1258.918	0.67376	0.2778
		775.367	0.80425	0.1433
		443.869	0.89232	0.0740
		241.871	0.94238	0.0382
		128.266	0.96857	0.0197
75.02	41	8782.963	1.33189	0.9805
		1952.500	0.57385	0.5059
		1206.355	0.68716	0.2610
		737.823	0.81454	0.1347
		419.921	0.89848	0.0695
		228.078	0.94581	0.0359
		120.731	0.97033	0.0185
75.01	42	5835.299	0.97881	0.8864
		1790.150	0.58197	0.4574
		1125.214	0.70897	0.2360
		680.209	0.83064	0.1218
		383.722	0.90817	0.0324
		109.475	0.97324	0.0167
75.02	43	3020.494	0.64303	0.6984
		1504.315	0.62069	0.3604
		948.188	0.75824	0.1859
		557.636	0.86426	0.0959
		308.857	0.92774	0.0495
		165.211	0.96181	0.0255

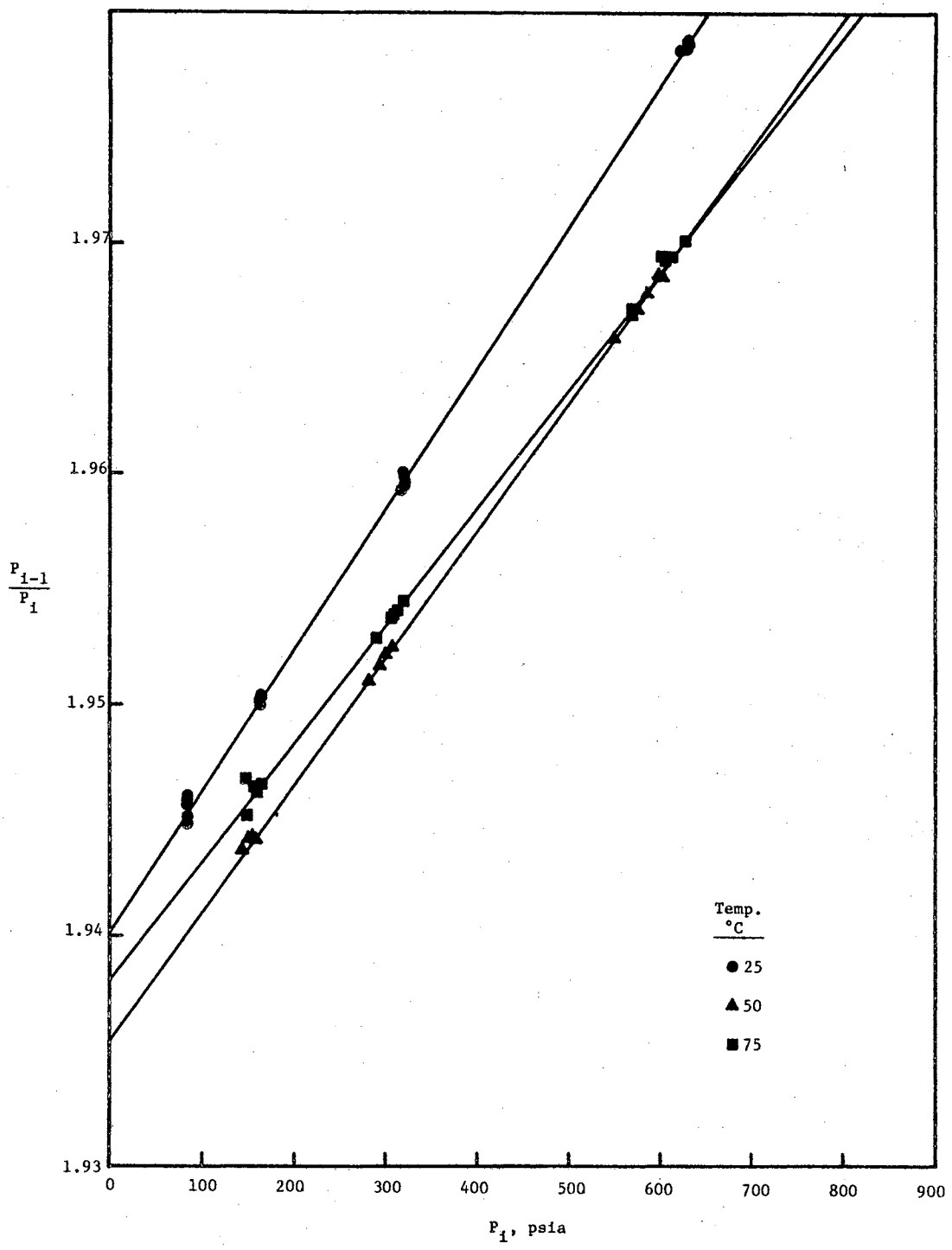

Figure 23. Helium Pressure Ratio Data

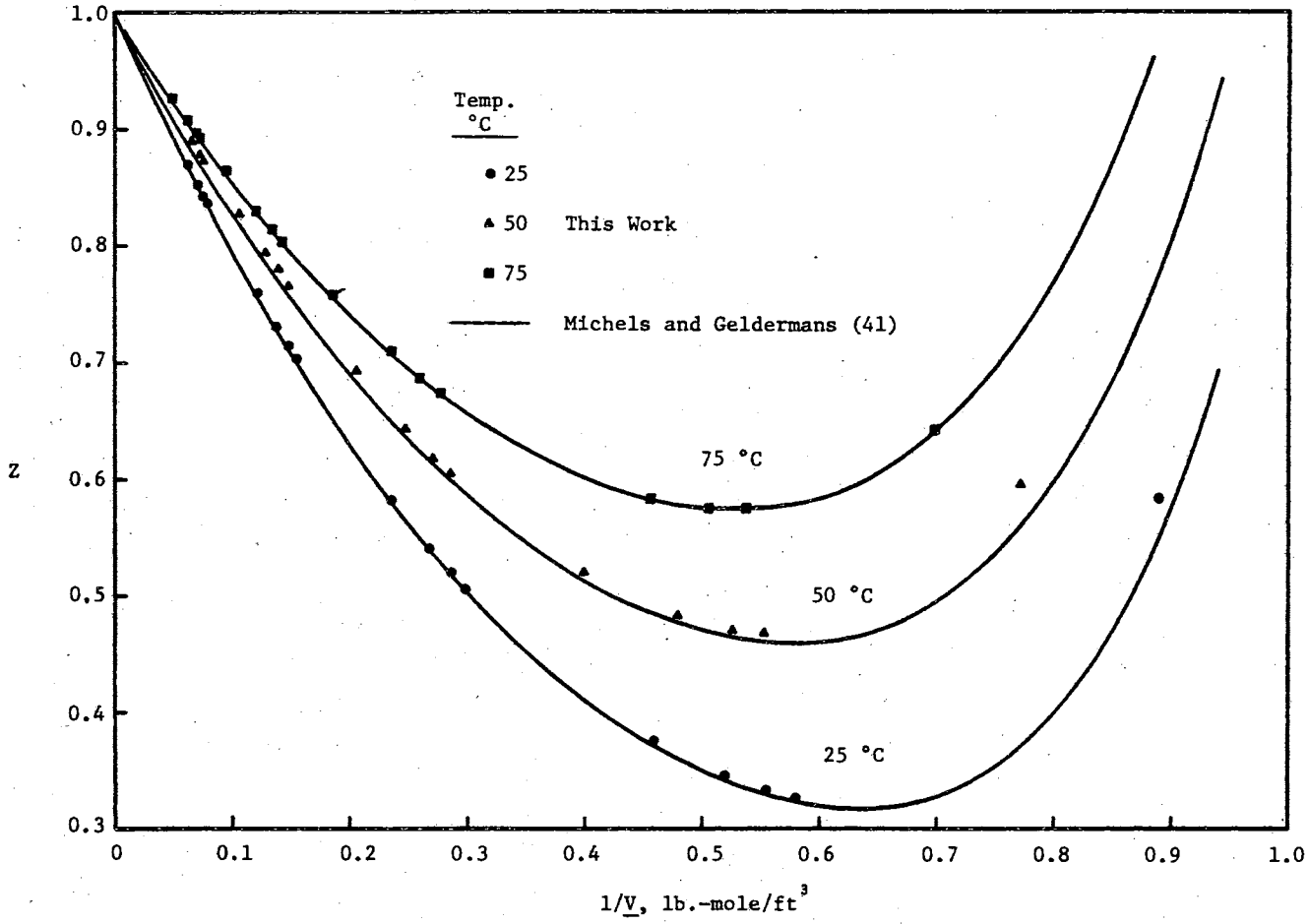

Figure 24. Comparison of Ethylene Data Calculated From the Helium Cell Constant With Literature Data

NOMENCLATURE

A	=	First Leiden virial coefficient
A'	=	First Berlin virial coefficient
A_o, A'_o, a, a'	=	Constants in empirical equations of state
a	=	Regression coefficient
A_E	=	Effective area of Ruska piston at pressure P_g and gage temperature $\underline{t}$
$A_{o,t}$	=	Area of Ruska piston at zero pressure and temperature $\underline{t}$
A_o	=	Area of Ruska piston at zero pressure and 25 °C
B	=	Second Leiden virial coefficient
B'	=	Second Berlin virial coefficient
B_o, B'_o, b, b'	=	Constants in empirical equations of state
b	=	Coefficient of pressure distortion for Ruska piston
	=	Regression coefficient
B_{ij}	=	Second cross coefficient between species i and j
C	=	Third Leiden virial coefficient
C'	=	Third Berlin virial coefficient
C_o, C'_o, c, c'	=	Constants in empirical equations of state
c	=	Coefficient of thermal expansion for Ruska piston
	=	Regression coefficient
C_{ijk}	=	Third cross coefficient between species i,j,k
C_{nm}	=	Term in expression for second virial coefficient in terms of the Lennard-Jones potential function

D	=	Fourth Leiden virial coefficient
D'	=	Fourth Berlin virial coefficient
E	=	Fifth Leiden virial coefficient
F	=	Sixth Leiden virial coefficient
f_I	=	Correction factor for estimating critical temperature for mixtures
f_s	=	Correction factor for estimating critical temperature for mixtures
g	=	Acceleration due to gravity at Stillwater, Oklahoma
g_c	=	Standard acceleration due to gravity
h	=	Head of oil above diaphragm in DPI cell when sitting zero point
I	=	Ionization potential
k	=	Boltzmann's constant
m	=	Exponent for repulsive term in Lennard-Jones potential function
n	=	Exponent for attractive term in Lennard-Jones potential function
n_o	=	Number of moles of gas in first bomb before first expansion
n_1	=	Number of moles of gas in bombs before second expansion
N	=	Volume ratio of expansion apparatus
$\overline{N}$	=	Avogadro's number
n	=	Number of components in mixture
P	=	Pressure
P_o	=	Pressure before first expansion
P_g	=	Pressure at reference level of Ruska gage
P_{oil}	=	Pressure correction for head of oil on top of diaphragm when setting zero of DPI cell
P_{DPI}	=	Pressure correction for zero shift of diaphragm with pressure

P_b = Barometric pressure

P_N = Nominal pressure

r = Number of expansions to reduce pressure to standard atmosphere

= Intermolecular distance

R = Scale reading of Texas Instruments barometer

= Universial gas constant

R_t = Resistance of platinum thermometer at temperature $\underline{t}$

R_o = Resistance of platinum thermometer at 0 °C

S = Coefficient for correcting for zero shift of DPI cell with pressure

s = Standard deviation of fit

s_{bi} = Standard deviation for i^{th} regression coefficients

T = Absolute temperature

t = Temperature

V_1 = Volume of first bomb

V_2 = Volume of second bomb

$\underline{V}$ = Molar volume

W = Force on Ruska piston due to "weights"

x = Mole fraction

z = Compressibility factor

z_o = Compressibility factor before first expansion

Creek Letters

α, α' = Constants in empirical equations of state

α = Regression coefficient

= Coefficient in calibration formula for platinum resistance thermometer

β = Regression coefficient

= Coefficient in calibration formula for platinum resistance thermometer

γ, γ' = Constants in empirical equations of state

γ_j = Exponent in expression for second virial coefficient in terms of Lennard-Jones potential function

Γ = Gamma function

δ = Coefficient in calibration formula for platinum resistance thermometer

Δt_p = Temperature correction to ice point of water for change in barometric pressure

Δt_d = Temperature correction to ice point for depth of submersion

ϕ = Intermolecular potential function

θ = Correlation for estimating B_{ij}

μ, λ = Parameters in Lennard-Jones potential function

σ, ε = Parameters in Lennard-Jones potential funtion

$\sigma_{12}, \varepsilon_{12}$ = Cross parameters for binary mixtures in Lennard-Jones potential function

$\sum$ = Summation

ρ = Molar density

$\rho_{1,T}$ = Molar density at standard atmosphere and temperature T

ρ_{AH} = Density of air at Houston

ρ_B = Density of brass

ρ_{oil} = Density of oil used in Ruska gage

ω = Accentric factor

Subscripts

c	=	Critical property
i,j	=	Number of expansions
i,j,k	=	i^{th}, j^{th}, k^{th} species in a mixture
m	=	Mixture

VITA

3

Roy Carlton Lee

Candidate for the Degree of

Doctor of Philosophy

Thesis: COMPRESSIBILITY FACTORS AND VIRIAL COEFFICIENTS FOR METHANE, ETHYLENE, AND THEIR MIXTURES, USING AN ISOTHERMAL EXPANSION RATIO APPARATUS

Major Field: Chemical Engineering

Biographical:

Personal Data: Born in Pampa, Texas, August 14, 1938, the son of Roy W. and Velma O. Lee.

Education: Attended grade school and two years of high school at Oilton, Oklahoma; finished high school at Fort Morgan, Colorado; graduated from Fort Morgan High School June, 1956; attended Colorado School of Mines from 1956-1958; transferred to Oklahoma State University in 1958; received the degree of Bachelor of Science in Chemical Engineering August, 1960; received the degree of Master of Science in Chemical Engineering at Oklahoma State University May, 1962; completed the requirements for Doctor of Philosophy degree May, 1969.

Professional Experience: Employed as Teaching Assistant during 1960-1961 and Research Assistant during 1962-1966 in the School of Chemical Engineering at Oklahoma State University; employed by Continental Oil Company during summer of 1965 in their Research Department; employed by Phillips Petroleum Company in their Research and Development Department since 1966.

Professional Societies: Associate Member of the American Institute of Chemical Engineers.